



UNIVERSITY OF TM
KWAZULU-NATAL
—
INYUVESI
YAKWAZULU-NATALI

**Synthesis and antibacterial studies of new cadmium,
silver and zinc dithiophosphonates**

By

Emmanuel R. Mkumbuzi

Dissertation submitted in fulfilment of the academic requirements for the degree of

Master of Science

School of Chemistry and Physics, University of KwaZulu-Natal, Durban

June 2018

**Synthesis and antibacterial studies of new cadmium,
silver and zinc dithiophosphonates**

By

Emmanuel R. Mkumbuzi

Dissertation submitted in fulfilment of the academic requirements for the degree of

Master of Science

School of Chemistry and Physics, University of KwaZulu-Natal, Durban

As the candidate's supervisor, I have approved this thesis for submission:

Supervisor: WERNER E. VAN ZYL

Signe



Date: 1 June 2018

DECLARATION: Plagiarism

I, Emmanuel R. Mkumbuzi, declare that the experimental work described in this dissertation was carried out at the School of Chemistry and Physics, University of KwaZulu-Natal, Westville campus, between March 2016 and November 2017, under the supervision of Professor W. E. van Zyl, and that:

1. The research reported in this thesis, except where otherwise indicated, and is my original research.
2. This thesis has not been submitted for any degree or examination at any other university.
3. This thesis does not contain other persons' data, pictures, graphs or other information, unless specifically acknowledged as being sourced from other persons.
4. This thesis does not contain other persons' writing, unless specifically acknowledged as being sourced from other researchers. Where other written sources have been quoted, then:
 - a. Their words have been re-written but the general information attributed to them has been referenced
 - b. Where their exact words have been used, then their writing has been placed in italics and inside quotation marks, and referenced.
5. This thesis does not contain text, graphics or tables copied and pasted from the Internet, unless specifically acknowledged, and the source being detailed in the thesis and in the References sections.

Signed

A solid black rectangular box used to redact the signature of Emmanuel R. Mkumbuzi.

Emmanuel R. Mkumbuzi

ABSTRACT

A variety of dithiophosphonate and bis(dithiophosphonate) compounds were synthesised from the reaction between a dithiophosphetane disulfide dimer, $[P(4-C_6H_4OMe)S(S)]_2$, commonly referred to as Lawesson's Reagent (LR), and alcohols. The LR was symmetrically cleaved by nucleophilic attack from primary or secondary alcohols, as well as diols. The alcohols used include isosorbide, 1, 4-cyclohexanol, 2-hexanol, isomannide, 2-butene 1, 4-diol, 2-methyl-cyclohexanol and 2-methyl-3-hexanol. The reaction of alcohols with LR resulted in the replacement of the P-S bond by a P-O bond due to the oxophilic nature of the phosphorous atom and consequent formation of dithiophosphonic acids ($pK_a \sim 3-4$) which were then readily deprotonated by ammonia gas to form the corresponding ammonium dithiophosphonate and bis(dithiophosphonate) ligand salts of the form $NH_4[S_2PR(OR')]$ and $(NH_4)_2[S_2PR(OR'O)PS_2R]$ respectively where ($R = 4-C_6H_4OMe$, and $R' =$ a spacer portion from a diol). The ligands were further reacted with aqueous metal nitrate salts of zinc(II), cadmium(II) and silver(I) precipitating copious amounts of dinuclear complexes with yields of at least 70% in most instances.

The characterisation of the compounds was achieved using solubility, stability, colour, melting point and several techniques which included FT-IR, mass spectrometry, 1H -NMR, ^{13}C -NMR, 2D-NMR and ^{31}P -NMR and SC-XRD. The ^{31}P -NMR spectra revealed singlet peaks indicative of a single phosphorous centre or equivalent phosphorous centres which were typically in the range *ca.* 90-110 ppm, values which are consistent with dithiophosphonate chemical shifts. Crystals of Cd(II) [**3B**] and Zn(II) [**3C**] complexes were successfully grown and subjected to single-crystal XRD analyses. The structures of the cadmium(II) and zinc(II) complexes were confirmed by SC-XRD as dinuclear complexes with an inversion centre within the molecular structure and comprising three ring structures including an eight-membered ring consisting of the metal, sulfur and phosphorus atoms. The dinuclear core $M_2S_4P_2$ formed via bridging of the ligands with the two metal centres and with a distorted tetrahedral geometry around the metal atoms. The Zn(II) and Cd(II) dinuclear metal

complexes had formulae of $[\text{Zn}_2\{\text{S}_2\text{PR}(\text{OCH}_2\text{HC}=\text{CHCH}_2\text{O})\text{PS}_2\text{R}\}_2]$ and $[\text{Cd}_2\{\text{S}_2\text{PR}(\text{OCH}_2\text{HC}=\text{CHCH}_2\text{O})\text{PS}_2\text{R}\}_2]$, respectively, where (R =4-C₆H₄OMe).

The synthesised dithiophosphonate ligands and complexes were subsequently investigated as antimicrobial agents against Methicillin resistant *Staphylococcus Aureus*, *Staphylococcus Aureus*, *Pseudomonas aeruginosa*, *Klebsiella pneumoniae*, *Escherichia Coli* and *Salmonella Typhimurium* bacterial strains. In general, the metal complexes were found to be more efficacious than the ammonium salts against these virulent bacterial strains. Silver(I) complexes were the most effective, consistent with the general observation that silver is a good antibacterial agent while cadmium generally had poor effectiveness. The most susceptible bacteria was *Klebsiella pneumoniae*, while the most resistant bacterial strains were *Salmonella Typhimurium* and *Escherichia Coli*. Most compounds, especially ammonium salts, were ineffective against these two bacterial strains in particular *Salmonella Typhimurium*. In general, each of the synthesised compounds had some degree of antibacterial activity against at least two strains.

To my family

“All you need in this life is ignorance and confidence, and then success is sure.”

Mark Twain

ACKNOWLEDGEMENTS

- My family for their love and support, they always pushed me to be a better person and for this I will forever be indebted to you.
- Prof. Werner E. van Zyl for allowing me an opportunity to experience life as a researcher. I also thank you for your faith, guidance and support.
- Mr Sizwe Zamisa, UKZN, School of Chemistry and Physics, Westville Campus, for the data collection and refinement of the crystal structures presented in this study.
- My colleagues in the Synthetics labs for guiding me while learning new techniques and for making my research worthwhile.
- My friends for their moral support and motivation through trying times when good results were hard to come by.
- The Technical Staff at UKZN, School of Chemistry, Westville campus. With special mention to Mr. Dilip Jagjivan.

LIST OF ABBREVIATIONS

°C	degrees Celsius
Å	Angstrom
MHz	mega Hertz
cm ⁻¹	wavenumbers
λ	wavelength
ppm	parts per million
DCM	dichloromethane (CH ₂ Cl ₂)
CDCl ₃	deuterated chloroform
Methanol- <i>d</i> ₄ /CD ₃ OD	Deuterated methanol
NMR	Nuclear Magnetic Resonance
• ¹ H	Proton Nuclei
• ¹³ C	Carbon-13 Nuclei
• ³¹ P	Phosphorus-31 Nuclei
• s	singlet
• d	doublet
• t	triplet
• q	quartet
• dd	doublet of doublets
• m	multiplet
FT-IR	Fourier Transform Infrared
IR	Infrared
• s	strong
• m	medium
• w	Weak
IUPAC	International Union Of Pure And Applied Chemistry
PIN	Preferred IUPAC Name
ORTEP	Oak Ridge thermal ellipsoid plot

TABLE OF CONTENTS

DECLARATION: Plagiarism	iii
ABSTRACT	iv
ACKNOWLEDGEMENTS	viii
LIST OF ABBREVIATIONS	ix
TABLE OF CONTENTS	x
LIST OF FIGURES	xiv
LIST OF TABLES	xvi
LIST OF SCHEMES	xvii
1 CHAPTER 1	1
1. INTRODUCTION	1
1.1 An overview of dithiophosphonate compounds	1
1.2 Lawesson’s Reagent	2
1.2.1 The history of the synthesis of Lawesson’s Reagent	2
1.2.2 Reactions of Lawesson’s Reagent	3
1.3 Dithiophosphonate ligands: nomenclature, bonding, resonance, structures and coordination	6
1.4 The application of dithiophosphonates	11
1.4.1 Technological, industrial and agricultural applications	11
1.4.2 Medical applications	12
1.5 Hypothesis, aims and objectives of this study	14

2	CHAPTER 2	16
	EXPERIMENTAL	16
2.1	General considerations	16
2.2	Instrumentation	16
2.3	Starting materials	17
2.3.1	Preparation of 2, 4-bis (4-methoxyphenyl)-1, 3, 2, 4-dithiadiphosphetane-2, 4-disulfide (Lawesson's Reagent)	17
2.4	Synthesis of dithiophosphonate ligand salts.	18
2.4.1	<i>1,4 Cyclohexanediol derived dithiophosphonate salt [1]</i>	18
2.4.2	<i>2-Hexanol derived dithiophosphonate salt [2]</i>	19
2.4.3	<i>2-Butene 1, 4 diol derived dithiophosphonate salt [3]</i>	19
2.4.4	<i>2-Methyl cyclohexanol derived dithiophosphonate salt [4]</i>	20
2.4.5	<i>2-Methyl -3- hexanol derived dithiophosphonate salt [5]</i>	20
2.5	Silver complexes (A)	21
2.5.1	<i>1,4 Cyclohexanol derived dithiophosphonate Ag(I) complex [1A]</i>	21
2.5.2	<i>2-Butene-1, 4-diol derived dithiophosphonate Ag(I) complex [3A]</i>	22
2.5.3	<i>2-Methyl cyclohexanol derived dithiophosphonate Ag(I) complex [4A]</i>	23
2.5.4	<i>2-Methyl 3-hexanol derived dithiophosphonate Ag(I) complex [5A]</i>	23
2.6	Cadmium complexes (B)	24
2.6.1	<i>1,4 Cyclohexanediol derived dithiophosphonate Cd(II) complex [1B]</i>	24
2.6.2	<i>2-Hexanol derived dithiophosphonate Cd(II) complex [2B]</i>	24
2.6.3	<i>2-Butene 1, 4-diol derived dithiophosphonate Cd(II) complex [3B]</i>	25

2.6.4	2-Methyl cyclohexanol derived dithiophosphonate Cd(II) complex [4B].....	25
2.6.5	2-Methyl 3 hexanol derived dithiophosphonate Cd(II) complex [5B]	26
2.7	Zinc complexes(C)	27
2.7.1	1,4 Cyclohexanediol derived dithiophosphonate Zn(II) complex [1C].....	27
2.7.2	2-Butene-1, 4-diol derived dithiophosphonate Zn(II) complex [3C]	27
2.7.3	2-Methyl cyclohexanol derived dithiophosphonate Zn(II) complex [4C]	28
2.7.4	2-Methyl 3 hexanol derived dithiophosphonate Zn(II) complex [5C].....	28
2.8	In-vitro antimicrobial studies methodology	29
3	CHAPTER 3	31
	SYNTHESIS OF NEW DITHIOPHOSPHONATE LIGANDS, SILVER(I), CADMIUM(II) AND ZINC(II) COMPLEXES	31
3.1.1	Characterisation of dithiophosphonate compounds	32
3.2	Conclusion	61
4	CHAPTER 4	62
	APPLICATION OF NEW DITHIOPHOSPHONATE COMPOUNDS IN ANTIBACTERIAL STUDIES	62
4.1	Introduction	62
4.2	Results and discussion	65
3.3	Minimum inhibitory concentration (MIC)	67
4.3	Conclusion	69
	CHAPTER 5	70
	CONCLUSIONS AND FUTURE WORK	70

6	CHAPTER 6	72
6.1	REFERENCES	72
	SUPPORTING INFORMATION	a

LIST OF FIGURES

Figure 1-1: Lawesson's Reagent and its analogues	3
Figure 1-2: An ammonium bis (dithiophosphonate) salt showing two monoanionic dithio moieties. ...	5
Figure 1-3: Types of phosphor-1, 1-dithiolates.	6
Figure 1-4: Resonance structures of dithiophosphonato ligands.	7
Figure 1-5: Various known and potential coordination bonding modes of dithiophosphonato ligands towards dithiophosphonate complexes. The most common bonding modes have been highlighted.	8
Figure 1-6: The quintessential structure of dinuclear cadmium(II) and zinc(II) dithiophosphonate complexes, binding in a 1:2 molar ratio.....	9
Figure 1-7: Monomeric and dimeric complex structures in solution.	10
Figure 1-8: The structure of dinuclear silver(I) dithiophosphonate complexes.	11
Figure 3-1: FT-IR spectrum for compound 1	34
Figure 3-2: ³¹ P-NMR spectrum for compound 1	34
Figure 3-3: ¹ H-NMR spectrum for compound 1	35
Figure 3-4: ¹³ C-NMR spectrum of compound 1	35
Figure 3-5: ESI (-) mass spectrum showing fragments of 1B	37
Figure 3-6: FT-IR spectrum for compound 2	39
Figure 3-7: ³¹ P-NMR spectrum for compound 2	39
Figure 3-8: ¹ H-NMR spectrum for compound 2	40
Figure 3-9: ¹³ C-NMR spectrum for compound 2	40
Figure 3-10: ESI (-) mass spectrum showing fragments of 2B	43
Figure 3-11: FT-IR spectrum for compound 3	44
Figure 3-12: ³¹ P-NMR spectrum for compound 3	44
Figure 3-13: ¹ H-NMR spectrum for compound 3	45
Figure 3-14: ¹³ C-NMR for compound 3	45
Figure 3-15 : ESI (-) mass spectrum showing fragments of 3B	47

Figure 3-16: ORTEP diagram for compound 3B , thermal ellipsoids drawn at 50% probability	48
Figure 3-17: ORTEP diagram for compound 3C , thermal ellipsoids drawn at 50% probability	49
Figure 3-18: Packing of 3C viewed along the a axis	49
Figure 3-19: FT-IR spectrum for compound 4	50
Figure 3-20: ³¹ P-NMR spectrum for compound 4	51
Figure 3-21: ¹ H-NMR spectrum of compound 4	51
Figure 3-22: ¹³ C-NMR spectrum for compound 4	52
Figure 3-23: ESI (-) mass spectrum showing fragments of 4B	54
Figure 3-24: FT-IR spectrum for compound 5	55
Figure 3-25: ³¹ P-NMR spectrum for compound 5	55
Figure 3-26: ¹ H-NMR spectrum for compound 5	56
Figure 3-27: ¹³ C-NMR spectrum for compound 5	57
Figure 3-28: HSQC spectrum for compound 5	57
Figure 3-29: ESI(-) mass spectrum for compound 5B	60
Figure 4-1: Structural comparison between gram positive and negative bacteria cell walls.	63

LIST OF TABLES

Table 3-1: ^{13}C -NMR chemical shifts for 1, 4 cyclohexanediol derived compounds.....	37
Table 3-2: ^{13}C -NMR chemical shifts for 2-hexanol derived compounds.....	42
Table 3-3: ^{13}C NMR chemical shifts for 2-butene -1, 4 diol derived compounds	46
Table 3-4: ^{13}C -NMR chemical shifts for 2-methyl hexanol derived compounds.....	53
Table 3-5: ^{13}C -NMR chemical shifts for 2-methyl-3-hexanol derived compounds	59
Table 4-1: Initial screening tests for synthesized dithiophosphonate compounds at 10 000ppm showing the diameter of zones of inhibition (mm)	66
Table 4-2: Minimum inhibitory concentrations (MICs) for dithiophosphonate complexes $\mu\text{g/mL}$ (ppm).....	67

LIST OF SCHEMES

Scheme 1-1: The synthesis of a diphosphetane disulfide dimer	2
Scheme 1-2: The synthesis of Lawesson's Reagent	2
Scheme 1-3: The synthesis of dithiophosphonate salts from Lawesson's Reagent.....	4

CHAPTER 1

INTRODUCTION

1.1 An overview of dithiophosphonate compounds

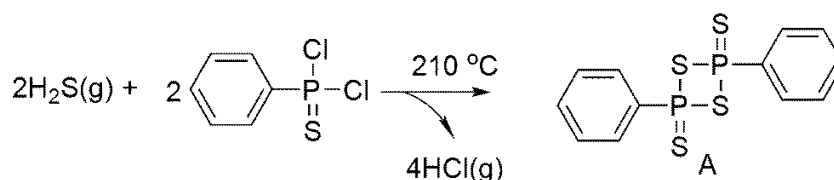
Approximately 1 wt.% of the human body consists of the element phosphorus,¹ which is essential for the existence of all life forms as part of the phosphate group found in genetic Ribonucleic acid (RNA) and Deoxyribonucleic acid (DNA) codes.² Ironically, phosphorus is also central to the most toxic and infamous synthetic poisons in the form of nerve gases that have been used in previous conflicts and terrorist attacks.³

The phosphor-1,1-dithiolate class of compounds contains the S₂P functionality, and comprise the dithiophosphates, dithiophosphinates, and dithiophosphonates.⁴ The phosphor-1,1,-dithiolato set of ligands can coordinate to most main group and transition metals, resulting in various coordination patterns. The chemistry of dithiophosphates has flourished,^{5,6} unlike the closely related dithiophosphinates and particularly the dithiophosphonates whose development has not been as forthcoming. Dithiophosphonates are a class of S-donor ligands⁷ which have been studied since the beginning of the twentieth century.⁸ The synthesis of dithiophosphonates is relatively easy because it is driven by the oxophilic nature of the phosphorous resulting in the P–S bond being replaced by a P–O bond via a nucleophilic attack a property which has proven indispensable in the synthesis of these ligands in this chemistry.⁶ The versatility of the ligands from these compounds produces a broad variety of coordination patterns which lead to a great diversity of molecular and supramolecular structures.⁴ There are numerous other sulphur or phosphorous containing ligands which are beyond the scope of this research and they include dithioarsinates, dichalcogenoimidodiphosphinates and dithioimidodiphosphinates.⁹

1.2 Lawesson's Reagent

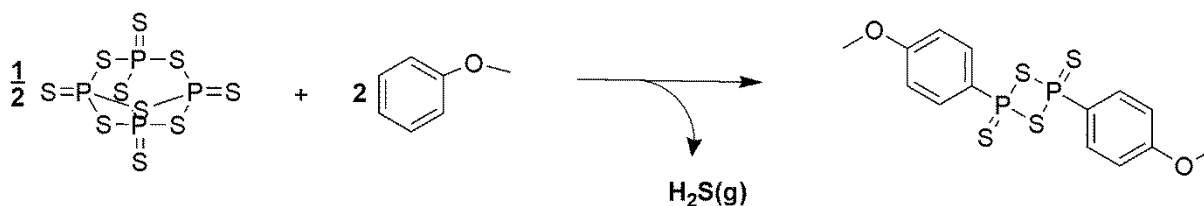
1.2.1 The history of the synthesis of Lawesson's Reagent

Thiophosphorus compounds are an important class of S-donor ligands.¹⁰ Diphosphetane disulphides were first reported in the mid-1950s by Fay and Lankelma although the synthetic method and characterisation was only reported in 1962. Initially the synthesis of such dimers involved inconvenient and hazardous methods involving the introduction of H₂S at 210°C into PhP(S)Cl₂. The reaction was extremely exothermic and also released copious amounts of corrosive HCl as a by-product¹¹ as represented by **Scheme 1-1**



Scheme 1-1: The synthesis of a diphosphetane disulfide dimer

An safer improved and simpler methodology was devised by Lawesson *et al.* in 1978 to succeed this inconvenient method to form a new related dimer [RP(S)S]₂ (R = 4-C₆H₄-OMe) in which anisyl took the convenient dual role of being the reagent as well as the solvent as shown in **Scheme 1-2**.



Scheme 1-2: The synthesis of Lawesson's Reagent.

In these reactions the diphosphetane disulfide dimer is synthesised when electron rich aromatics like anisole, phenetole and ferrocene are reacted with P₄S₁₀. Woollins and co-workers introduced ferrocene¹² as a substitute for an electron rich aromatic such as anisole in performing similar electrophilic substitution chemistry.⁶ A selenium analogue now generally known as Woollins's Reagent (commercially available) has gained popular use as an excellent selenation reagent introducing selenium into organic compounds via both electrophilic and nucleophilic pathways.¹²⁻¹⁴

Several other LR analogues are now available including fluorinated LR reagents which are less odiferous than regular LR.¹⁵ Zwitterions have also been reported when aminoalcohols and ferrocenyl Lawesson's Reagent (FcLR) were reacted.^{5,16} **Figure 1-1** shows Lawesson's Reagent and some of its analogues, (A-E)

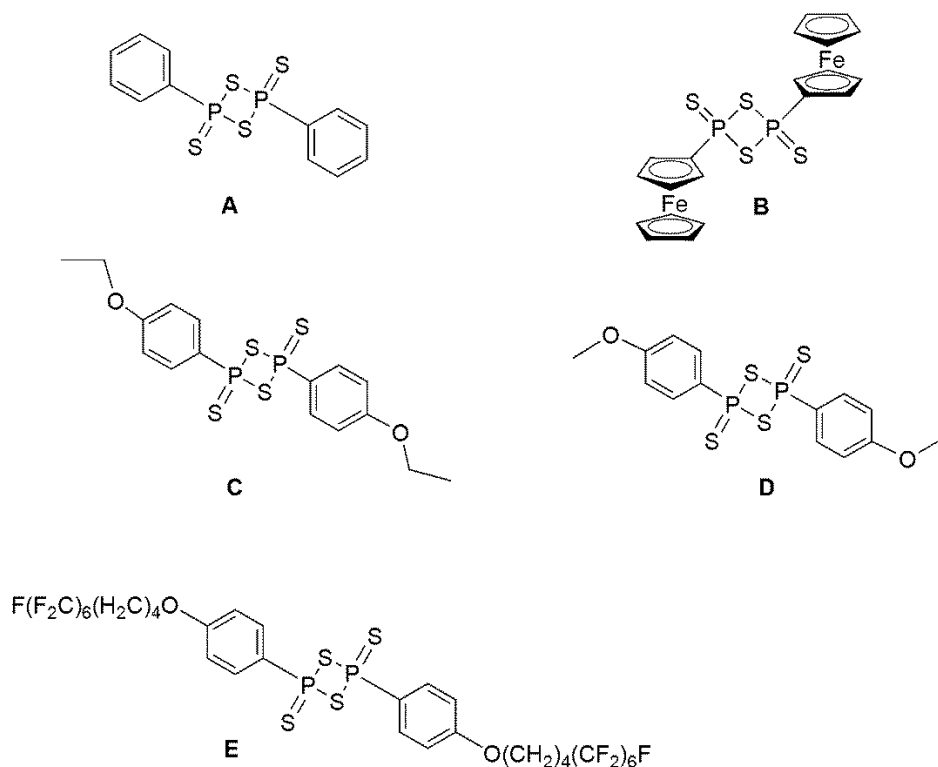


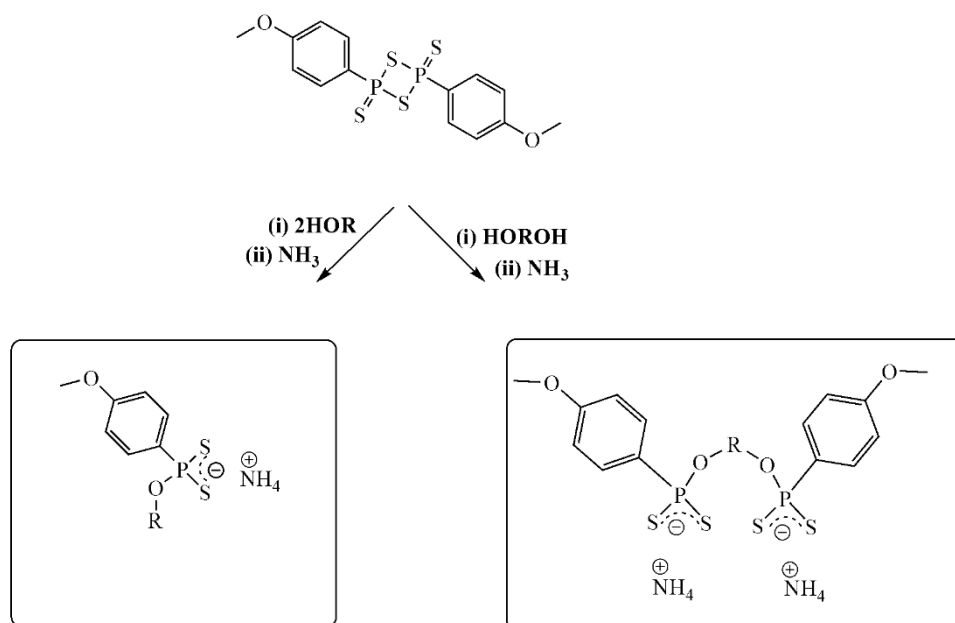
Figure 1-1: Lawesson's Reagent and its analogues

1.2.2 Reactions of Lawesson's Reagent

LR has found use as a good thionation reagent in the conversion of ketones, amides, and esters into their thio-analogues.^{6,13,17,18} It is a commonly preferred powerful thionation agent when compared to classical thionation agents such as P_2S_5 and P_4S_{10} .¹⁹ The availability, high yields and usage for soft thionation reactions are among the reasons that contribute to the popularity of LR in these thionation reaction, in addition, LR is also commercially available.²⁰ The main thermodynamic driving force behind the success of LR as a thionation reagent is the oxophilic nature of the phosphorus centre.

Lawesson's Reagent (LR) is also an important starting material for the synthesis of organodithiophosphorus compounds.²¹ Under suitable conditions LR can undergo a ring opening

reaction by nucleophilic attack.¹⁰ The use of LR as an excellent precursor to form dithiophosphonic acids which are then converted to ammonium salts as shown by **Scheme 1-3** is now well established.²²



Scheme 1-3: The synthesis of dithiophosphonate salts from Lawesson's Reagent

Dithiophosphonic acids (DTPs) are formed in a relatively straightforward reaction between LR and primary and secondary alcohols, but not with tertiary alcohols, as there is a tendency of elimination reactions to occur. An example is *tert*-butanol which eliminates isobutene. However, the dimer does react with triphenylsilanol (a silicon analogue of a tertiary alcohol) to eventually give the DTP salt.^{16,23} Trialkylsilyl alcohols also work well with no elimination reaction.^{6,24} Other reactions of LR, with carboxylic acid chlorides, esters, acetals, epoxides, sodium alkoxide, and thiols have been reported.^{5,16} Halogen-containing alcohols also form the DTP acid as expected, but the subsequent reaction with ammonia to form an ammonium salt has a tendency of resulting in dehydrohalogenation instead of the anticipated deprotonation of the acidic S-H moiety.²⁴

With the development of dithiophosphonate chemistry, a great variety of dithiophosphonic acids have been synthesised by reacting LR with various types of alcohols.^{4,25,26} Other researchers have synthesised dithiophosphonate derivatives using other analogues of Lawesson's Reagent as to explore the properties of the resultant ligands and complexes. Pillay *et al.* reacted the ferrocenyl analogue of

LR with ethanediol, *trans*-1,2-cyclohexanediol, and pentaerythritol to form the respective dithiophosphonic acids as stable di-ammonium salts in high yield.²² The products of the reactions with alkanediols showed two bridging dithiophosphonic acids with the formation of a ligand with four S atoms for coordination.^{26,27} Other diols such as 2,2 dimethyl-1,3 propanediol and 2,2' biphenol have also been used, and characterised by mass spectroscopy as well as ³¹P, ¹³C and ¹H-NMR.²⁵

The use of diols in this chemistry is interesting in that it offers new perspectives in forming dithiophosphonates because they introduce two monoanionic dithio moieties in close proximity on the same molecule, as shown in **Figure 1-2**. They also introduce stereoisomerism into the ligands and complexes resulting in less predictable and interesting molecular structures when compared to other “flat diols” for example 1,2-dihydroxybenzene. There is also increased ligand flexibility due to several *sp*³ hybridized atoms.²⁸

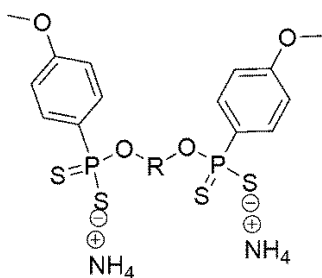


Figure 1-2: An ammonium bis (dithiophosphonate) salt showing two monoanionic dithio moieties.

Shabana reported the synthesis of bis-anisilyldithiophosphonic acids from aliphatic and aromatic diols but without isolating the acids contrary to his expectations, but instead the products of elimination of hydrogen sulphide namely 2-aryl-1, 3, 2-diox- aphospholane-2-sulfides, cyclic trithiopyrophosphonates, and thioacetamide.²⁹ He also reported the reaction of LR with aromatic ortho dihydroxy compounds in toluene at reflux temperature giving rise to 1,3,2-dioxaphos- pholane-2-sulfide derivatives.³⁰ Bis-dithiophosphonic acids were also successfully obtained by reacting diols with anisole LR.²⁵

Recently new synthesis methods have been reported. A one-pot synthesis of nickel(II) dithiophosphonate complexes by reacting LR and NiCl₂ dissolved in the appropriate alcohol, instead

of first synthesising the dithiophosphonic acid as expected. Environmental considerations have also taken centre-stage with the advent of green chemistry culminating in the use of solvent-less techniques like mechanochemistry in the synthesis of DTP to minimise the environmental impact of the fossil derived solvents for example *n*-hexane, toluene and benzene while also improving the atom efficiency of the processes.³¹

1.3 Dithiophosphonate ligands: nomenclature, bonding, resonance, structures and coordination

Dithiophosphonates are well known bidentate ligands²⁶ though relatively rare in literature compared to the other phosphor-1, 1-dithiolates, the dithiophosphates and dithiophosphinates.^{4,22} The systematic naming (nomenclature) of the class of the ligands that are the subject of this dissertation has been inconsistently used in literature. The compounds have been indiscriminately referred to as phosphonodithiolates, organodithiophosphonates or dithiophosphonates.^{6,13,16} This inconsistent use of names has often resulted in confusion.³² Systematic names are seldom used as they are cumbersome, instead the so-called “preferred IUPAC names” (PIN) are used. This PIN refers to a preferred name among two or more IUPAC names, however, other names can still be used regardless.⁵ Phosphor-1, 1-dithiolato compounds include phosphorodithioates, phosphonodithioates and phosphinodithioates which correspond to dithiophosphates, dithiophosphonates and dithiophosphinates, respectively, which are commonly used names. **Figure 1-3** shows the structures of the different types of phosphor-1, 1-dithiolate. Dithiophosphonate ligands can be thought of as “hybrids” of dithiophosphinates and dithiophosphates. One of the key features of the dithiophosphonates is that they are asymmetric thereby enabling the formation of stereoisomers, unlike dithiophosphonates and dithiophosphates.

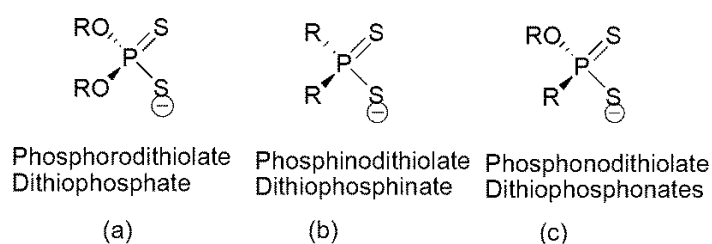


Figure 1-3: Types of phosphor-1, 1-dithiolates.

In the interest of clarity, the term “dithiophosphonates” will be used throughout this dissertation or “dithiophosphonato” when referring to the free monoanion, typically in the context of the deprotonated acid.

In dithiophosphonic acids, the electrons can be situated at one of the sulphur atoms resulting in a monodentate binding configuration, or they can be delocalized between the S-P-S atoms, producing a bidentate ligand in the same structure. In literature P-S bonds of ca 2.0 Å and longer are classified as single bonds while bonds shorter than 1.95 Å are classified as double bonds.³³ Depending on the metal type and the oxidation state several resonance structures shown in **Figure 1-4** are possible upon complexation.⁶ Such versatility in dithiophosphonate binding modes has motivated the application of such ligands in supramolecular chemistry.¹³ In this branch of chemistry, the ligand’s ability to provide strongly covalent and secondary dative coordinative interactions which bridge several metal centres is exploited. The supramolecular structures produced rely on the coordination geometry of the metal and also the functional groups present.³⁴

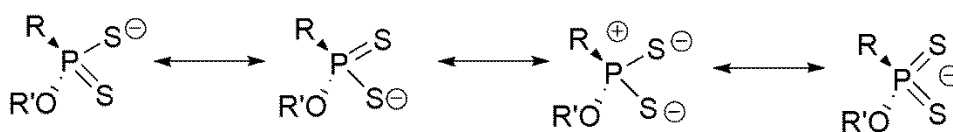


Figure 1-4: Resonance structures of dithiophosphonato ligands.

The S-P-S group can behave as isobidentate³⁵ (symmetrical) or anisobidentate³⁶ (unsymmetrical), both in chelating and bridging situations. The dithiophosphorus ligands display various coordination patterns, which include, monodentate, bidentate chelating and bridging.⁹

These different coordination patterns lead to a great diversity of molecular and supramolecular structures.^{4,9} It is known that a considerable number of dithiophosphonates and their metal complexes have been synthesized in a straightforward manner using Lawesson’s Reagent (or any of its analogues) and its respective alcohols via a ring opening nucleophilic attack as mentioned earlier.³⁷

The major coordination patterns include mono- to tetranuclear metal centres and from mono- to tetra-

connectivity with some of the known and potential coordination bonding modes of dithiophosphonato ligands being shown in **Figure 1-5**

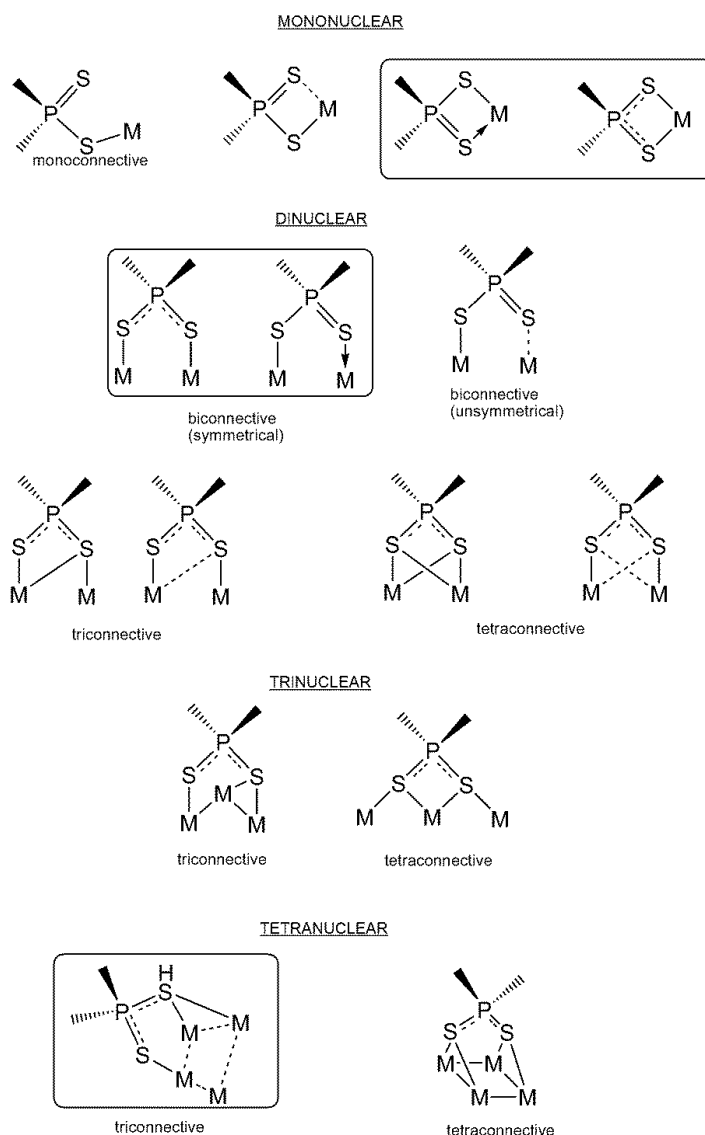


Figure 1-5: Various known and potential coordination bonding modes of dithiophosphonato ligands towards dithiophosphonate complexes. The most common bonding modes have been highlighted.

The dithiophosphonato ligand, $[S_2PR(OR')]^-$ is of interest and can still be considered comparatively rare in literature compared to the dithiophosphonates and the dithiophosphinates. The synthesis of dithiophosphonates is relatively easy to conduct and therefore many new complexes can be synthesised using almost any primary and secondary alcohol or hydroxy moiety. Such new complexes typically have slightly different properties compared to similar complexes with the dithiophosphonato

ligand. The asymmetric nature of the ligand allows for the synthesis of isomers which may result in applications in medicine and technology where isomerism can play a role in the antibacterial efficacy of a compound.³⁸

Metal complexes with sulfur ligands are significant in the investigation of biological metal–sulfur interactions as models.³⁹ As with many other thiophosphorus compounds, the DTPOAs are prone to form complexes with transition metals,²³ though no alkali metal or group 3 metal complexes are known, unlike the well-developed dithiophosphates.⁵ Group 10 and group 12 metal cations are known to form stable complexes with DTPO, which is dominated by Ni(II) complexes.⁴⁰ In most cases, their complexes form *trans* isomers with a crystallographic inversion centre present within the molecule which can be attributed to steric effects. The first *cis* isomer was of a Ni(II) dithiophosphonate complex formed from aminated LR and Ni(II). This complex was stabilized in the solid matrix by extensive hydrogen bonding involving the released ethylenediamine and a water molecule.⁵

Eight membered group 12 complexes that adopt dimeric M_2L_4 structures have been reported.²⁶ Examples in literature show various group 12 metal dithiophosphonate complexes of dithiophosphonates exhibiting dimeric structural motifs in virtually all cases in which eight membered $M_2P_2S_4$ rings occur. They have two terminal bidentate ligands each bound to one metal atom via both sulfur atoms, while the other two act as bridging ligands with their sulfur atoms binding to two different metal atoms as shown in **Figure 1-6**

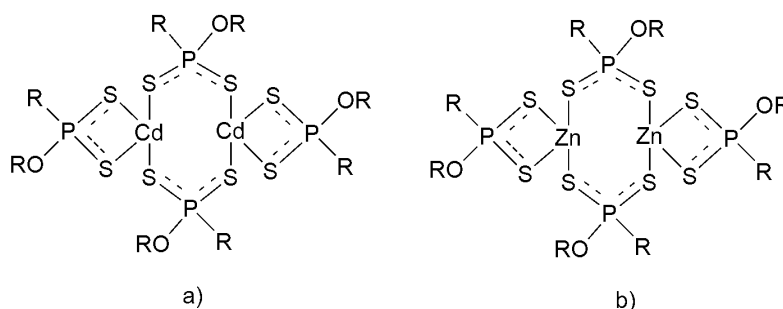


Figure 1-6: The quintessential structure of dinuclear cadmium(II) and zinc(II) dithiophosphonate complexes, binding in a 1:2 molar ratio.

However, literature is devoid of examples of confirmed molecular structures of bis-dithiophosphonates complexes. Earlier studies conducted on bis-dithiophosphonate complexes of group 12 metals (cadmium and zinc) suggested an equilibrium with a rapid exchange between monomeric and dimeric structures.^{26,41,42} **Figure 1-7** shows the monomeric and dimeric forms suggested.

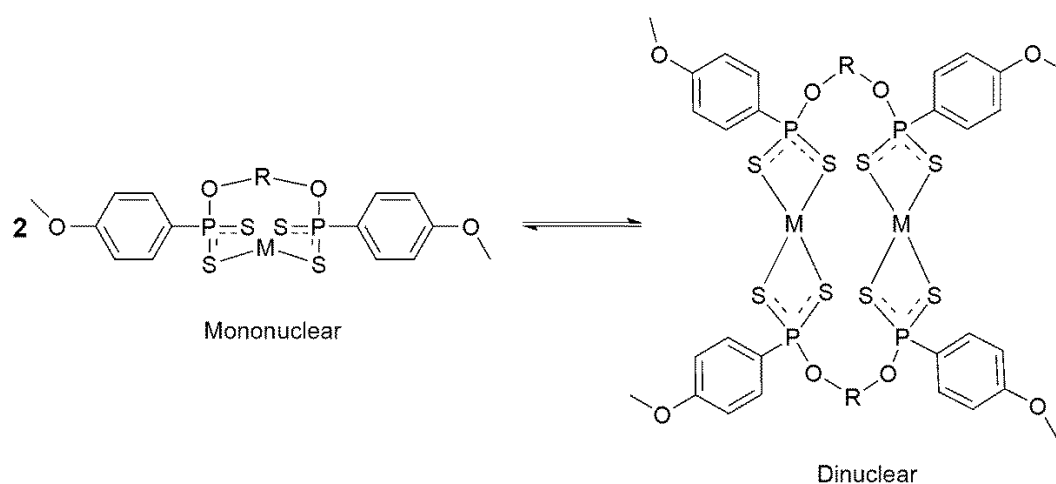


Figure 1-7: Monomeric and dimeric complex structures in solution.

The complexation properties of bis(dithiophosphinates), bis(dithiophosphonates) and bis(dithiophosphates), especially containing functionalized bridging moieties, have been much less investigated.⁴² Physicochemical properties of bis-dithiophosphonic acids are particularly interesting since as bidentate chelating ligands they are able to produce much more stable complexes with metal ions.³⁹ However, in general, metal complexes of dithiophosphonates are particularly vulnerable to hydrolysis, the ligand progressively becomes oxidized, especially during prolonged crystal growth, resulting in substitution of a terminal P=S bond with a P=O bond, presumably due to moisture or dissolved oxygen present in the solvents.⁵

Group 11 dithiophosphonate complexes including gold(I) and silver(I) form dimeric, eight-membered rings, containing two bridging dithiophosphonate ligands like the previously mentioned group 10 metal complexes⁴³, as shown in **Figure 1-8**.

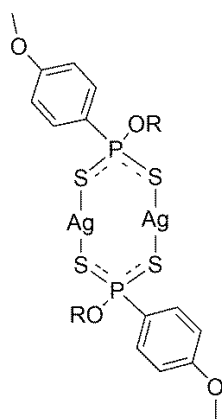


Figure 1-8: The structure of dinuclear silver(I) dithiophosphonate complexes.

1.4 The application of dithiophosphonates

Dithiophosphonates are an important group of compounds that have found applications in technology, agriculture and medicine⁴⁴ as precursors in materials chemistry, and reagents in biological and medicinal chemistry.³⁶ These commercial applications of dithiophosphonates exploit the ability of the ligand to form stable metal chelates.¹³

1.4.1 Technological, industrial and agricultural applications

Thiophosphorus species are used in a variety of applications encompassing technology, agriculture and industry as nematicides, vulcanization accelerators, stabilisers for polymer compositions, insecticides, chemical warfare agents, metal ore extraction reagents, flotation agents for mineral ores, antiwear agents, fireproofing agents,^{45,46} as antioxidants in extreme pressure engine lubricants and in plastics.^{5,13,32,33,37,39,47} While metal phosphate chemistry has flourished owing to its relative ease of synthesis and diverse applications which include photophysics, microelectronics, catalysis, sensors, ion exchanges and materials, applications of the heavier dithiophosphonate ligands are not as plentiful. The commercial unavailability of this ligand and sensitivity towards hydrolysis may be a reason for its scarcity in applications.^{6,13,17}

The insecticidal activity of dithiophosphonates against *Plutella xylostella*, a polyphagous insect, quite prevalent in the vegetable crops of northern India has been investigated where novel

dithiophosphonate (DTP) complexes exhibited substantial insecticidal activity. Some of the compounds were found to be more effective than endosulfan, a common but environmentally dangerous insecticide.⁴⁷

Kir *et al.* devised a method of utilising solid liquid membranes in a single stage to achieve simultaneous extraction, stripping, and regeneration operations. Their investigation used supported liquid membranes with dithiophosphonates dissolved in methanol, dichloromethane, chloroform and tetrachloromethane as mobile carriers in the facilitated transport of toxic heavy metals for the selective removal and recovery of toxic metals like mercury and nickel.⁴⁵ Phosphorus-1,1-dithiolates have also been used to synthesise liquid transition metal complexes for use in the preparation of thin layers by chemical vapour deposition (CVD) of polymer-inorganic nanocomposites.²³

Some bis-dithiophosphonic acids also form cyclic disulfides,²² with potential use in thiol-disulfide interchange reactions which is a process of great biochemical significance.³⁹

Gold(I) thiolate complexes have been used in a variety of applications in modern technology such as photosensitizers for photographic emulsions and luminescence-based chemical sensors.⁷ Numerous gold(I) dithiophosphonate complexes have luminescence properties at 77K. It would appear that this luminescence is determined by the presence of intermolecular interactions in a series of dithiophosphates and dithiophosphonates in the form of Au...Au interactions in the dinuclear complex.^{22,52} Potential applications are also being developed for aurophilic bonds and possible biological functions.⁵¹

1.4.2 Medical applications

In recent years the outbreak of new and re-emerging infectious diseases has posed a significant burden on global economies and public health. The growth of population and urbanization along with poor water supply and environmental hygiene are usually cited as the possible reasons for this increase in outbreaks.⁵²⁻⁵⁴ Multidrug-resistant bacteria have become more prevalent in the past few decades which has been blamed on the careless use of antibacterial agents⁵⁵ resulting in bacteria resistance.⁵⁶

Transmission of infectious pathogens to the community has caused outbreaks of diseases in developing countries, as well as developed countries.⁵⁷

In response to the reduced number of effective antibacterial drugs, it is imperative to develop new drugs to combat these bacteria. Lawesson's Reagent has been instrumental in the thionation of cephalosporins and penicillins to produce β -thiolactams as the bacteria has developed resistance to β -lactam antibiotics by producing β -lactamase enzymes.⁵⁸ Although there are numerous dithiophosphonates, only few antibacterial activity studies related to this class of compounds are present in literature.^{37,59} Thiophosphonoformic acid (TPFA), a thio-analogue of the anti-viral agent phosphonoformic acid (PFA), synthesised after thionation with LR, has been found to inhibit human immunodeficiency virus (HIV-1) reverse transcriptase.⁶⁰

Several studies have proven that some DTPs have greater efficacy than common antibacterial agents like vancomycin. Investigations by Aydemir *et al.* revealed that amidodithiophosphonate and dithiophosphonate compounds with more ionic character were more effective during an investigation carried out on several gram positive and negative bacteria which also included Methicillin resistant *staphylococcus aureus* (MRSA).⁵⁹ The studies also showed that complexes are generally more effective than free dithiophosphonates. In another study, Ni(II) complexes displayed greater efficacy against gram negative bacteria compared to the free ligands.⁶¹ The heavy metals within the complexes react with the proteins by combining the thiol (SH) groups, thereby inactivating the proteins.³⁷ A combination of historical antibacterial metals, for example silver, in complexes with dithiophosphonates is anticipated to have significant antibacterial action.

1.5 Hypothesis, aims and objectives of this study

Hypothesis

Dithiophosphonate complexes of silver, cadmium and zinc compounds are well known dinuclear complexes. Zn(II) and Cd(II) complexes form an eight membered ring of $M_2S_4P_2$ with the ligand behaving as chelating and bridging ligands between the two metal centres. However the crystal structures with bis(dithiophosphonate) ligands are yet to be reported. It is anticipated that the synthesised complexes will also be dinuclear complexes with ligands forming chelating and bridging coordinations with the metal centres as reported. In this research two of the five alcohols are diols, namely 2-butene 1, 4 diol and 1, 4 cyclohexanediol. There will be used to synthesise bis(dithiophosphonate) ligands for complexation with Ag(I), Cd(II) and Zn(II) and thereafter grow high quality single crystals for use in SC-XRD. Some dithiophosphonate compounds have been shown to have antibacterial properties against some common bacterial strains, the newly synthesised DTPs are expected to have some degree of activity against similar bacterial strains.

Aims

- To synthesize new dithiophosphonate ligands and their silver, zinc and cadmium complexes.
- To determine the structures of the synthesised compounds using SC-XRD.
- To determine the antibacterial properties of the synthesised compounds.
-

Objectives:-

- Fully characterize the compounds isolated using multinuclear NMR spectroscopy (^{31}P , ^{13}C , 1H), FT-infrared spectroscopy and mass spectrometry.
- Draw comparison and highlight differences (if any) in structures obtained to previously reported data of related complexes.

- Compare the antibacterial efficacy of DTP ligands and complexes on various common bacterial strains.
- Determine the minimum inhibitory concentrations (MICs) of selected compounds.

Overview

This dissertation has been divided into 6 chapters.

Chapter 1: This chapter serves as an introductory chapter into the dithiophosphonate ligand class giving a brief history of Lawesson's Reagent and its role as a crucial starting material in ligand synthesis and consequently complex synthesis. The chapter also details the phosphor-1, 1-dithiolato compounds, the main synthetic routes to dithiophosphonates, as well as dithiophosphonate complexes. This chapter also introduces the current and potential applications in industry, medicine and agriculture of this class of ligands as well as related dithiolates (dithiophosphinates and dithiophosphates).

Chapter 2: This chapter comprises experimental data detailing the preparation from P_4S_{10} and anisole of the primary starting material, anisole Lawesson's Reagent. It also shows the preparation of new ligands and complexes. A concise summary of characterisation data is contained herein including NMR (^{31}P , ^{13}C , 1H) spectroscopic data, selected FT-IR bands, mass spectra, melting points and single crystal XRD.

Chapter 3: This chapter contains the concise synthesis routes, results, characterisation and discussions of several new cadmium(II), silver(II) and zinc(II) complexes. Crystallographic data of the obtained structures of the cadmium and zinc complexes are also included in this chapter.

Chapter 4: This chapter contains the results and discussion of the antibacterial study conducted on the 7 ligands and the twenty complexes synthesised against the six virulent bacterial strains used.

Chapter 5: This chapter serves as the concluding chapter highlighting the notable and overall findings of this study as well as future research that can emanate from this work.

Chapter 6: This chapter contains the citations of the information included in this work.

CHAPTER 2

EXPERIMENTAL

2.1 General considerations

All commercially available reagents were purchased from Sigma-Aldrich and were reagent grade and used without further purification. Ammonia gas was obtained from Afrox (South Africa). Diethyl ether, THF, benzene, and hexane were distilled under dinitrogen over a sodium wire with the formation of a benzophenone ketyl indicator. Dichloromethane was distilled over P_4O_{10} .

All ligand preparations were conducted under an inert and dry N_2 atmosphere using standard Schlenk techniques and pre-dried solvents. Complexation reactions were conducted in open air in a fume hood. All glassware was cleaned and dried at $140^\circ C$ for at least 24 hours before use. Stirring was achieved using a magnetic stirrer bar and all heating was conducted by means of immersion in a silicone oil bath. Room temperature refers to 296-298 K.

The organophosphorus compounds are malodorous and highly toxic. All organophosphorus compounds synthesised in this study evolve H_2S upon exposure to the atmosphere as such caution must be taken when handling them. All manipulations of these compounds were performed in a well-ventilated fume-hood with great caution being exercised to minimize exposure to fumes.^{13,16,24}

2.2 Instrumentation

1H , ^{13}C and ^{31}P NMR spectra were obtained using a Bruker 400 MHz NMR spectrometer under ambient conditions. NMR data are expressed in parts per million (ppm). 1H spectra are referenced internally to residual proton impurity in the deuterated solvents. ^{31}P NMR spectra chemical shifts were referenced relative to an 85% H_3PO_4 in D_2O external standard solution. The data are reported as resonance position (δH), multiplicity, assignment, and relative integral intensity. Infrared spectra were collected on a Perkin Elmer Spectrum 100 FT-IR spectrophotometer. Mass spectra were recorded with a Waters Micromass LCT Premier TOF-MS. The mode of ionization was ESI (electrospray)

negative and ESI positive. Samples were prepared to ~2ppm concentration in the desired solvent and infused into the mass spectrometer. Crystallographic data collection and refinement of compounds was conducted at the University of KwaZulu-Natal, Westville Campus. Crystals of **3B** and **3C** were selected, attached onto the tip of glass fibres using epoxy glue, and centred in the X-ray beam by the aid of a video camera. Crystal evaluation and data collection were done on a Bruker Smart APEX2 diffractometer with Mo $K\alpha$ radiation ($\lambda = 0.71073 \text{ \AA}$) equipped with an Oxford Cryostream low-temperature apparatus operating at 100(1) K. The initial cell matrix was determined from three series of scans consisting of twelve frames collected at intervals of 0.5° in a 6° range with the exposure time of ten seconds per frame. Each of the three series of scans was collected at different starting angles and the *APEXII*⁸ program suite used to index the reflections. The data collection involved using omega scans of 0.5° width with an exposure time of 20 s per frame. The total number of images was based on results from the programme *COSMO*⁹ whereby the expected redundancy was to be 4.0 and completeness of 100% out to 0.75 \AA . Cell parameters were retrieved using *APEXII*⁸ and refined using *SAINT* on all observed reflections. Data reduction was performed using *SAINT* software, and the scaling and absorption corrections were applied using *SADABS*¹¹ multi-scan technique. The structures were solved by the direct method using the *SHELXS*¹² program and refined. The visual crystal structures were presented using *ORTEP-3*,¹³ *MERCURY*,¹⁴ and *DIAMOND*,¹⁵ system software. Non-hydrogen atoms were first refined isotropically and then by anisotropic refinement with full-matrix least squares based on F^2 using *SHELXL*¹². All hydrogens were positioned geometrically, allowed to ride on their parent atoms, and refined isotropically.

2.3 Starting materials

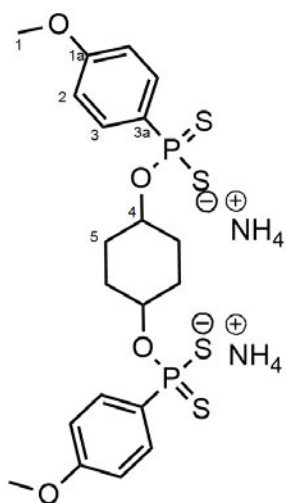
2.3.1 Preparation of 2, 4-bis (4-methoxyphenyl)-1, 3, 2, 4-dithiadiphosphetane-2, 4-disulfide (Lawesson's Reagent)

Lawesson's Reagent was prepared according to established procedure.¹³ Phosphorus pentasulfide dimer (P_4S_{10}) (44.4 g, 0.1 mol) was placed in a 500 mL two neck round bottom flask equipped with a nitrogen inlet. Anisole (108 g, 1.0 mol) was added to the flask. The mixture was stirred and refluxed

until all solids had dissolved over a period of approximately 6 hours. The resulting clear yellow solution was allowed to cool down slowly to room temperature, resulting in the formation of a yellow crystalline material. This material was isolated by vacuum filtration and washed with 100 mL of toluene and washed with 4 portions of 20 mL dry diethyl ether. All reactions and manipulations were carried out under an inert atmosphere with a positive nitrogen gas flow using standard Schlenk techniques. The yellow powder was dried, closed in an airtight container and stored in a vacuum desiccator under nitrogen. Yield: 76.04g (94%). Melting point: 228-229°C. NMR data could not be obtained as the product was not soluble in any deuterated solvents.

2.4 Synthesis of dithiophosphonate ligand salts.

2.4.1 1,4 Cyclohexanediol derived dithiophosphonate salt [1]

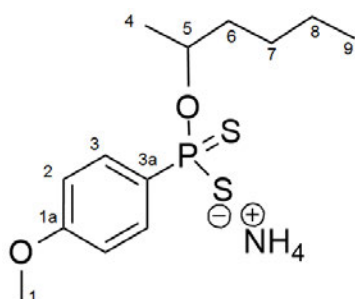


Lawesson's Reagent (LR) (4.05 g, 10 mmol) was charged in a Schlenk tube. The tube was put under vacuum for 15 minutes and purged with gaseous nitrogen. 1, 4 cyclohexanediol (1.163 g, 10 mmol.) was dissolved in 3 mL of THF and added drop wise to the Schlenk tube. The mixture was stirred using a magnetic stirrer until no visible solids were observed after approximately 10 minutes. The resultant colourless liquid was placed into an ice-cold water-bath and bubbled with ammonia for 30 seconds via a pasteur pipette resulting in the formation of a white precipitate. 10 mL of hexane was added to further precipitate and then consolidate the salt. More ammonia was bubbled for 30 seconds thereafter and the mixture stirred overnight to consolidate the salt further. The hexane was removed *in vacuo* overnight and the resultant white powder was stored in a vacuum desiccator. Yield: 4.351 g (78 %). Melting point 209-210°C. ^{31}P -NMR (Methanol- d_4) δ (ppm): 104.93. ^1H -NMR (Methanol- d_4) δ (ppm): 1.57 (4H, m, $\text{H}_{a/b-5}$), 1.91 (4H, m, $\text{H}_{a/b-5}$), 3.83 (6H, s, H-1), 4.41 (1H, m, H-4), 6.87 (4H, dd, $J=10.9, 5.4$ Hz, H-2), 8.03 (4H, dd, $J=13.5, 8.18$ Hz, H-3). ^{13}C -NMR (Methanol- d_4) δ (ppm): 162.37(C-1a), 138.24(C-3a), 132.78(C-3), 113.62(C-2), 68.90(C-4), 55.78(C-1), 26.53(C-5).

Selected IR data ν/cm^{-1} : 3176(N-H), 1012(P-O-C), 649(P-S_{as}), 544(P-S_s). ESI (-) Mass spec m/z: [M + Na]⁻ = 541.97.

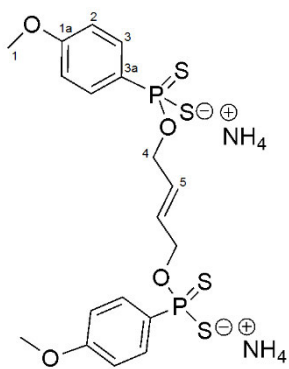
Similar reaction conditions and techniques were used in the preparation of compounds **2-5**.

2.4.2 2-Hexanol derived dithiophosphonate salt [2]



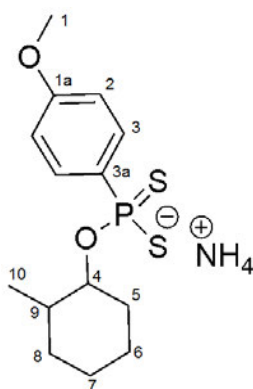
Mass of LR used: (2.384 g, 5.8 mmol). Alcohol used: 2-hexanol. Alcohol mass: (1.204 g, 11.8 mmol). Reaction time: 10 min. Product appearance: White powder. Yield: 3.399 g (90%). Melting point 154-156°C. ³¹P-NMR (Methanol-*d*₄) δ (ppm): 104.27. ¹H-NMR (Methanol-*d*₄) δ (ppm): 0.87 (3H, t, J=6.92 Hz, H-9), 1.21 (3H, d, J=6.24 Hz, H-4), 1.39 (6H, m, H-6/7/8), 3.83 (3H, s, H-1), 4.60 (1H, m, H-5), 6.90 (2H, dd, J= 8.78, 2.38 Hz, H-2), 8.07 (2H, dd, J=13.36, 8.64 Hz, H-3). ¹³C-NMR (Methanol-*d*₄) δ (ppm): 162.38(C-1a), 137.25(C-3a), 132.92(C-2), 113.40(C-3), 73.36(C-5), 55.78(C-1), 38.78(C-6), 28.62(C-7), 23.78(C-4), 22.16(C-8), 14.45(C-9). Selected IR data ν/cm^{-1} : 3173(N-H), 1011(P-O-C), 649(P-S_{as}), 556(P-S_s). ESI (-) Mass spec m/z: [M]⁻ = 303.07.

2.4.3 2-Butene 1, 4 diol derived dithiophosphonate salt [3]



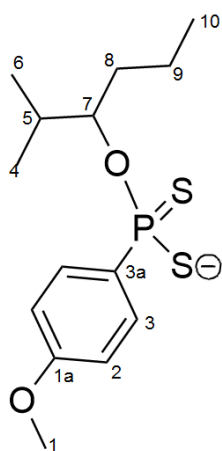
Mass of LR used: (3.863 g, 9.6 mmol). Alcohol used: 2-butene 1, 4 diol. Alcohol mass: (0.841 g, 9.6 mmol). Reaction time: 10 mins. Product: White powder. Yield: 3.032 g (59%). Melting point 149-150°C. ³¹P-NMR (Methanol-*d*₄) δ (ppm): 107.74. ¹H-NMR (Methanol-*d*₄) δ (ppm): 3.83 (6H, s, H-1), 4.44 (4H, dd, J= 9.92, 4.08 Hz, H-4), 5.66 (2H, t, J=4.04 Hz, H-5), 6.92 (4H, dd, J= 8.36, 2.04 Hz, H-2), 8.03 (4H, dd, J= 13.3, 8.8 Hz, H-3). ¹³C-NMR (Methanol-*d*₄) δ (ppm): 162.60(C-1a), 136.85(C-3a), 133.08(C-3), 130.23(C-5), 113.91(C-2), 61.18(C-4), 55.92(C-1). Selected IR data ν/cm^{-1} : 3189(N-H), 1023(P-O-C), 650(P-S_{asy}), 555(P-S_{sym}). ESI (-) Mass spec m/z: [M + Na]⁺ = 512.93.

2.4.4 2-Methyl cyclohexanol derived dithiophosphonate salt [4]



Mass of LR used: (3.87 g, 9.6 mmol). Alcohol used: 2-methyl cyclohexanol. Alcohol mass: (2.185 g, 19.1 mmol). Reaction time: 10 min. Product appearance: White powder. Yield: 4.59 g (72%). Melting point 130-132°C. ^{31}P -NMR (Methanol- d_4) δ (ppm): 103.67. ^1H -NMR (Methanol- d_4) δ (ppm): 0.93 (3H, d, $J=2,40$ Hz, H-10), 1.26 (3H, m, H-5/6/7/8), 1.28 (2H, m, H-5/6/7/8), 1.43 (3H, m, H-5/6/7/8), 1.72 (1H, q, $J= 2.79$ Hz, H-9), 3.82 (3H, s, H-1), 4.13 (1H, m, H-4), 6.89 (2H, dd, $J= 8.46, 1.66$ Hz, H-2), 8.08 (2H, dd, 13.36, 3.24 Hz, H-3). ^{13}C -NMR (Methanol- d_4) δ (ppm): 162.13(C-1a), 137.52(C-3a), 132.67(C-3), 113.47(C-2), 81.36(C-4), 55.71(C-1), 39.81(C-9), 36.63(C-5), 34.68(C-8), 31.55(C-7), 22.83(C-6), 19.89(C-10). Selected IR data ν/cm^{-1} : 3141(N-H), 1022(P-O-C), 648(P-S_{as}), 545(P-S_s). ESI (-) Mass spec m/z : $[\text{M}]^- = 315.07$.

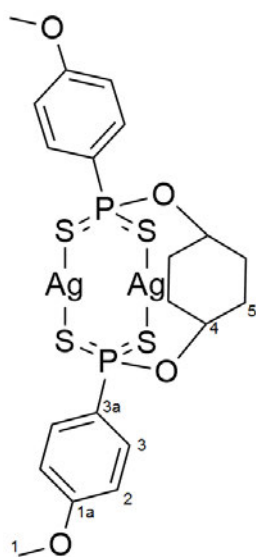
2.4.5 2-Methyl -3- hexanol derived dithiophosphonate salt [5]



Mass of LR used: (3.87 g, 9.6 mmol). Alcohol used: 2-methyl-3-hexanol. Alcohol mass: (2.184 g, 18.8 mmol). Reaction time: 10 min. Product appearance: White powder. Yield: 4.59 g (71%). Melting point 137-139°C. ^{31}P -NMR (Methanol- d_4) δ (ppm): 103.83 ppm. ^1H -NMR (Methanol- d_4) δ (ppm): 0.87 (10H, m, H-4/6/10), 1.42 (1H, m, H-8), 1.46 (3H, m, H-8/9), 2.04 (1H, m, H-5), 3.82 (1H, s), 4.45 (1H, m, H-7), 6.90 (2H, dd, $J= 8.72, 2.44$ Hz-H-2), 8.08 (2H, dd, $J= 13.40, 8.60$ Hz, H-3). ^{13}C -NMR (Methanol- d_4) δ (ppm): 162.29(C-1a), 139.06(C-3a), 132.88 (C-2), 113.58(C-3), 81.91(C-7), 55.93(C-1), 34.43(C-8), 32.55(C-5), 19.77(C-9), 18.82(C-4/C-6), 18.24(C-6/C-4), 14.79(C-10). Selected IR data ν/cm^{-1} : 3192(N-H), 1017(P-S_{as}), 646(s), 540(P-S_s). ESI (-) Mass spec m/z : $[\text{M}]^- = 317.09$.

2.5 Silver complexes (A)

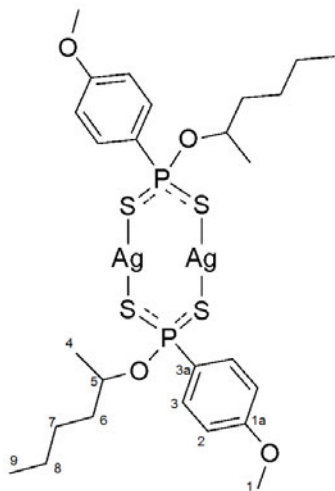
2.5.1 1,4 Cyclohexanol derived dithiophosphonate Ag(I) complex [1A]



Ligand **1** (0.183 g, 0.3 mmol) was dissolved in water (30 mL). A solution of silver nitrate (AgNO_3) (0.122 g, 0.66 mmol) in water was prepared. The silver nitrate solution was added drop wise using a pasteur pipette to the solution of the ligand **1** over 5 minutes yielding a yellow precipitate which was dried using a benchtop vacuum overnight. Reaction time: 20 min. Product appearance: Yellow powder. Melting point: 145°C (Decomp). Yield: 0.209 g (86%). ^{31}P -NMR ($\text{DMSO-}d_6$) δ (ppm): 104.10. ^1H -NMR ($\text{DMSO-}d_6$) δ (ppm): 1.33 (4H, m, $\text{H}_{a/b-5}$), 1.86 (4H, m, $\text{H}_{a/b-5}$), 3.76 (6H, s, H-1), 4.73 (2H, m, H-4), 6.90 (4H, dd, $J= 8.64, 2.36$ Hz, H-2), 7.90 (4H, dd, $J= 9.06, 3.38$ Hz, H-3). ^{13}C -NMR $\text{DMSO-}d_6$ δ (ppm): 162.90(C-1a), 133.44(C-3), 128.47(C-3a), 114.15(C-2), 69.43(C-4), 56.31(C-1), 27.06(C-5). Selected IR data ν/cm^{-1} : 1021(P–O–C), 653(P–S_{as}), 518(P–S_s). ESI (-) Mass spec m/z : $[\text{M} - \text{Ag}]^- = 626.91$.

Similar preparation methods and techniques were used to prepare compounds **2A-5C**.

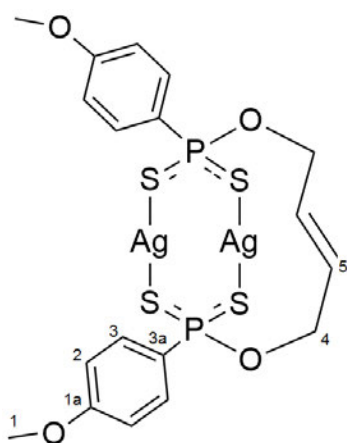
2-Hexanol derived dithiophosphonate Ag(I) complex [2A]



Mass of **2** (0.205 g, 0.64 mmol), mass of AgNO₃ (0.108 g, 0.64 mmol). Reaction time: 20 min. Product appearance: Yellow powder. Melting point: 154-156°C. Yield: 0.225 g (86%). ³¹P NMR (CDCl₃) δ (ppm): 104.06. ¹H-NMR (CDCl₃) δ (ppm): 0.89 (6H, t, J=6.86 Hz, H-9), 1.34 (16H, m, H-4/6/7/8), 1.73 (2H, m, H-6), 3.84 (6H, s, H-1), 4.94 (2H, m, H-5), 6.93 (4H, dd, J= 8.76, 3.12 Hz, H-3), 8.01 (4H, dd, J= 10.48, 8.64 Hz, H-3). ¹³C-NMR (CDCl₃) δ (ppm): 162.95(C-1a), 132.95(C-2), 128.56(C-3a), 113.48(C-3), 72.68(C-5), 55.52(C-

1), 37.35(C-6), 27.31(C-7), 22.63(C-4), 21.71(C-8). Selected IR data ν/cm^{-1} : 1023(P-O-C), 652(P-S_{as}), 531(P-S_s). ESI (-) Mass spec m/z: [M -Ag]⁻ = 715.02.

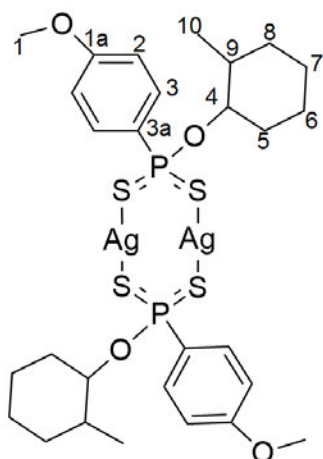
2.5.2 2-Butene-1, 4-diol derived dithiophosphonate Ag(I) complex [3A]



Mass of **3** (0.268 g, 0.5 mmol), mass of AgNO₃ (0.173 g, 1.0 mmol), Reaction time: 20 min. Product appearance: Yellow powder. Melting point: 113.6°C (Decomp.). Yield: 0.256 g (71%). ³¹P-NMR (DMSO-*d*₆): 106.77. ¹H-NMR (DMSO-*d*₆) δ (ppm): 3.78 (6H, s, H-1), 4.38 (2H, d, J=4.92 Hz, H_{a/b}-4), 4.84 (2H, d, J=8.32 Hz, H_{b/a}-4), 5.59 (2H, t, J= 6 Hz, H-5); 6.99 (4H, dd, J= 8.32, 2.56 Hz, H-2), 7.60(4H, dd, J= 12.44, 8.52 Hz, H-3). ¹³C-NMR (DMSO-*d*₆): δ

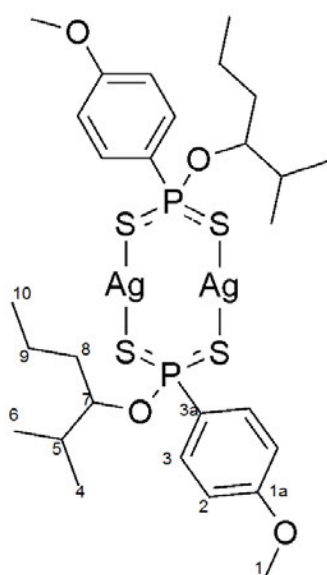
(ppm): 159.74(C-1a), 132.01(C-3), 131.26(C-5), 128.28(C-3a), 112.20(C-2), 58.44(C-4), 55.42(C-1). Selected IR data ν/cm^{-1} : 1020(P-O-C), 653(P-S_{as}), 531(P-S_s). ESI (-) mass spec m/z: [M-Ag]⁻ = 598.87.

2.5.3 2-Methyl cyclohexanol derived dithiophosphonate Ag(I) complex [4A]



Mass of **4** (0.672 g, 2.0 mmol). Mass of AgNO₃ (0.342 g, 2.0 mmol). Reaction time: 20 mins. Product appearance: Yellow powder. Melting point: 107.6°C (Decomp.). Yield: 0.581 g (68%). ³¹P-NMR (CDCl₃) δ (ppm): 103.83. ¹H-NMR (CDCl₃) δ (ppm): 0.87 (6H, dd, J=12.73 Hz, H-10), 1.40 (18H, m, H-5/6/7/8), 3.87 (6H, s, H-1), 4.14 (2H, q, J= 7.72 Hz, H-4), 6.92 (4H, dd, J= 26.62, 6.22 Hz, H-2), 7.90 (4H, dd, J= 18.66, 6.52 Hz, H-3). ¹³C-NMR (CDCl₃) δ (ppm): 161.59(C-1a), 131.90(C-3), 129.86(C-3a), 112.86(C-2), 80.15(C-4), 54.57(C-1), 37.67(C-9), 34.89(C-5), 32.54(C-8), 24.88(C-7), 24.23(C-6), 18.49(C-10). Selected IR data ν/cm⁻¹: 1026(P-O-C), 655(P-S_{as}), 532(P-S_s). ESI (-) Mass spec m/z: [M-Ag]⁻=737.03.

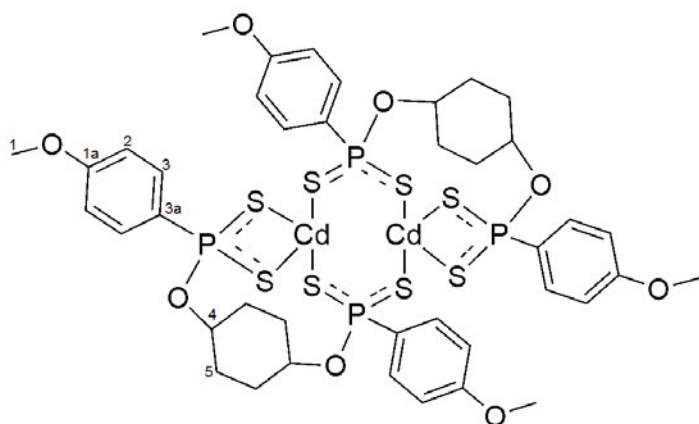
2.5.4 2-Methyl 3-hexanol derived dithiophosphonate Ag(I) complex [5A]



Mass of **5** (0.817 g, 2.44 mmol). Mass of AgNO₃ (0.413 g, 2.44 mmol). Reaction time: 20 min. Product appearance: Yellow product. Yield: 0.932 g (96%). ³¹P-NMR (CDCl₃) δ (ppm): 103.84. ¹H-NMR (CDCl₃) δ (ppm): 0.73 (18H, m, H-4/6/10), 1.30 (8H, m, H-8/9), 1.90 (2H, m, H-5), 3.67 (6H, s, H-1), 4.31 (2H, m, H-7), 6.75 (4H, dd, J= 8.60, 2.16 Hz, H-2), 7.94 (4H, dd, J= 13.36, 8.60 Hz, H-3). ¹³C-NMR (CDCl₃) δ (ppm): 162.41(C-1a), 131.72(C-2), 130.44(C-3a), 113.66(C-3), 84.04(C-7), 55.45(C-1), 33.10(C-8), 31.49(C-5), 19.86(C-9), 18.80(C-4/C-6), 18.01(C-4/6), 14.26(C-10). Selected IR data ν/cm⁻¹: 1024(P-O-C), 653(P-S_{as}), 534(P-S_s). ESI (-) Mass spec m/z: [M-Ag]⁻= 741.07

2.6 Cadmium complexes (B)

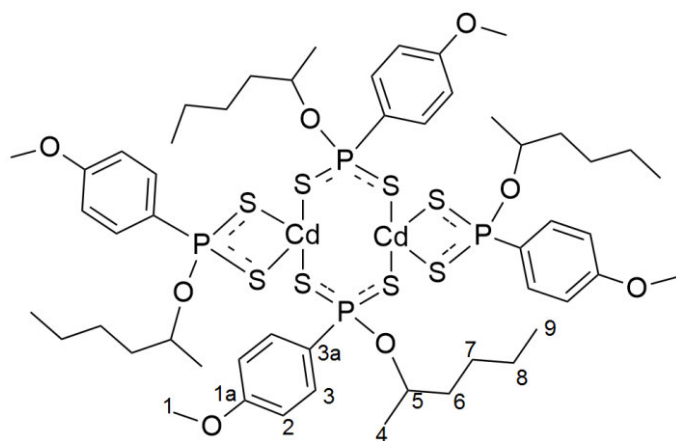
2.6.1 1,4 Cyclohexanediol derived dithiophosphonate Cd(II) complex [1B]



Mass of **1** (0.876 g, 1.58 mmol). Mass of $\text{Cd}(\text{NO}_3)_2 \cdot 4\text{H}_2\text{O}$ (0.487 g, 1.58 mmol), Reaction time: 20 mins. Product appearance: White powder. Melting point: 146°C (Decomp.). Yield: 0.846 g (85%). ^{31}P -NMR ($\text{DMSO}-d_6$) δ (ppm): 102.50. ^1H -NMR ($\text{DMSO}-d_6$) δ (ppm):

1.43 (5H, m, H-5), 1.73 (8H, m, H-5), 3.78 (12H, s, H-1), 4.44 (4H, m, H-4), 6.96 (8H, dd, $J = 8.60, 2.72$ Hz, H-2), 7.89 (8H, dd, $J = 19.98, 6.30$ Hz, H-3). ^{13}C -NMR ($\text{DMSO}-d_6$) δ (ppm): 161.94(C-1a), 132.47(C-3), 128.85(C-3a) 113.19(C-2), 68.47(C-4), 55.35(C-1), 26.10(C-5). Selected IR data ν/cm^{-1} : 1021(P-O-C), 635(P-S_{as}), 534(P-S_s). ESI (+) Mass spec m/z : $[\text{M} + \text{Na}]^+ = 1285.73$

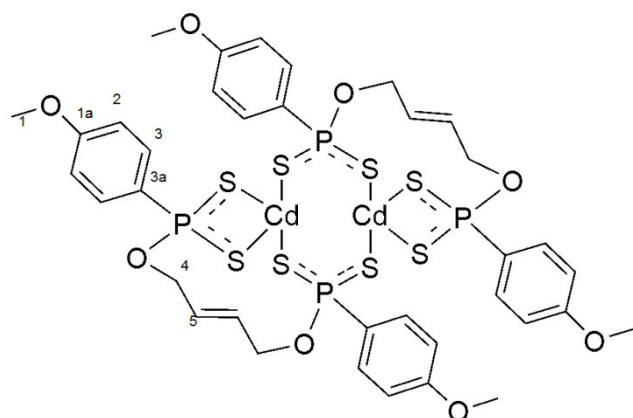
2.6.2 2-Hexanol derived dithiophosphonate Cd(II) complex [2B]



Mass of **2** (1 g, 3.1 mmol), mass of $\text{Cd}(\text{NO}_3)_2 \cdot 4\text{H}_2\text{O}$ (0.48 g, 1.56 mmol). Reaction time: 20 min. Product appearance: White powder, Melting point: 154-156°C. Yield: 0.826 g (74%). ^{31}P NMR (CDCl_3) δ (ppm): 102.50. ^1H -NMR (CDCl_3) δ (ppm): 0.90 (12H, t, $J = 6.86$ Hz,

H-9), 1.33-1.42 (32H, m, H-4/6/7/8), 1.74 (4H, q, $J = 7.28$ Hz, H-6), 3.85 (12H, s, H-1), 4.97 (4H, m, H-5), 6.94 (8H, dd, 8.76, 3.12, H-2), 8.02 (8H, dd, $J = 14.48, 8.64$ Hz, H-3). ^{13}C -NMR (CDCl_3) δ (ppm): 162.40 (C-1a), 132.36(C-2), 129.02(C-3a), 113.64(C-3), 75.56(C-5), 55.41(C-1), 37.41(C-6), 27.42(C-7), 22.65(C-4), 21.78(C-8), 14.04(C-9). Selected IR data ν/cm^{-1} : 1027(P-O-C), 645(P-S_{as}), 529(P-S_s). ESI (+) Mass spec m/z : $[\text{M} + \text{Na}]^+ = 1461.95$.

2.6.3 2-Butene 1, 4-diol derived dithiophosphonate Cd(II) complex [3B]

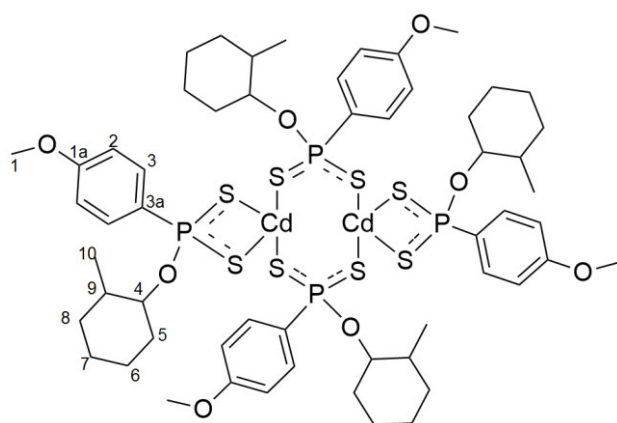


Mass of **3** (1.802 g, 3.42 mmol), mass of Cd(NO₃)₂•4H₂O (2.136 g, 3.42 mmol), Reaction time: 20 min. Product appearance: White powder. Melting point: 104°C (Decomp.). Yield: 1.73 g (84%). ³¹P-NMR (DMSO-*d*₆) δ (ppm): 105.88 ppm. ¹H-NMR (DMSO-*d*₆) δ (ppm): 3.79 (12H, s, H-1), 4.82

(8H, q, J=5.02 Hz, H-4), 5.76 (4H, t, J= 2.59 Hz, H-5), 6.99 (8H, dd, 8.72, 2.76 Hz, H-2), 7.87 (8H, dd, J= 13.96, 8.68 Hz, H-3). ¹³C-NMR (DMSO-*d*₆) δ (ppm): 161.99(C-1a), 132.48(C-3), 131.13(C-5), 129.62(C-3a), 113.16(C-2), 58.14(C-4), 55.31(C-1). Selected IR data ν/cm⁻¹: 1003(P–O–C), 642(P–S_{as}), 544(P–S_s). ESI (+) Mass spec m/z: [M + Na]⁺ = 1228.70.

Colourless single crystals suitable for single crystal X-ray diffraction analysis were obtained from the slow diffusion of hexane into a dichloromethane solution of **3B**.

2.6.4 2-Methyl cyclohexanol derived dithiophosphonate Cd(II) complex [4B]

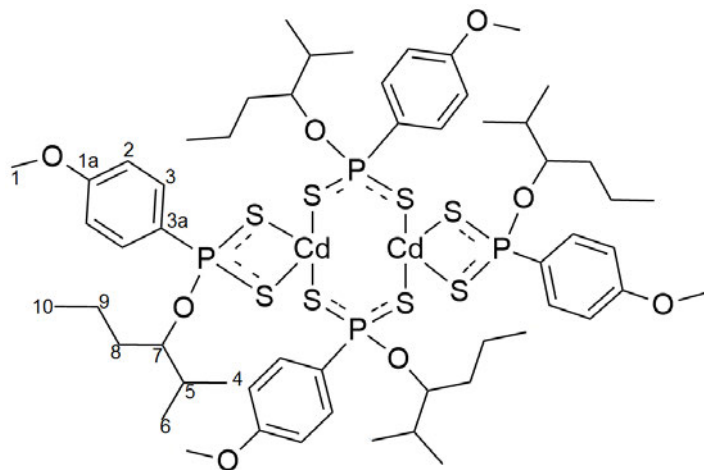


Mass **4** (0.997 g, 3.0 mmol), mass of Cd(NO₃)₂•4H₂O (0.461 g, 1.5 mmol), Reaction time: 20 min, Product appearance: White powder. Melting point: 193°C (decomp.). Yield 0.956 g (86%). ³¹P-NMR (CDCl₃): δ (ppm): 102.21. ¹H-NMR (CDCl₃): 1.02 (12H, dd, J= 14.54, 2.98 Hz, H-10), 1.56 (32H, m,

J=15.81 Hz, H-5/6/7/8), 2.29 (2H, d, J=9.73 Hz, H-9), 2.50 (2H, q, J=4.07 Hz, H-9), 3.85 (12H, s, H-1), 4.48 (2H, q, J=6.08 Hz, H-4), 5.02 (2H, q, J=5.84 Hz, H-4), 6.94 (8H, dd, J= 5.58, 3.06 Hz, H-2), 8.03 (8H, dd, J= 14.36, 8.18 Hz, H-3). ¹³C-NMR CDCl₃: 162.31(C-1a), 132.18(C-3), 129.67(C-3a), 113.67(C-2), 83.07(C-4), 55.41(C-1), 38.64(C-9), 35.68(C-5), 33.85(C-8), 25.18(C-7), 24.74(C-6),

19.49(C-10). Selected IR data ν/cm^{-1} : 1026(P–O–C), 647(P–S_{as}), 536(P–S_s). ESI (+) mass spec m/z : [M + Na]⁺ = 1509.99.

2.6.5 2-Methyl 3 hexanol derived dithiophosphonate Cd(II) complex [5B]

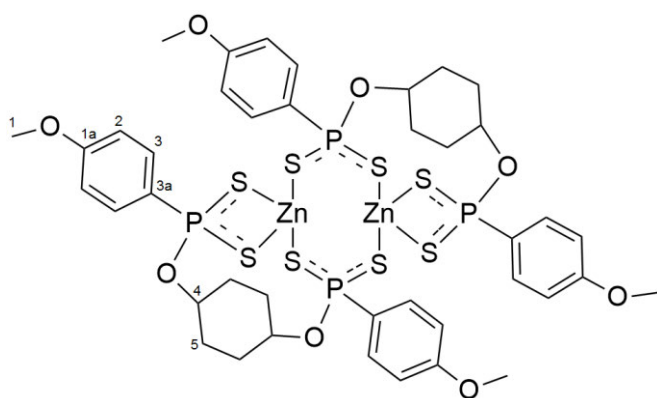


Mass of **5** (0.755 g, 2.25 mmol), mass of Cd(NO₃)₂•4H₂O (0.3470 g, 1.125 mmol), Reaction time: 20 mins, Product appearance: White powder. Melting point: 88-91°C. Yield: 0.5884 g (70%). ³¹P-NMR (CDCl₃) δ (ppm): 100.17. ¹H-NMR (CDCl₃) δ (ppm): 0.99 (36H, m, H-4/ 6/10), 1.50 (8H,

m, H-9), 1.75 (8H, m, H-8), 2.28 (4H, q, J=6.03 Hz, H-5), 3.88 (12H, s, H-1), 4.79 (4H, q, J=6.98 Hz, H-7), 6.99 (8H, dd, J= 8.68, 3.00 Hz, H-2), 7.99 (8H, dd, J= 14.62, 8.62) Hz, H-3). ¹³C-NMR (CDCl₃) δ (ppm): 162.49(C-1a), 131.91(C-3), 130.11(C-3a), 113.71(C-3), 84.09(C-7/), 55.50(C-1), 33.19(C-8), 31.58(C-5), 18.85(C-9), 18.05(C-4/6), 17.81(C-4/6), 14.31(C-10). Selected IR data ν/cm : 1027(P–O–C), 642(P–S_{as}), 540(P–S_s). ESI (+) Mass spec m/z : [M + Na]⁺ = 1517.06

2.7 Zinc complexes(C)

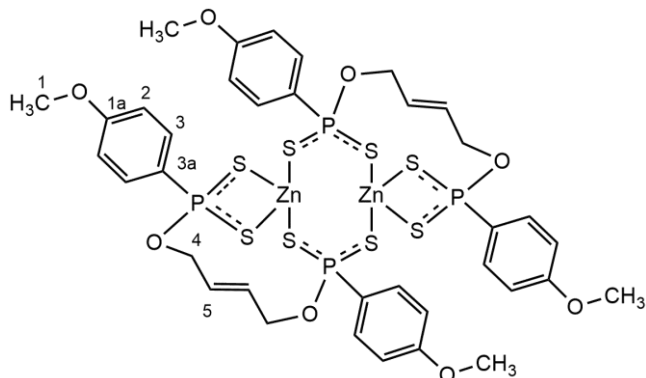
2.7.1 1,4 Cyclohexanediol derived dithiophosphonate Zn(II) complex [1C]



Mass of **1** (0,952 g, 1.72 mmol), mass of $Zn(NO_3)_2 \cdot 6H_2O$ (0.51 g 1.72 mmol), Reaction time: 20 min. Product appearance: White powder. Melting point: 242-245°C. Yield: 0.716 g (71%). ^{31}P -NMR (DMSO- d_6) δ (ppm): 101.70, 101,19, 100.73. 1H -NMR (DMSO- d_6) δ

(ppm): 1.47 (8H, m, H-5), 1.72 (8H, m, H-5), 3.76 (12H, s, H-1), 4.42 (4H, m, H-4), 6.90 (8H, dd, J= 11.78, 3.38 Hz, H-2), 7.87 (8H, dd, J=13.24, 8.16 Hz, H-3). ^{13}C -NMR (DMSO- d_6) δ (ppm): 162.87(C-1a), 133.28(C-3), 128.52(C-3a), 114.12(C-2), 69.40(C-4), 56.28(C-1), 27.03(C-5). Selected IR data ν/cm^{-1} : 1016(P-O-C), 634(P-S_{as}), 534(P-S_s). ESI (+) Mass spec m/z : $[M+ Na]^+ = 1192.75$

2.7.2 2-Butene-1, 4-diol derived dithiophosphonate Zn(II) complex [3C]

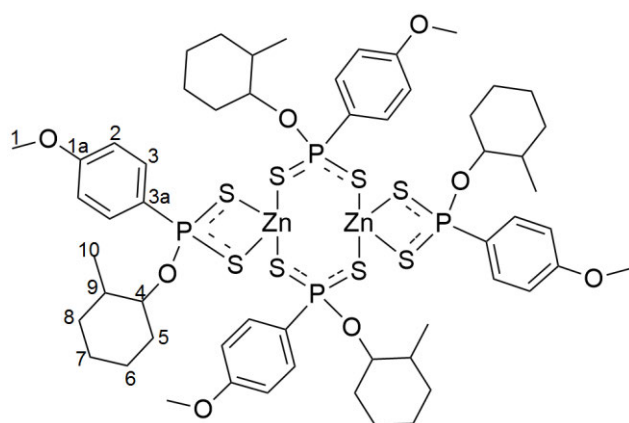


Mass of **3** (1.715 g, 3.3 mmol). Mass of $Zn(NO_3)_2 \cdot 6H_2O$ (0.969 g, 3.3 mmol. Reaction time: 20 min. Product appearance: White powder. Melting point: 200°C (decomp.), yield: 1.537 g (85%). ^{31}P -NMR (DMSO- d_6) δ (ppm): 104.81. 1H -NMR (DMSO- d_6) δ (ppm)

3.75 (1H, s, H-1), 4.18 (8H, m, J=6.27 Hz, H-4), 5.45 (1H, t, J=3.88 Hz, H-5), 6.84 (8H, dd, J= 8.64, 2.2 Hz, H-2), 7.86 (8H, dd, J= 12.96, 8.60 Hz, H-3). ^{13}C -NMR (DMSO- d_6) δ (ppm): 159.89 (C-1a), 132.20(C-3), 131.43(C-5), 128.28(C-3a), 112.06(C-2), 58.49(C-4), 55.02(C-1). Selected IR data ν/cm^{-1} : 1022(P-O-C), 646(P-S_{as}), 522(P-S_s). ESI(+) Mass spec m/z : $M^+ = 1112.80$.

Colourless single crystals suitable for X-ray analysis were obtained from the slow diffusion of hexane into a dichloromethane solution of **3C**.

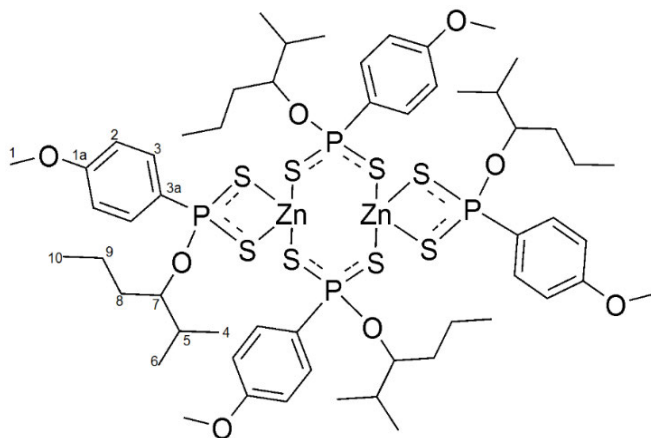
2.7.3 2-Methyl cyclohexanol derived dithiophosphonate Zn(II) complex [4C]



Mass of **4** (1.021 g, 3.0 mmol), mass of $\text{Zn}(\text{NO}_3)_2 \cdot 6\text{H}_2\text{O}$ (0.455 g, 1.5 mmol). Reaction time: 20 min. Product appearance: White powder. Melting point (128-130°C), yield 0.959 g (90%). ^{31}P -NMR ($\text{DMSO}-d_6$) δ (ppm): 101.47. ^1H -NMR (CDCl_3) δ (ppm): 1.05 (1H, dd, $J=7.98$ Hz, H-10), 1.51 (32H, m, H-5/6/7/8),

2.36 (2H, q, $J=4.62$ Hz, H-9), 2.51 (2H, q, $J=5.28$ Hz, H-9), 3.88 (12, s, H-1), 4.47 (2H, m, H-4), 5.03 (2H, d, $J=14.77$ Hz, H-4), 6.99 (8H, dd, $J=8.52, 3.42$ Hz, H-2), 7.98 (8H, dd, $J=14.56, 8.76$ Hz, H-3). ^{13}C -NMR CDCl_3 : 162.46(C-1a), 131.76(C-3), 129.81(C-3a), 113.73(C-2), 79.14(C-4), 55.44(C-1), 38.54(C-9), 35.76(C-5), 33.41(C-8), 25.50(C-7), 24.73(C-6), 19.36(C-10). Selected IR data ν/cm^{-1} : 1024(P-O-C), 642(P-S_{as}), 537(P-S_s). HR-MS m/z : $\text{M}^+ = 1392.14$.

2.7.4 2-Methyl 3 hexanol derived dithiophosphonate Zn(II) complex [5C]



Mass of **5** (0.720 g, 2.15 mmol) mass of $\text{Zn}(\text{NO}_3)_2 \cdot 6\text{H}_2\text{O}$ (0.319g, 1.075 mmol). Reaction time: 20 mins. Product appearance: White powder. Melting point (112-114°C). Yield: 0.586 g (78%). ^{31}P NMR ($\text{DMSO}-d_6$) δ (ppm): 97.00. (^1H -NMR (CDCl_3) δ (ppm): 0.98 (36H, m, H-4/6/10), 1.48 (8H, m, H-9),

1.71 (8H, m, H-8), 2.27 (4H, m, H-5), 3.87 (12H, s, H-1), 4.78 (4H, m, $J=5.11$ Hz, H-7), 6.98 (8H, dd, $J=8.66, 3.02$ Hz, H-2), 7.98 (8H, dd, $J=14.62, 8.42$ Hz, H-3). ^{13}C NMR (CDCl_3) δ (ppm): 162.42(C-1), 131.84(C-2/), 129.78(C-3a), 113.48(C-3), 84.02(C-7), 55.43(C-1), 33.12C-8), 31.51(C-5), 18.78(C-9), 17.98(C-4/6), 17.75(C-4/6), 14.24(C-10). Selected IR data ν/cm^{-1} : 1020(P-O-C), 656(P-S_{as}), 532(P-S_s). ESI (-) m/z : $[\text{M-L} + \text{Na}]^- = 1168.07$.

2.8 In-vitro antimicrobial studies methodology

In-vitro antibacterial activity of the synthesized compounds was tested against 6 bacterial strains namely *Klebsiella pneumoniae* ATCC 314588, *Staphylococcus Aureus* ATCC 25923, Methicillin resistant *Staphylococcus Aureus* ATCC BAA-1683, *Pseudomonas aeruginosa* ATCC 27853, *Salmonella Typhimurium* ATCC 14026 and *Escherichia coli* ATCC 25922 using ciprofloxacin as a standard for comparison. The diffusion method was used for initial screening for antibacterial susceptibility. The bacterial strains were obtained from the Department of Pharmacy at the University of Kwa-Zulu Natal, Westville campus.

10 mg of each synthesised compound was dissolved in 1 mL of DMSO to make a solution of 10 000 ppm. Broth cultures of the test organisms were then standardised using a spectrophotometer. Mueller Hinton agar (MHA) was prepared according to the manufacturer's specification and melted to obtain a homogenous solution. 20 mL each of the MHA was dispensed into McCartney bottles and autoclaved at 121°C for 15 min and allowed to cool to about 45°C. The agar was aseptically poured into a sterile disposable petri dish and allowed to solidify. Thereafter, the plates were incubated for 24 hrs to confirm their sterility. The plates were labelled accordingly and 50 µL of the test compounds were carefully dropped on the agar gel. The plates were then incubated at 35°C for 24 hours after which the diameter of the zones of inhibition were measured using a colourless 30 cm ruler. The most effective compound against each bacterial strain, as shown by the largest zone of inhibition against a particular bacterial strain was chosen to determine the Minimum inhibitory concentration (MIC).

Solutions of the most effective compounds against each strain were diluted using serial dilution to a concentration of 10 ppm. After which the same procedure as outlined above was repeated using the diluted compounds against each bacterial strain and the zones of inhibition noted. The lowest effective concentration was noted as the minimum inhibitory concentration (MIC).

DMSO was used as a control and showed no zones of inhibition to any of the bacterial strains tested against. Solutions of AgNO₃, Cd(NO₃)₂ and Zn(NO₃)₂ were also used and showed some levels of

activity. Ciprofloxacin served as the standard drug for all antimicrobial studies. All experiments were conducted in triplicate.

CHAPTER 3

SYNTHESIS OF NEW DITHIOPHOSPHONATE LIGANDS, SILVER(I), CADMIUM(II) AND ZINC(II) COMPLEXES

Overview

The literature on complexes with bis (monoanionic) dithiophosphonate ligands is still limited and the available reports often lack sufficient structural characterisation. Considering the potential of synthesizing new complexes from simple alcohols and complex diols within the dithiophosphonate motif, this work explores the preparation and characterization of new multinuclear metal complexes.

This study consists of five dithiophosphonate ligands and their Ag(I), Cd(II) and Zn(II) complexes. The synthesized compounds were subsequently tested for antibacterial activity, the results and discussion are presented in Chapter 4. Metal complexation preparations were carried out in open air at room temperature. Complexes of Ag(I) were however, sensitive to UV/light, which necessitated complexation to be done in a dark fume hood to avoid decomposition. However, Ag(I) complexes were stable to light as powders. Generally, metal complexes were isolated in good yields, which could be due to the short reaction time and rapid isolation by filtration. The ionic nature of the ammonium salt by-products (NH_4NO_3) also makes isolation and purification easier as they were easily filtered off in the aqueous media.

The synthesized compounds were stable enough to be stored indefinitely under nitrogen, although prolonged exposure to air does eventually lead to decomposition with the release of the distinct smell of H_2S .^{26,22} The ammonium salts slowly hydrolyse in air and can be safely stored in a vacuum desiccator.⁶² The reaction can be scaled-up but special preparative precautions are necessary due to large amounts of H_2S gas that are evolved during synthesis.

3.1.1 Characterisation of dithiophosphonate compounds

3.1.1.1.1 Nuclear magnetic resonance (NMR) multinuclear spectroscopic analyses

Structural elucidation of synthesized complexes was done using solution multinuclear NMR spectroscopy (^1H , ^{31}P and ^{13}C) in $\text{DMSO-}d_6$, CDCl_3 and MeOD and in one instance 2D- NMR. ^{31}P NMR spectra were used to indicate the synthesis of dithiophosphonates.⁵ Obtained ^{31}P -NMR spectra showed singlets within the expected range of 90-110 ppm which agrees with reported literature.^{63,13}

The ^1H NMR of compounds **1-5C** was well resolved and integrated to the number of the corresponding hydrogen atoms. ^1H -NMR spectra of the compounds displayed expected chemical shift values with the predicted splitting pattern²⁶ The ^1H -NMR spectra of all synthesized compounds showed two doublet of doublets at *ca.* 8.00 ppm and *ca.* 6.90 ppm which were assigned to the *ortho* and *meta* protons on the anisyl moiety respectively,⁵⁹ as well as a singlet *ca.* 3.8 ppm due to the methoxy protons (relative to the P atom).

^{13}C -NMR spectra of the compounds showed four common resonances at approximately 162 ppm, 133 ppm, 114 ppm and 55.6 ppm due to the *para*, *ortho*, *meta* and methoxy carbon atoms respectively (relative to the P atom).

3.1.1.1.2 Fourier-Transform Infrared spectroscopic analysis

The FT-IR spectra of the dithiophosphonate ligands showed a broad strong band in the region 3102-3158 cm^{-1} which was assigned to the $\nu(\text{N}-\text{H})$ stretching vibration of the ammonium ion.¹⁷ A comparison of the FT-IR spectra between the synthesized ligands and their metals complexes are discussed in subsequent sections. Selected bands at 1020-1030 cm^{-1} , 540-570 cm^{-1} and 650-680 cm^{-1} were assigned to $\nu(\text{P}-\text{O}-\text{C})$, $\nu_{as}(\text{P}-\text{S})$ and $\nu_s(\text{P}-\text{S})$ vibrations, respectively.^{8,45,64}

3.1.1.1.3 Mass spectrometry

ESI (-) was mostly used for ligands while ESI(+) was mostly used to characterise the metal complexes.

3.1.1.1.4 Single crystal X-ray diffraction

Fourteen new dithiophosphonate complexes were prepared. Crystals of Cd(II) and Zn(II) bis(dithiophosphonate) complexes (**5B** and **5C** respectively) suitable for X-ray analysis were grown and their molecular structures obtained.

3.1.1.2 1, 4-Cyclohexane diol derived compounds

3.1.1.2.1 1, 4-Cyclohexane diol derived ligand

The ligand was synthesized from the reaction between Lawesson's Reagent with 1, 4 cyclohexanediol. The compounds were characterized using FT-IR, ¹H-NMR, ¹³C-NMR, ³¹P-NMR and mass spectroscopy. The proton NMR of the ligand were well resolved and integrated to the number of the corresponding hydrogen atoms.

FT-IR analysis of compound **1** indicated the presence of $\nu(\text{P-O-C})$, $\nu_s(\text{P-S})$ and $\nu_{as}(\text{P-S})$ vibrations associated with dithiophosphonate, as well as the $\nu(\text{N-H})$ stretching associated with the ammonium ion. Vibrations at 3176 cm^{-1} , 1012 cm^{-1} and 649 cm^{-1} and 544 cm^{-1} were assigned to the $\nu(\text{N-H})$, $\nu(\text{P-O-C})$, $\nu_{as}(\text{P-S})$ and $\nu_s(\text{P-S})$ respectively as shown in **Figure 3-1**.

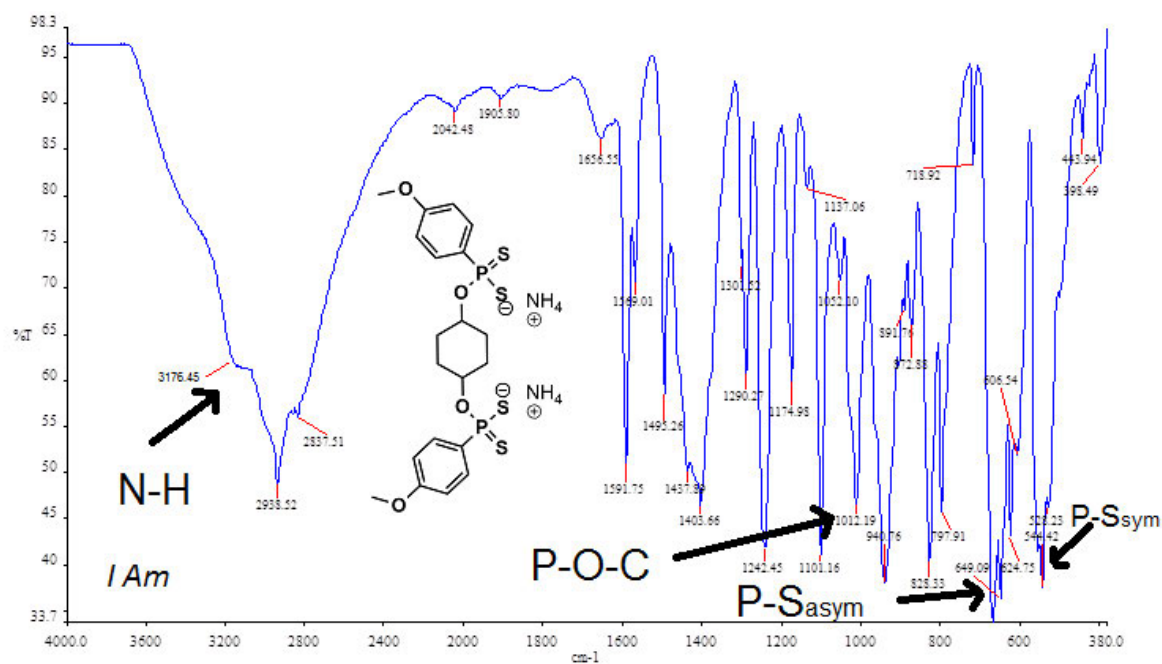


Figure 3-1: FT-IR spectrum for compound **1**

The ^{31}P -NMR of the ligand indicated the presence of a phosphorous centre in the expected range of the dithiophosphonate group. The spectrum obtained showed a singlet at 104.93 ppm as shown in **Figure 3-2**.

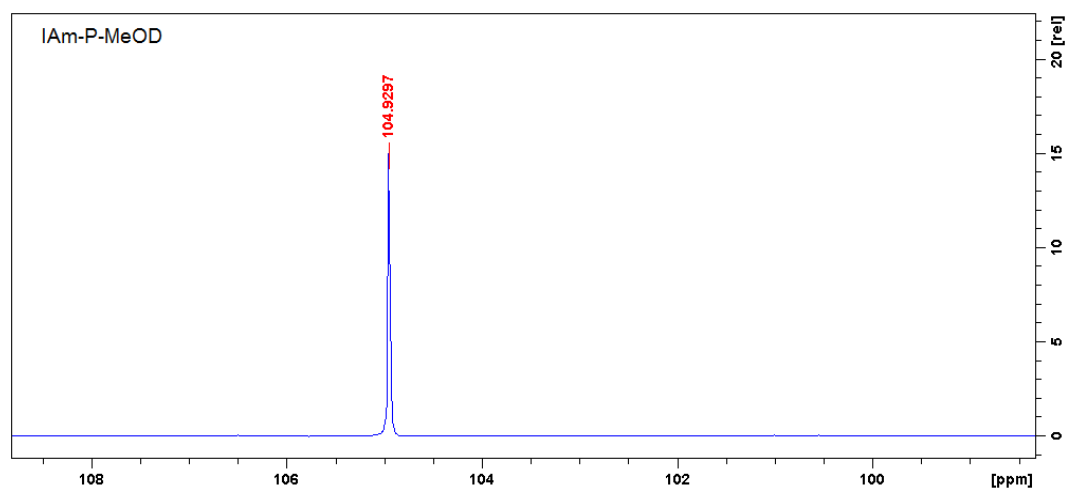


Figure 3-2: ^{31}P -NMR spectrum for compound **1**

1 was also analysed with ^1H -NMR and ^{13}C -NMR. **Figure 3-3** shows the ^1H -NMR spectrum of **1** and the assignment of the peaks done using their chemical shifts and their splitting pattern.

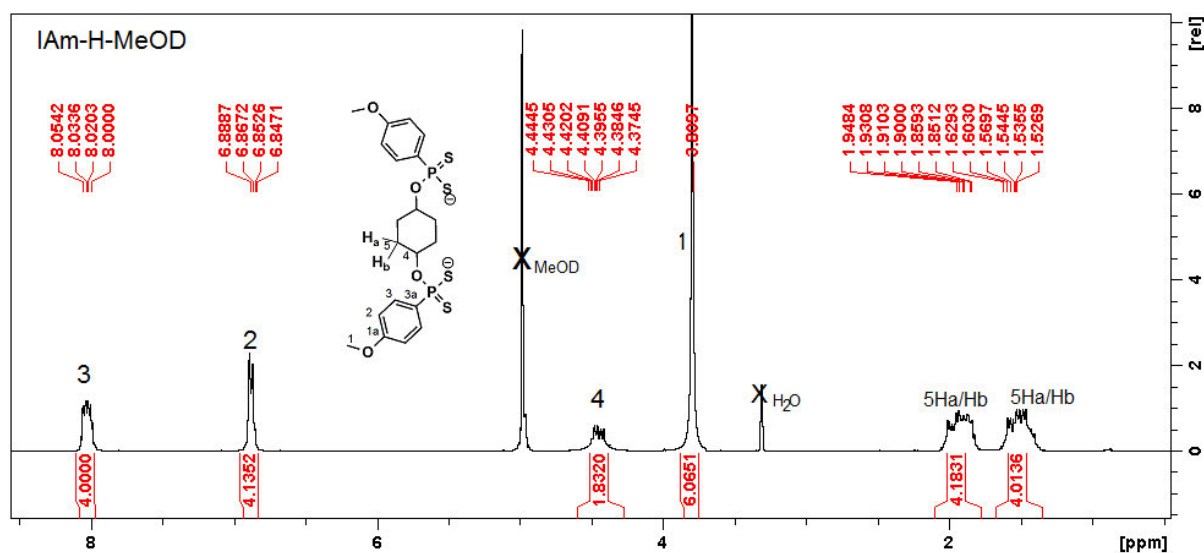


Figure 3-3: ¹H-NMR spectrum for compound **1**

The multiplet on 4.42 ppm was assigned to H-4 due to the downfield chemical shift value as it was deshielded by an oxygen atom on the POS₂⁻ moiety. The peaks 1.85-1.95 ppm and 1.52-1.62 ppm were assigned to the axial and equatorial protons on C-5. The ¹³C-NMR spectrum of **1** as shown in **Figure 3-4** showed seven signals. The resonance at 68.90 ppm was assigned to C-4 while 26.53 ppm was assigned to C-5.

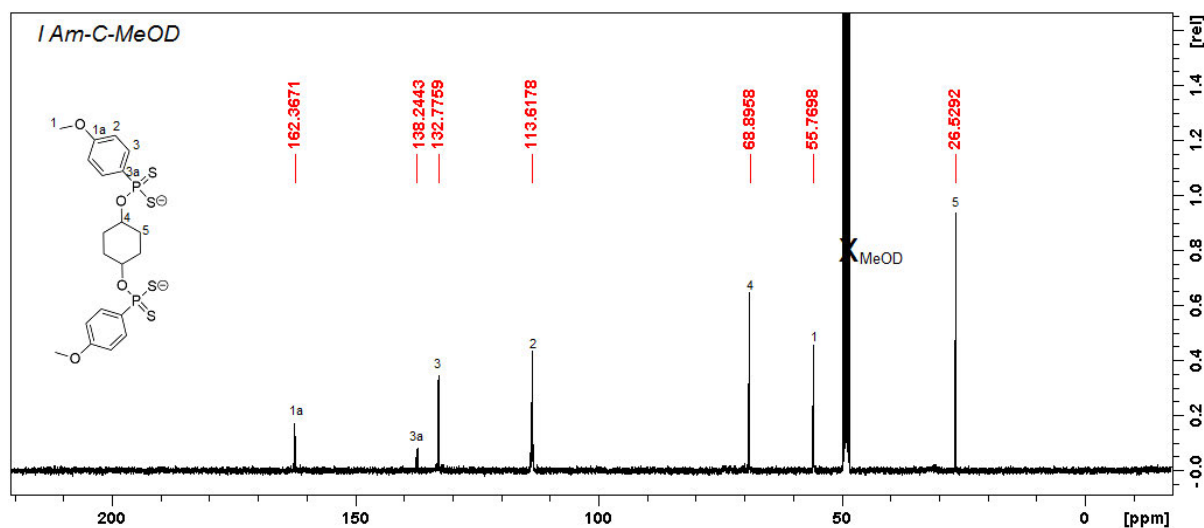


Figure 3-4: ¹³C-NMR spectrum of compound **1**

1 was further analysed with ESI (-) mass spectrometry, a fragment ion peak was observed as $[M+Na]^- = 540.97$ m/z which confirmed the molecular formula of the ligand as $C_{20}H_{24}O_4P_2S_4^{2-}$.

3.1.1.2.2 Silver(I), cadmium(II) and zinc(II) complexes

Complex **1A** was isolated as a yellow free flowing powder, while **1B** and **1C** were obtained as white free flowing powders. The complexes were characterized in a similar way as outlined for **1**. The FT-IR spectra of **1A**, **1B** and **1C** showed the disappearance of the (N-H) band at 3176 cm^{-1} indicating metal complexation, other bands corresponding to $\nu(\text{P-O-C})$ and $\nu_{as}(\text{P-S})$ and $\nu_s(\text{P-S})$ vibrations were also observed. $\nu(\text{P-O-C})$ - 1021 cm^{-1} , $\nu_{as}(\text{P-S})$ - 653 cm^{-1} , $\nu_s(\text{P-S})$ - 518 cm^{-1} for **1A**; $\nu(\text{P-O-C})$ - 1021 cm^{-1} , $\nu_{as}(\text{P-S})$ - 635 cm^{-1} , $\nu(\text{P-S})$ - 534 cm^{-1} for **1B**; $\nu(\text{P-O-C})$ - 1016 , $\nu_{as}(\text{P-S})$ - 634 , $\nu(\text{P-S})$ - 534 cm^{-1} for **1C** indicating the formation of DTP complexes.

The complexes were analysed by ^{31}P -NMR, ^1H -NMR and ^{13}C -NMR. Single peaks at 104.10 ppm, 102.59 ppm and 101.70 ppm were observed for **1A**, **1B** and **1C** respectively using ^{31}P -NMR. ^1H -NMR spectra of **1A**, **1B** and **1C** showed signals with similar splitting and chemical shifts to **1**. Characteristic signals included doublets of doublet associated with the anisyl protons at approximately 7.9 ppm and 6.9 ppm as well as a singlet *ca.* 3.8 ppm. A multiplet due to the most deshielded proton H-4 was observed at 4.72-4.76 ppm, 4.39-4.45 ppm and 4.39-4.49 ppm for **1A**, **2A** and **1C** respectively. The methylene protons (H-5) were observed as two separate multiplets in all complexes *ca.* 1.70-1.76 ppm and *ca.* 1.40-1.5 ppm. The ^{13}C -NMR spectra chemical shifts of the 1, 4-cyclohexanediol derived compounds are shown in **Table 3-1**. They show similar chemical shift values for most of the carbon atoms. Significant difference was observed on the *ipso*-carbon (C-3a), **1** had a value of 138.42 ppm while **1A**, **1B** and **1C** had relatively upfield chemical shifts of 128.47 ppm, 128.85 ppm and 128.52 ppm respectively compared to **1**, consistent with the reported chemical shifts of ligands and complexes.⁴¹

Compounds **1A**, **1B** and **1C** were also analysed using ESI (-) and ESI (+) mass spectrometry. A fragment ion peak for **1A** was observed as $[M-Ag]^- = 626.91$, **1B** as $[M + Na]^+ = 1285.73$ and **1C** as $[M+ Na]^+ = 1192.75$. The ESI (-) mass spectrum shown in **Figure 3-5** shows some notable fragments of **1B**.

Table 3-1: ^{13}C -NMR chemical shifts for 1, 4 cyclohexanediol derived compounds

Carbon atoms and their chemical shifts (ppm)							
	C-1	C-1a	C-2	C-3	C-3a	C-4	C-5
1	55.77	162.37	132.78	113.62	138.42	68.90	26.53
1A	56.31	162.90	133.44	114.15	128.47	69.43	27.06
1B	55.36	161.94	132.47	113.19	128.85	68.47	26.10
1C	56.27	162.87	133.28	114.12	128.52	69.40	27.03

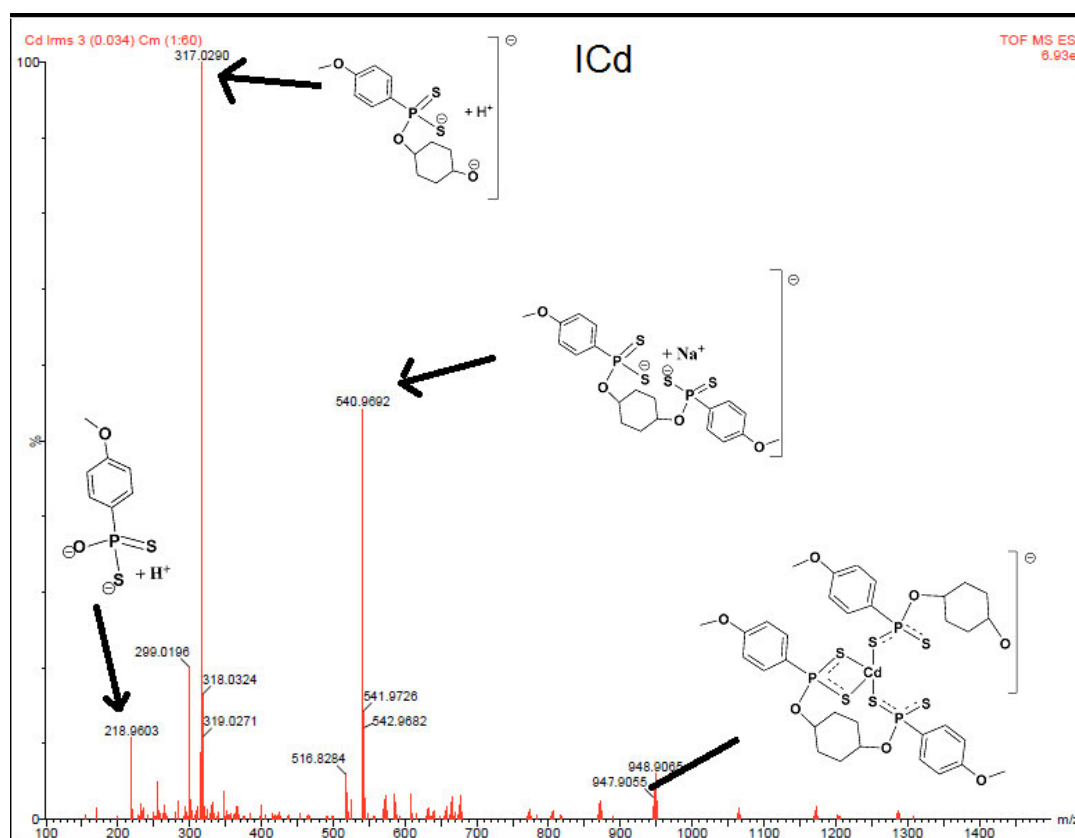


Figure 3-5: ESI (-) mass spectrum showing fragments of **1B**

The fragment ion at 947.9 shows that **1B** lost a cadmium ion and the anisyl part of the ligand. The mass spectra also shows a fragment ion at 540.97 assigned to the ligand. **1A** and **1C** also follow a similar fragmentation pattern and are shown in the supporting information.

3.1.1.3 2-hexanol derived compounds

3.1.1.3.1 2-hexanol derived ligand (2)

The ligand was synthesized using LR and 2-hexanol and complexed with silver and cadmium salts.

The ligand was analysed with FT-IR spectroscopy which indicated the presence of $\nu(\text{P-O-C})$, $\nu(\text{P-S})$ as well as the $\nu(\text{N-H})$ bands. **Figure 3-6** shows the FT-IR spectrum of compound **2**. The $\nu(\text{N-H})$, $\nu(\text{P-O-C})$, $\nu_{as}(\text{P-S})$ and $\nu_s(\text{P-S})$ stretchings were observed at 3174 cm^{-1} , 1011 cm^{-1} , 649 cm^{-1} and 556 cm^{-1} respectively as shown in the annotated spectrum

The $^{31}\text{P-NMR}$ spectrum showed a single peak at 104.27 ppm indicating the presence of the desired dithiophosphonate species as shown in **Figure 3-7** while **Figure 3-8** shows the $^1\text{H-NMR}$ spectrum for compound **2**. Of the remaining signals, the signal at 4.58 ppm (H-5) was assigned to the most deshielded proton on the methine C-5 attached to the oxygen atom. H-6, H-7 and H-8 were assigned based on peak integration as well as the chemical shift values which are typical of methylene protons, while the doublet at *ca.* 1.21 ppm was assigned to H-4. The triplet at 0.89 ppm was assigned to H-9 which was the least deshielded and integrated for three protons.

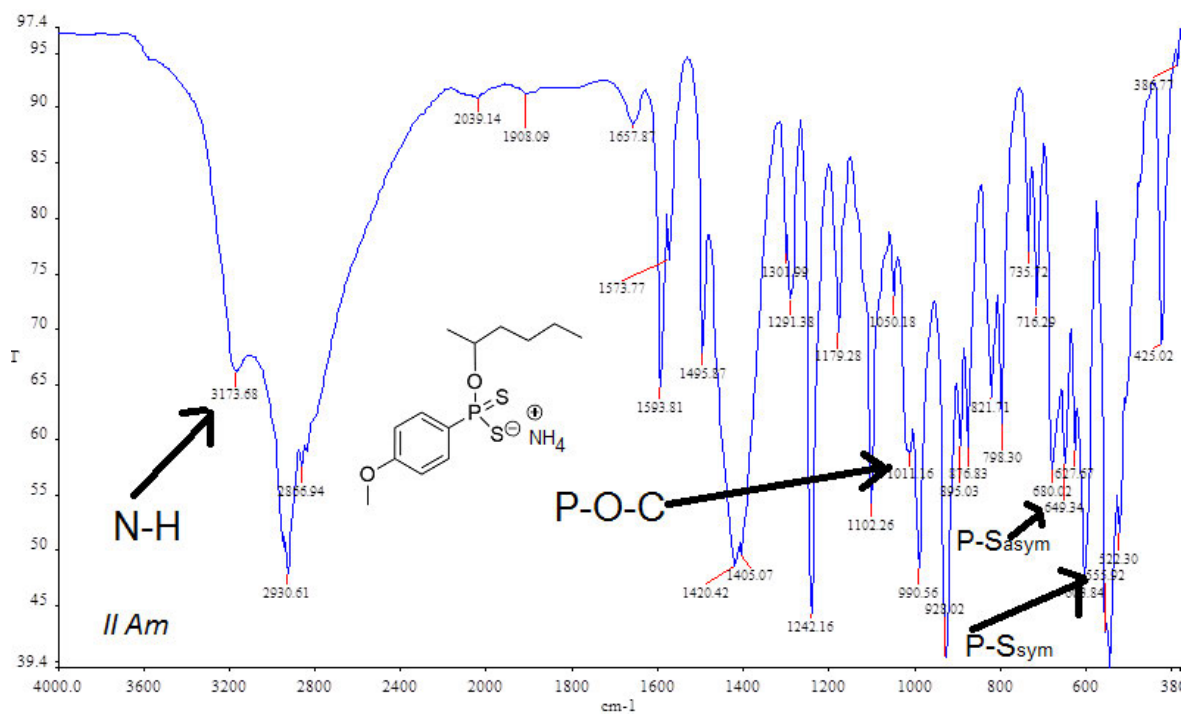


Figure 3-6: FT-IR spectrum for compound 2

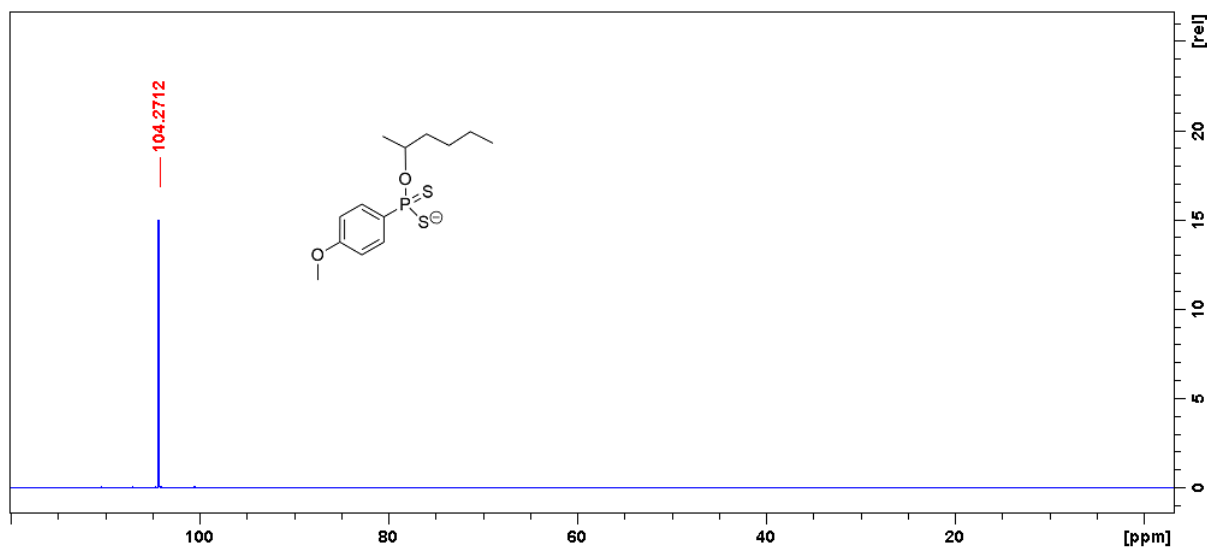


Figure 3-7: ^{31}P -NMR spectrum for compound 2

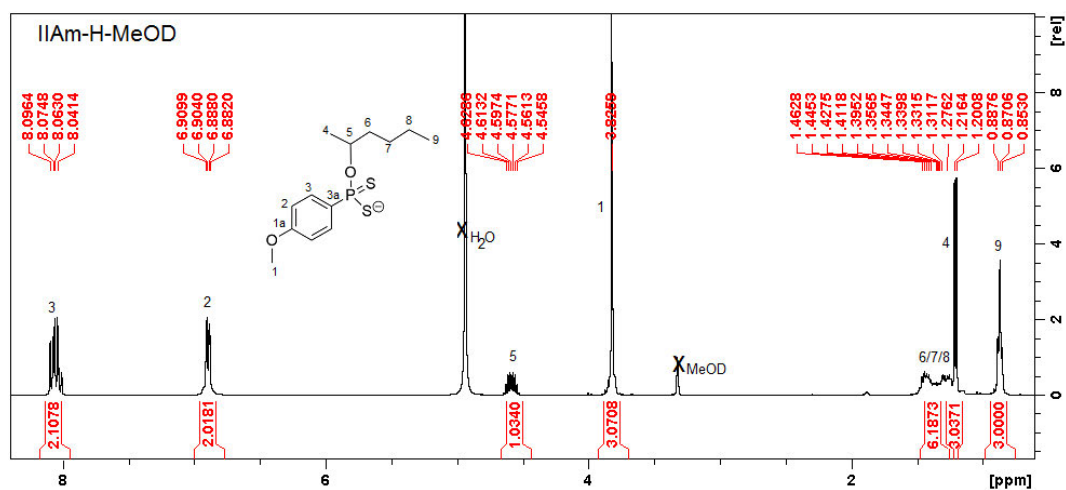


Figure 3-8: ^1H -NMR spectrum for compound 2

Eleven signals were observed with ^{13}C -NMR and assigned using their chemical shifts. The peak at 73.56 ppm was assigned to C-5, followed by the peak at 38.77 ppm which was assigned to C-6 while 28.62 ppm was assigned to C-7, the peaks at 23.78 ppm, 22.16 ppm and 14.45 ppm were assigned to C-4, C-8 and C-9 respectively as shown by **Figure 3-9**. The assignments were verified using HSQC-NMR (shown in the supporting information) which confirmed the correlations between the assigned carbons and protons.

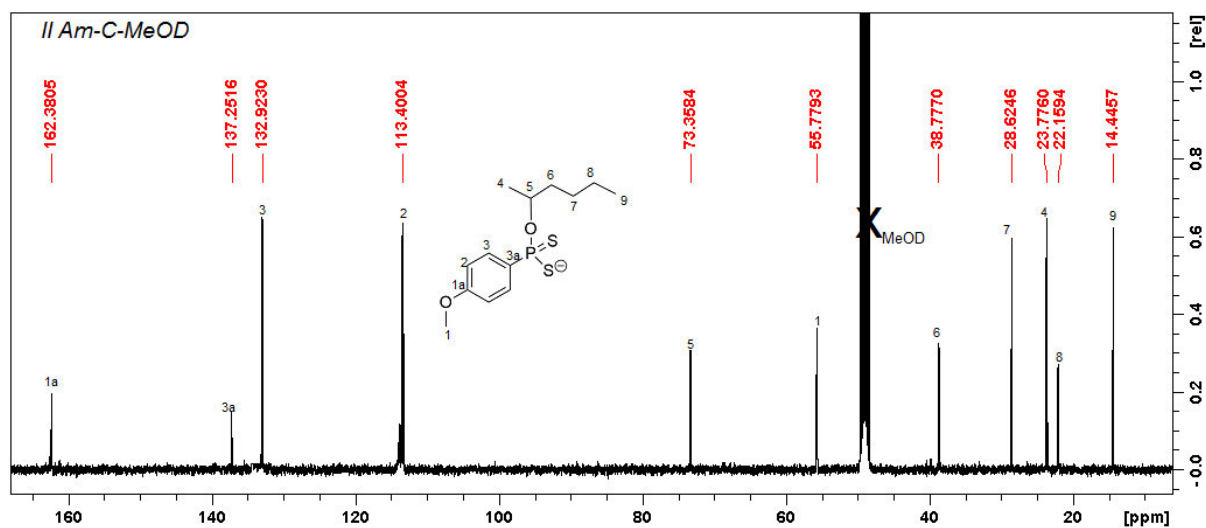


Figure 3-9: ^{13}C -NMR spectrum for compound 2

A base peak $[M]^- = 303.07$ was observed on the ESI (-) mass spectrum corresponding to the desired ligand with the molecular formula $C_{13}H_{20}O_2PS_2^-$.

3.1.1.3.2 Silver(I) and cadmium(II) complexes

Compounds **2A** and **2B** were synthesized by a complexation reaction of a 2-hexanol derived ligand and silver(I) and cadmium(II) metal salts producing a yellow powder and a white powder respectively. The zinc derivative was attempted, but a powder could not be obtained as the complex remained as a sticky white paste which could not be characterised effectively by the methods employed in this work. As a result it was omitted.

The two complexes were analysed using FT-IR spectroscopy. The $\nu(P-O-C)$ band was at 1023 cm^{-1} and 1027 cm^{-1} for **2A** and **2B** respectively. The $\nu_s(P-S)$ vibrations were at 531 cm^{-1} and 529 cm^{-1} for **2A** and **2B** respectively while the $\nu_{as}(P-S)$ vibrations were at 651 cm^{-1} for **2A** and 645 cm^{-1} for **2B**. A comparison of the FT-IR spectrum of **2** and the spectra of **2A** and **2B** show the notable absence of the $\nu(N-H)$ band *ca.* 3173 cm^{-1} , however, as mentioned above bands of $\nu(P-O-C)$, $\nu_{as}(P-S)$ and $\nu_s(P-S)$ were observed which indicates the presence of a POS_2^- moiety.

The ^{31}P -NMR spectra showed singlets for **2A** and **2B** at 104.06 ppm and 102.50 ppm respectively. Comparison of the 1H -NMR spectra of **2A** and **2B** showed similar resonances to **2**. The resonances indicated the formation of **2A** and **2B** from **2**. ^{13}C -NMR spectra of **2A** and **2B** compared to **2** showed a difference of approximately 8 ppm on the *ipso*- carbon (C-3a). **2** had a chemical shift of 137.2 ppm while the **2A** and **2B** had chemical shifts of 128.5 ppm and 129.0 ppm respectively as shown by **Table 3-2**.

Table 3-2: ^{13}C -NMR chemical shifts for 2-hexanol derived compounds

Carbon atoms and their chemical shifts (ppm)											
	C-1	C-1a	C-2	C-3	C-3a	C-4	C-5	C-6	C-7	C-8	C-9
2	55.7	162.3	132.9	113.4	137.2	23.7	73.3	38.78	28.6	22.1	14.4
	8	8	2	0	5	7	6		2	5	5
2A	55.5	162.9	132.9	113.4	128.5	22.6	72.6	37.346	27.3	21.7	14.0
	1	4	5	8	7	3	7	8	1	1	5
2B	55.4	162.4	132.3	113.6	129.0	22.6	75.5	37.41	27.4	21.7	14.0
	1	0	6	4	1	5	3		2	8	3

Fragment ion peaks were observed corresponding to $[\text{M}-\text{Ag}]^- = 713.02 \text{ m/z}$ for **2A** and $[\text{M}+\text{Na}]^+ = 1461.95 \text{ m/z}$ for **2B** by the use of ESI (-) and ESI (+) mass spectrometry respectively. The fragments of **2B** are shown in **Figure 3-10**. **2A** also had a similar fragmentation pattern as shown in the supporting information, both complexes had base peaks at 303.06 m/z for the ligand fragment. **2A** showed the loss of a metal cation while of **2B** showed the loss of a metal ion and one ligand as shown in **Figure 3-10**

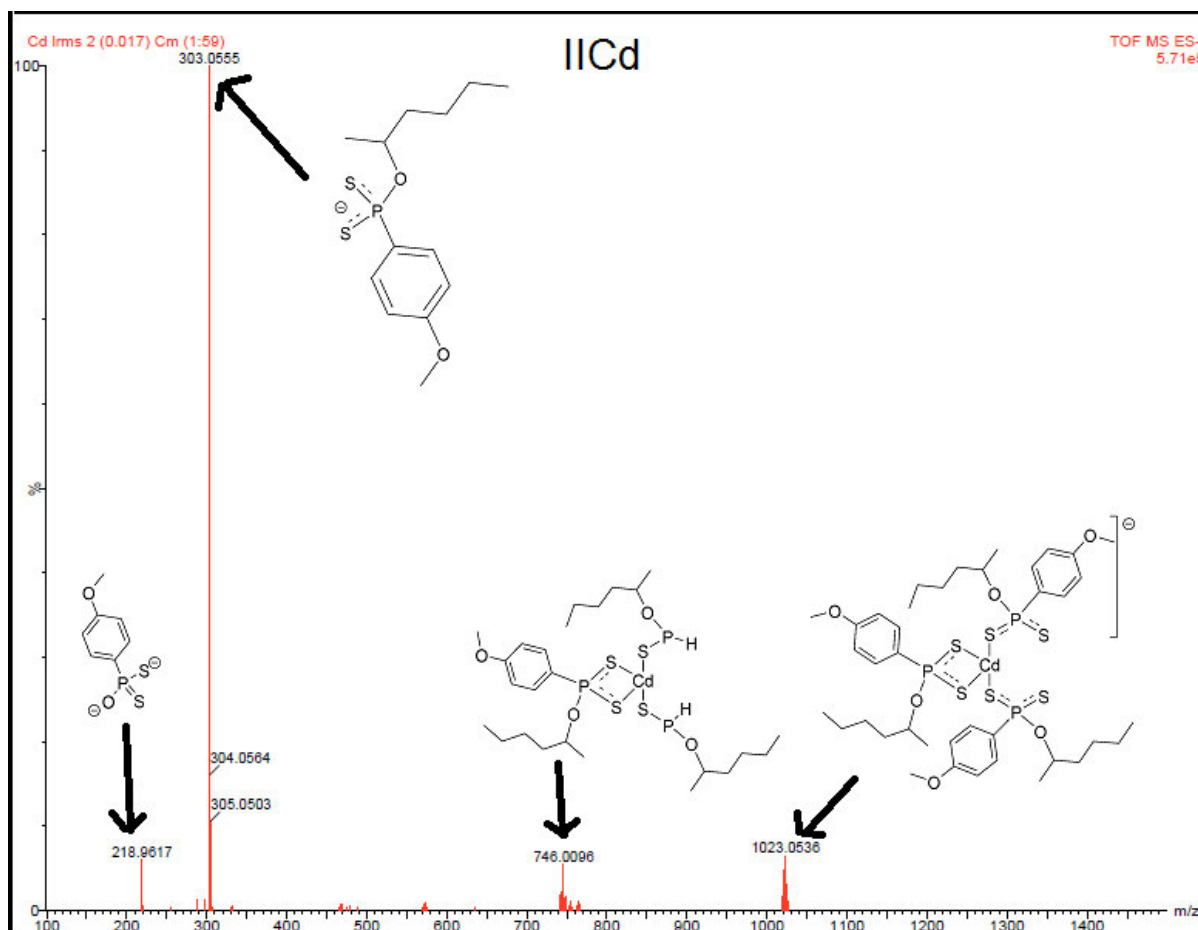


Figure 3-10: ESI (-) mass spectrum showing fragments of **2B**.

3.1.1.4 2-Butene 1, 4 diol derived compounds

3.1.1.4.1 2-Butene 1, 4 diol derived ligand (2)

A 2-butene 1, 4 derived ligand salt was synthesised after Lawesson's Reagent was reacted with 2-butene 1, 4 diol. The synthesized ligand was complexed with silver, zinc and cadmium metal salts.

FT-IR analysis showed $\nu(\text{N-H})$, $\nu(\text{P-O-C})$, $\nu_s(\text{P-S})$ and $\nu_{as}(\text{P-S})$ bands at expected vibrations of 3189 cm^{-1} , 1023 cm^{-1} , 650 cm^{-1} and 555 cm^{-1} respectively. This indicated the presence of an ammonium compound with a dithiophosphonate moiety. The obtained FT-IR spectrum is shown in **Figure 3-11**.

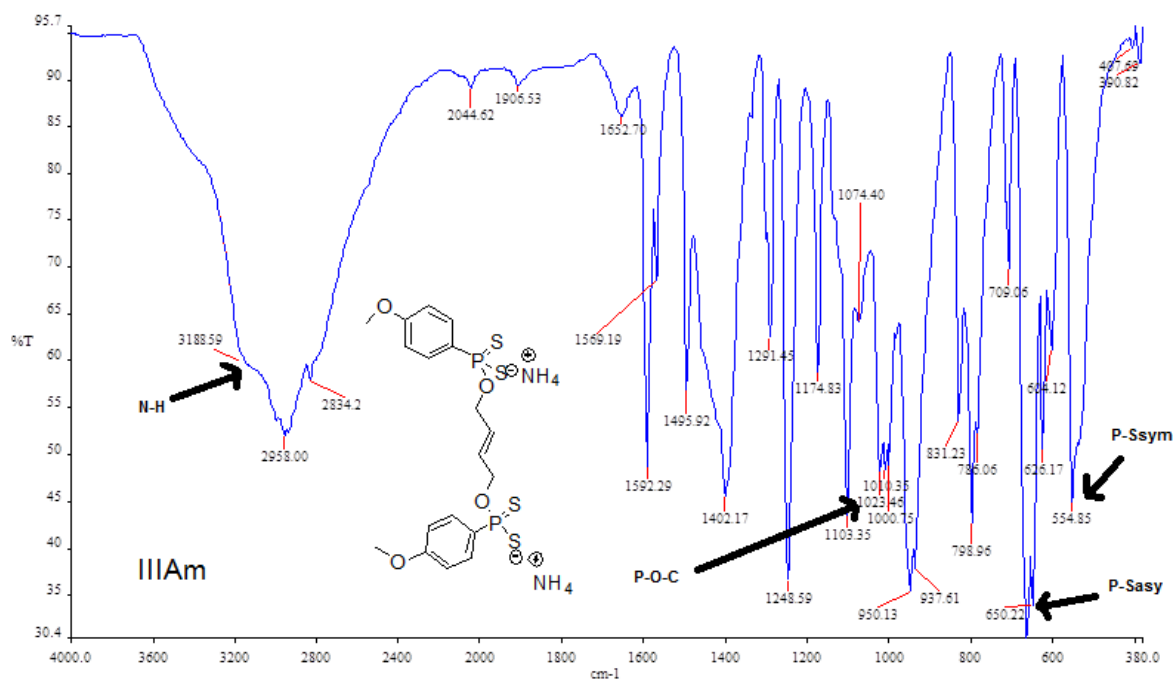


Figure 3-11: FT-IR spectrum for compound **3**

³¹P-NMR indicated the presence of the dithiophosphonate group shown by a singlet at 107.74 ppm in **Figure 3-12**. Analyses with ¹H-NMR and ¹³C-NMR were conducted to predict the structure of **3**. The ¹H-NMR spectrum for **3** is shown in **Figure 3-13**. The methine protons (H-5) from the parent alcohol were observed downfield at 5.66 ppm as a triplet owing to the deshielding effect of the *pi* bond on the protons. The methylene protons (H-4) were found upfield as a doublet of doublets.

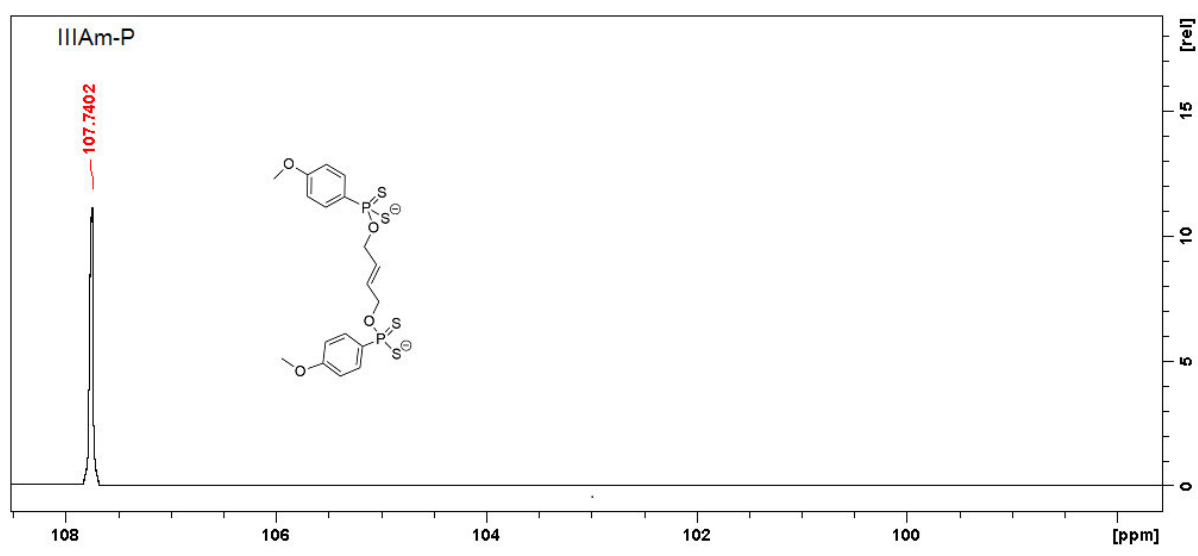


Figure 3-12: ³¹P-NMR spectrum for compound **3**

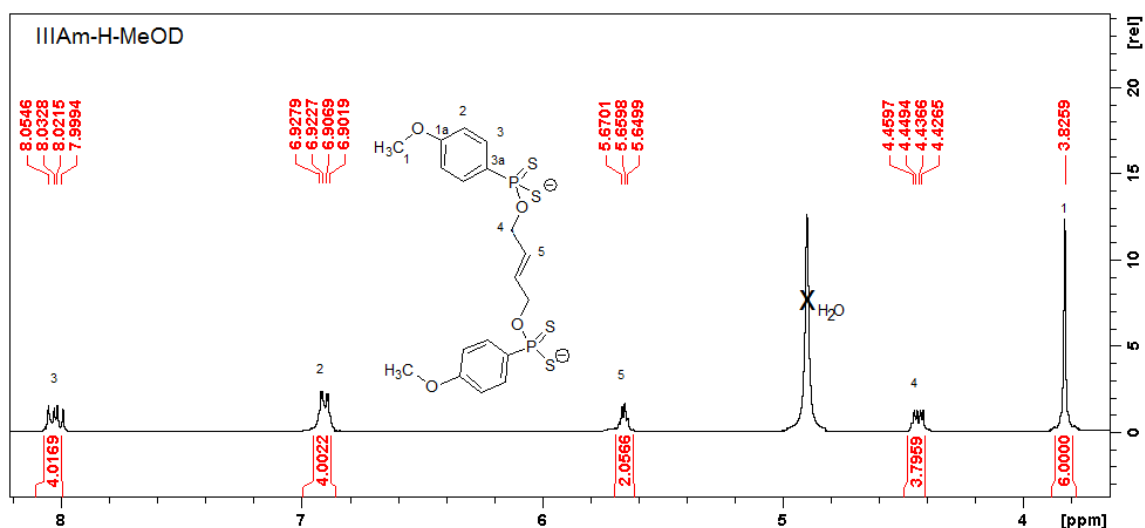


Figure 3-13: $^1\text{H-NMR}$ spectrum for compound **3**

The $^{13}\text{C-NMR}$ spectrum obtained for compound **3** shown in **Figure 3-14** had seven resonances consistent with the expected resonances. The two remaining resonances were assigned using the differences in their chemical shifts. The resonance at 130.23 ppm was assigned to C-5 which was downfield due to the deshielding effect of the π electron system in the $\text{C}=\text{C}$ double bond. The remaining resonance at 61.1 ppm was assigned to the methylene carbon (C-4)

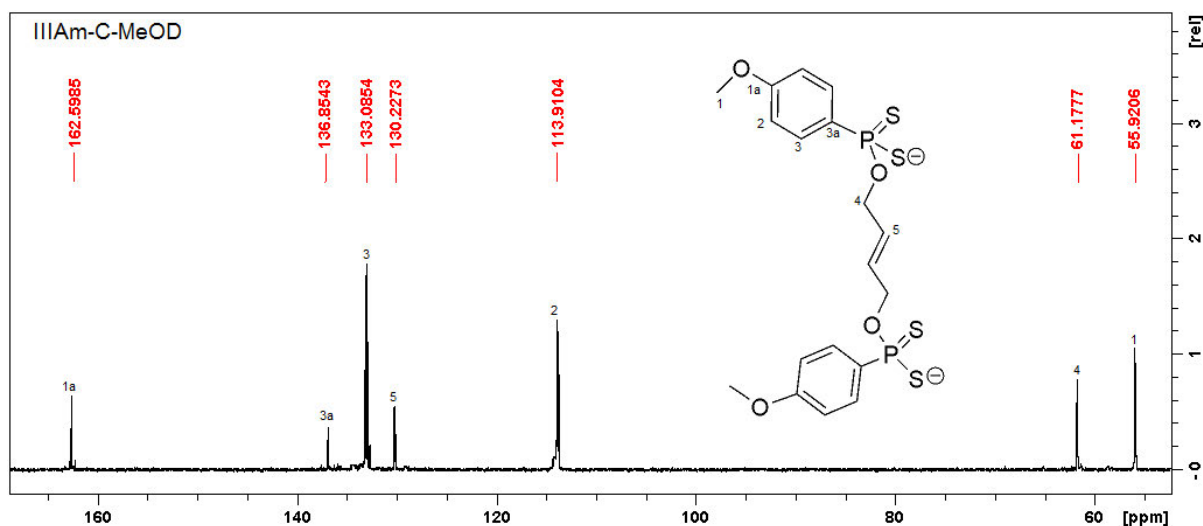


Figure 3-14: $^{13}\text{C-NMR}$ for compound **3**

The final analysis using ESI (-) mass spectrometry showed a base peak $[\text{M} + \text{Na}]^- = 512.93 \text{ m/z}$ thereby confirming the synthesis of the desired ligand with a molecular structure of $\text{C}_{18}\text{H}_{20}\text{O}_4\text{P}_2\text{S}_4^{2-}$.

3.1.1.4.2 Silver(II), cadmium(II) and silver(I) complexes

Cadmium, silver and zinc complexes were synthesized by the reaction of their respective metal nitrates with ligand **3**. White precipitates were obtained for the cadmium and zinc complexes and a yellow powder was obtained for the silver complex.

FT-IR analysis indicated the presence of the $\nu(\text{P-S})$ and $\nu(\text{P-O-C})$ bands and the absence of the $\nu(\text{N-H})$ vibrations and the formation of the desired complex from the ligand. The FT-IR spectra of the compounds are shown in the supporting information showing the disappearance of the $\nu(\text{N-H})$ peak at 3189 cm^{-1} .

Solution multinuclear NMR analyses were used to analyse **3A**, **3B** and **3C**. The ^{31}P -NMR analyses showed resonances due to the dithiophosphonate moiety at 106.77 ppm, 105.88 ppm and 104.81 ppm for **3A**, **3B** and **3C** respectively. The ^1H -NMR spectra of the complexes were similar to the ligand with regards to the signal splitting and chemical shifts as shown in the ^1H -NMR spectra of **3A**, **3B** and **3C**. The chemical shifts of the compounds were similar in most of the carbon atoms with the notable exception of C-3a which showed a significant difference of about 8 ppm between **3** and its derivatives. The resonance due to the *ipso* carbon (3a) on **3** was downfield compared to its derivatives **3A**, **3B** and **3C** as shown by the peaks at 136.85 ppm, 128.28 ppm, 129.62 ppm and 128.28 ppm for **3**, **3A**, **3B** and **3C** respectively.

Table 3-3 : ^{13}C NMR chemical shifts for 2-butene -1, 4 diol derived compounds

Carbon atom number and chemical shifts (ppm)							
	C-1	C-1a	C-2	C-3	C-3a	C-4	C-5
3	55.92	162.60	113.91	133.08	136.85	61.17	130.08
3A	55.42	159.74	112.20	132.01	128.28	58.43	131.26
3B	55.13	161.99	113.15	132.48	129.62	58.14	131.14
3C	55.02	159.89	112.06	132.20	128.28	58.48	131.43

Mass spectrometry analysis showed a base peak of $[M-Ag]^- = 598.87$ for **3A**. ESI (+) used for **3B** showed a peak for $[M+Na]^+ = 1228.70$ m/z, while HR-MS showed a peak for $M^+ = 1112.80$ m/z for **3C**. **Figure 3-15** shows the ESI (-) mass spectrum of **3B** and the fragments for the observed peaks. The spectrum shows a fragment ion peak at 891.85 m/z when **3B** lost a metal ion and $An-PS_2^-$ ($An=Anisyl$), another notable peak is the base peak at 512.94 m/z due to $[L+Na]^-$ ($L=Ligand$). **3A** and **3C** also showed similar fragments as shown in the supporting information.

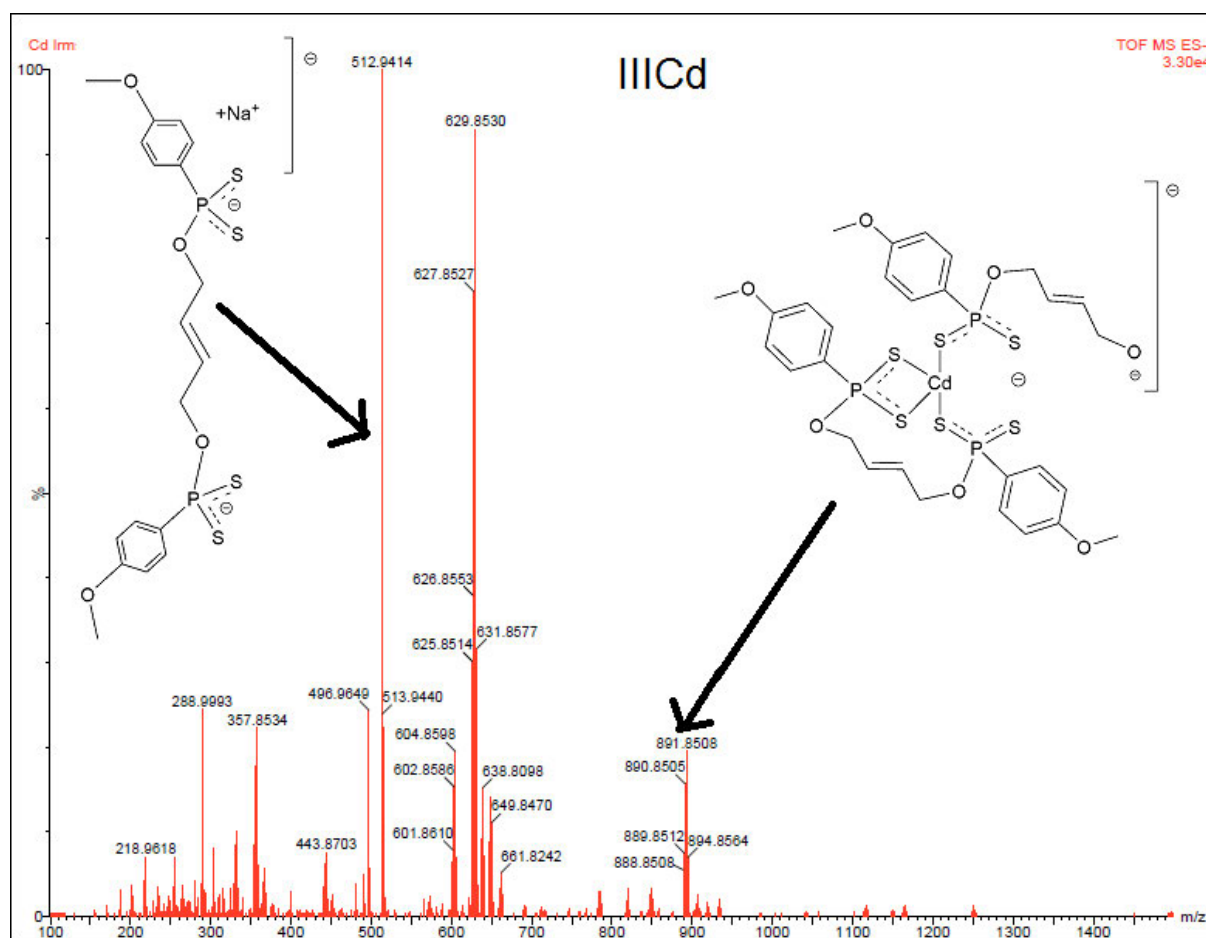


Figure 3-15 : ESI (-) mass spectrum showing fragments of **3B**

Colourless single crystals of compounds **3C** and **3B** suitable for SC-XRD were successfully grown in DCM/Hexane using the vapour diffusion technique. The crystal data and structure refinement for compounds **3B** and **3C** are shown in the supporting information. Both compounds had a distorted tetrahedral geometry around their metal centres. For complex **3B**, the S(3)-Cd(1) and S(4)-Cd(1) bond lengths were 2.6053(5) Å and 2.5367(5) Å, respectively, and the S(4)-Cd(1)-S(3) bite angle was

79.910(14)°. For complex **5C** the Zn(1)-S(4) and Zn(1)-S(1) bond lengths were 2.4164(9) and 2.3378(8) Å while the S(1)-Zn(1)-S(4) bite angle was 86.85°. **3B** and **3C** had similar structures which consisted of three ring structures including an eight membered $M_2S_4P_2$ ring comprising the metal, sulfur and phosphorus atoms which was formed *via* bridging coordination of the two ligands with two metal centres using their PS_2 moiety as shown by **Figure 3-16** and **Figure 3-17**. The result of this pattern was the formation of an inversion centre within the complexes between their two metal atoms. The crystal structures packed in a triclinic crystal system in a P-1 space group. Each of the complexes showed similar groups of ligands adjacent to one another within the complex molecule i.e. the anisyl groups of a bridging and chelating ligand were held adjacent to one another as shown by **Figure 3-16** and **Figure 3-17** which show the molecular solid state structure of compounds **3B** and **3C** respectively with atom numbering scheme. **Figure 3-18** shows the packing when viewed along the *a* axis

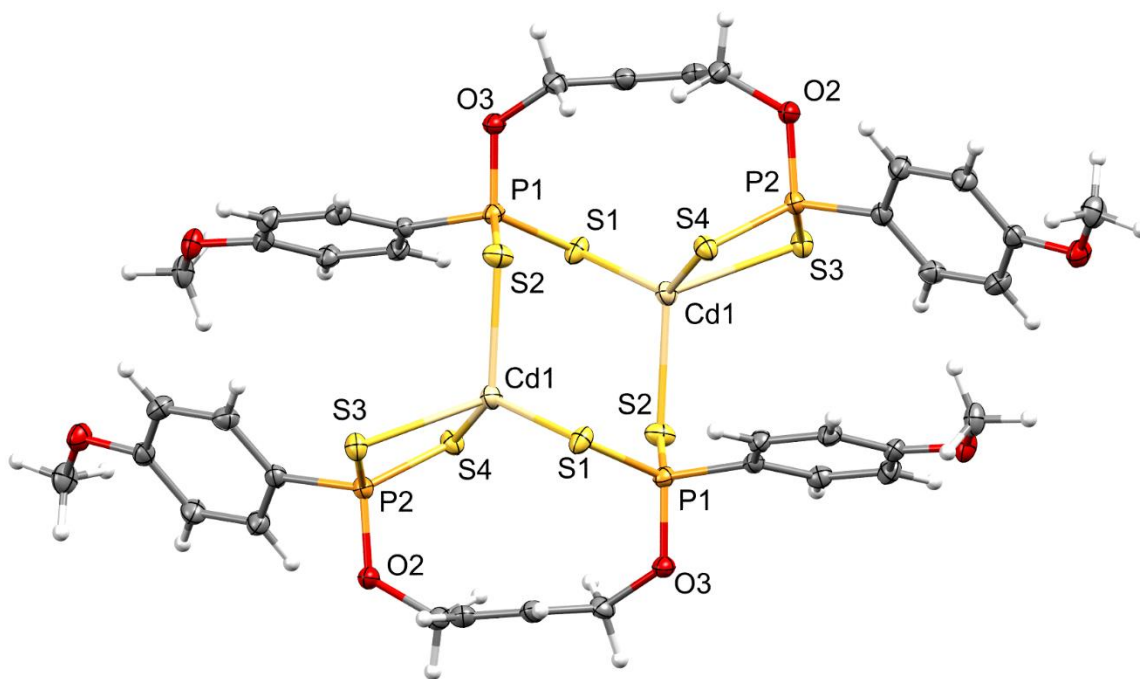


Figure 3-16: ORTEP diagram for compound **3B**, thermal ellipsoids drawn at 50% probability

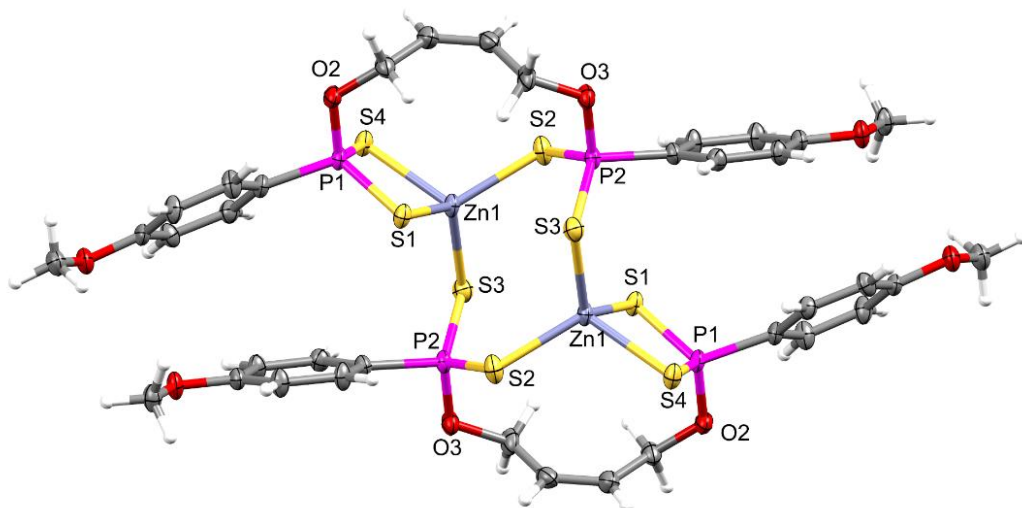


Figure 3-17: ORTEP diagram for compound **3C**, thermal ellipsoids drawn at 50% probability

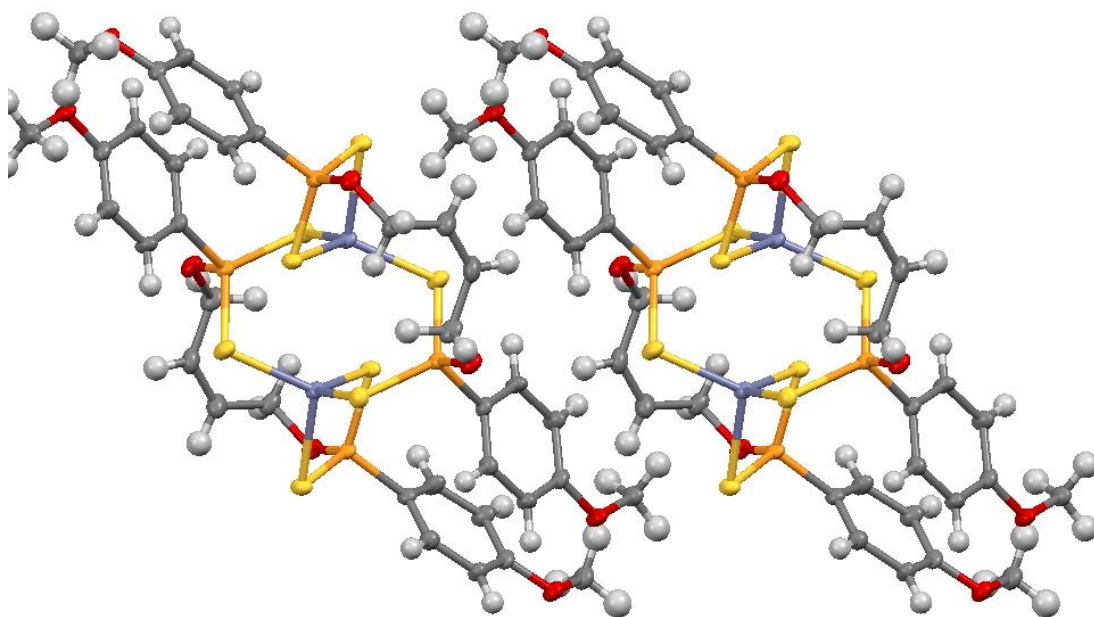


Figure 3-18: Packing of **3C** viewed along the *a* axis

3.1.1.5 2-methyl cyclohexanol derived compounds

The ligand was synthesized by the reaction between LR and 2-methyl cyclohexanol. The 2-methyl cyclohexanol derived ligand was thereafter complexed with the nitrate salts of silver, cadmium and zinc.

3.1.1.5.1 2-methyl cyclohexanol derived ligand (4)

Analysis with FT-IR revealed the presence of $\nu(\text{N-H})$, $\nu(\text{P-O-C})$, $\nu_s(\text{P-S})$ and $\nu_{as}(\text{P-S})$ bands at 3141 cm^{-1} , 1023 cm^{-1} , 648 cm^{-1} and 548 cm^{-1} respectively. This indicated the presence of an ammonium dithiophosphonate compound. The FT-IR spectrum for **4** is shown in **Figure 3-19**.

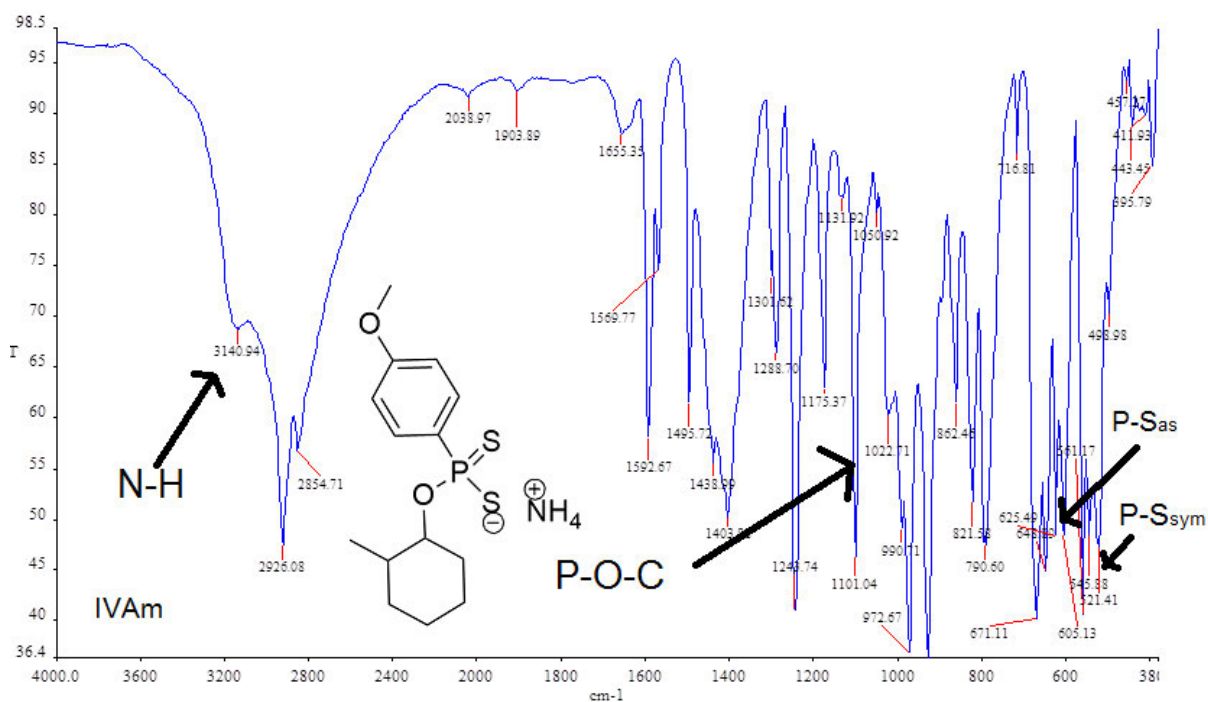


Figure 3-19: FT-IR spectrum for compound **4**

^{31}P -NMR indicated the presence of a dithiophosphonate moiety within the expected chemical shift range shown by a single peak at 103.67 ppm . **Figure 3-20** shows the ^{31}P -NMR spectrum for **4**.

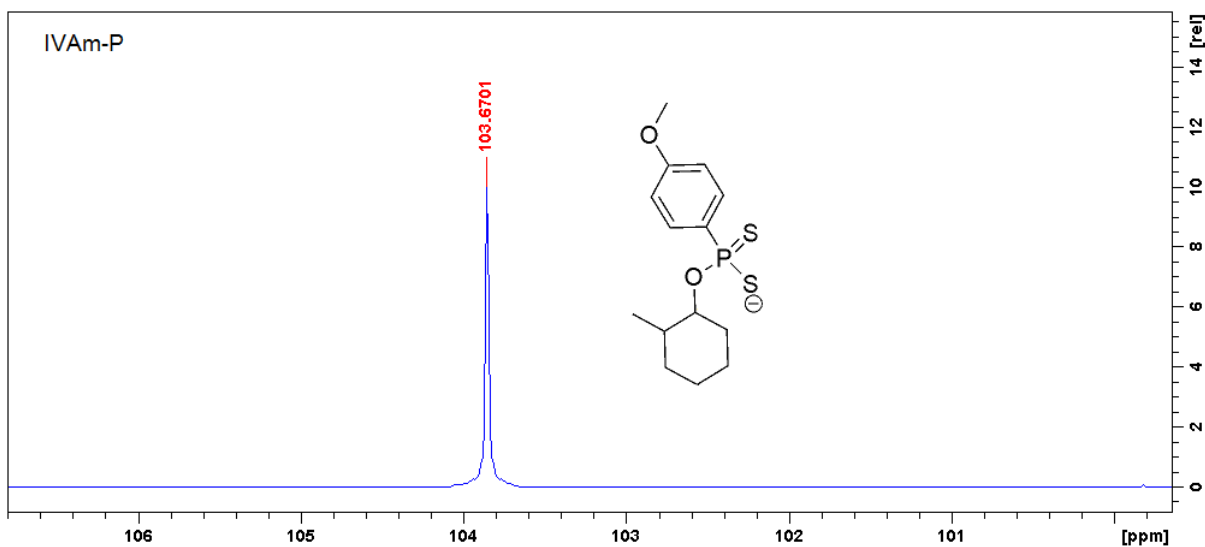


Figure 3-20: ^{31}P -NMR spectrum for compound 4

The ^1H -NMR spectrum showed a quartet at 4.14 ppm which was assigned to H-4 since it was more deshielded due to the oxygen higher than the upfield quartet at 2.02 ppm which was assigned to H-9. The multiplets at 1.25-1.73 ppm were assigned to the methylene protons H-5, H-6, H-7 and H-8. The doublet at 0.93 ppm was assigned to H-10 using its chemical shift, splitting pattern as well as a peak integral of 3 protons. **Figure 3-21** shows the ^1H -NMR spectrum of compound 4. **Figure 3-22** shows the ^{13}C -NMR spectrum of 4, the resonances were assigned using their chemical shifts as 81.36 ppm (C-4), 39.81 ppm (C-9), 36.63 ppm (C-5), 34.68 ppm (C-8), 31.55 ppm (C-7), 22.83 ppm (C-6) and 19.89 ppm (C-10) which was the least deshielded.

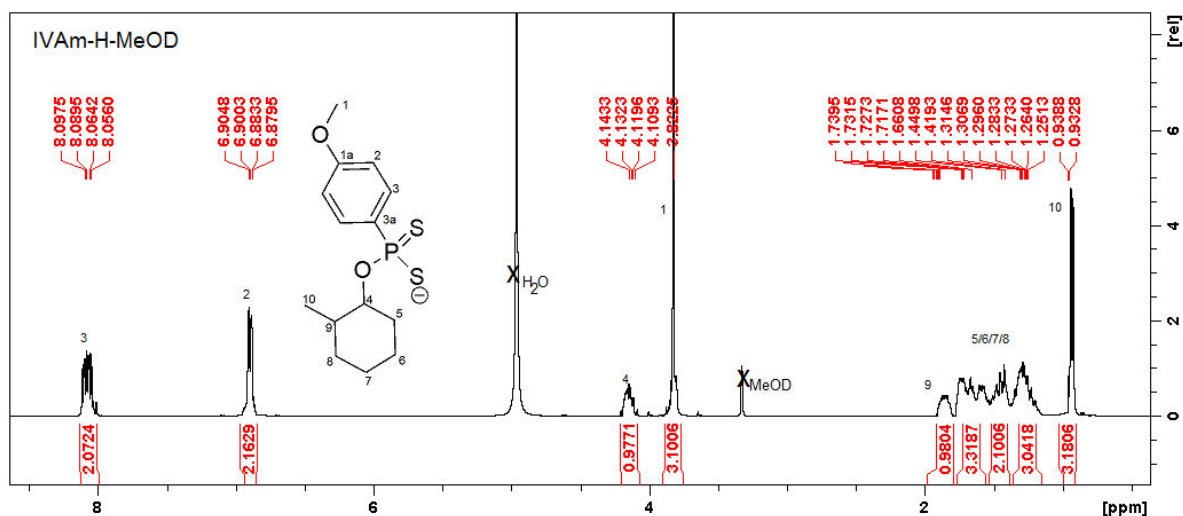


Figure 3-21: ^1H -NMR spectrum of compound 4

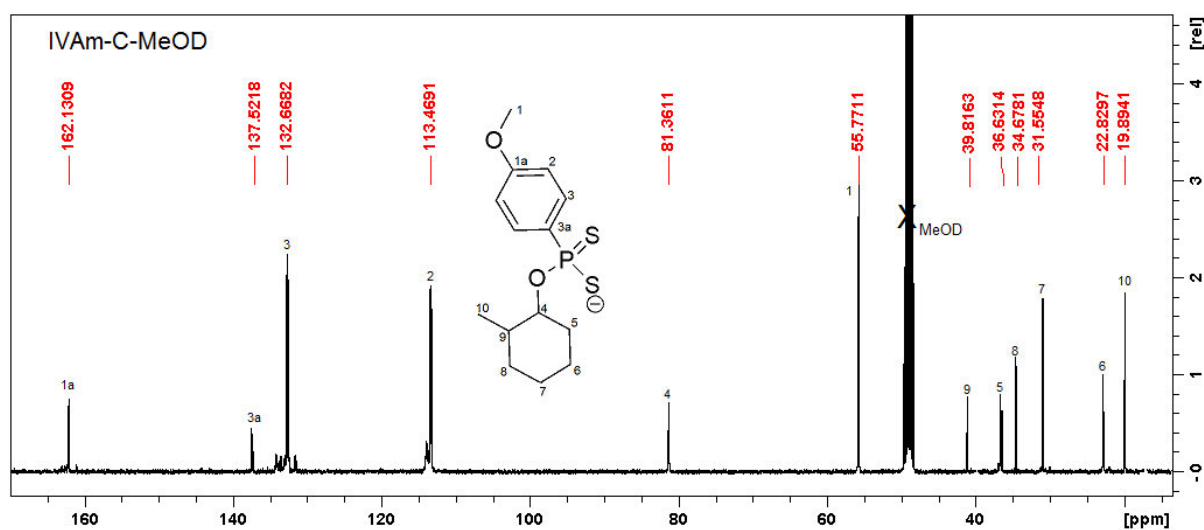


Figure 3-22: ^{13}C -NMR spectrum for compound **4**

A base peak was observed with ESI (-) mass spectrometry for compound **4** as $[\text{M}]^- = 317$ which confirmed the molecular formula of the ligand as $\text{C}_{14}\text{H}_{20}\text{O}_2\text{PS}_2^-$.

3.1.1.5.2 Silver Cadmium and Zinc complexes

4A, **4B** and **4C** were synthesized from ligand **4** and their characterisation data compared to their parent ligand. Complexes **4B** and **4C** were white powders while compound **4A** was a yellow powder.

The three compounds were analysed using FT-IR spectroscopy. The $\nu(\text{P-O-C})$ vibrations were at 1026 cm^{-1} , 1026 cm^{-1} and 1024 cm^{-1} for **4A**, **4B** and **4C** respectively. For the $\nu_s(\text{P-S})$ vibrations were at 532 cm^{-1} , 537 cm^{-1} and 537 cm^{-1} for the **4A**, **4B** and **4C** respectively. The $\nu_{as}(\text{P-S})$ vibrations were at 655 cm^{-1} , 647 cm^{-1} and 642 cm^{-1} for **4A**, **4B** and **4C** respectively. Comparison of the spectra of **4** and those of **4A**, **4B** and **4C** shows the disappearance of the $\nu(\text{N-H})$ vibration at 3141 cm^{-1} . This proves that **4** successfully complexed with metal ions to form **4A**, **4B** and **4C**.

^{31}P -NMR showed single peaks at 103.83 ppm , 102.21 ppm , and 101.47 ppm were for **4A**, **4B** and **4C** respectively. The ^1H -NMR signals of complexes **4A**, **4B** and **4C** were similar to the peaks that were observed with **4**. Table 3-4 shows the ^{13}C -NMR of **4** and its derivatives. For C-3a compound **4** was at

137.52 ppm compared to its derivatives **4A**, **4B**, and **4C** which were upfield at 129.86 ppm, 129.67 ppm and 129.81 ppm respectively.

Table 3-4: ^{13}C -NMR chemical shifts for 2-methyl hexanol derived compounds

Carbon atom number and chemical shifts (ppm)												
	C-1	C-1a	C-2	C-3	C-3a	C-4	C-5	C-6	C-7	C-8	C-9	C-10
4	55.7	162.1	113.4	132.6	137.5	81.3	36.6	22.8	31.5	34.6	38.8	19.8
	1	3	7	7	2	6	3	3	5	7	1	9
4	54.5	161.5	112.8	131.8	129.8	80.1	34.8	24.2	24.8	32.5	37.6	18.4
A	7	9	6	9	6	5	9	3	7	4	7	9
4B	55.4	162.3	113.6	132.1	129.6	83.0	35.6	24.7	25.1	33.8	38.6	19.5
	1	1	7	8	7	8	8	4	8	5	4	0
4	55.4	162.4	113.7	131.7	129.8	79.1	35.7	24.7	25.5	33.4	38.5	19.3
C	4	6	3	6	1	4	7	3	0	0	4	6

The peaks for the complexes were determined using ESI (-) MS as $[\text{M-Ag}]^- = 869.96$ m/z for **4A**, ESI (+) as $[\text{M+ Na}]^+ = 1506$ m/z for **4B** and $[\text{M}]^+ = 1392.14$ for **4C**. **Figure 3-23** shows the fragment of **4B** after the loss of a metal ion and An-PS_2^- (An = Anisyl) at 1059.05 m/z, as well as the ligand fragment at 315.05 m/z. **4A** also followed a similar pattern of fragmentation.

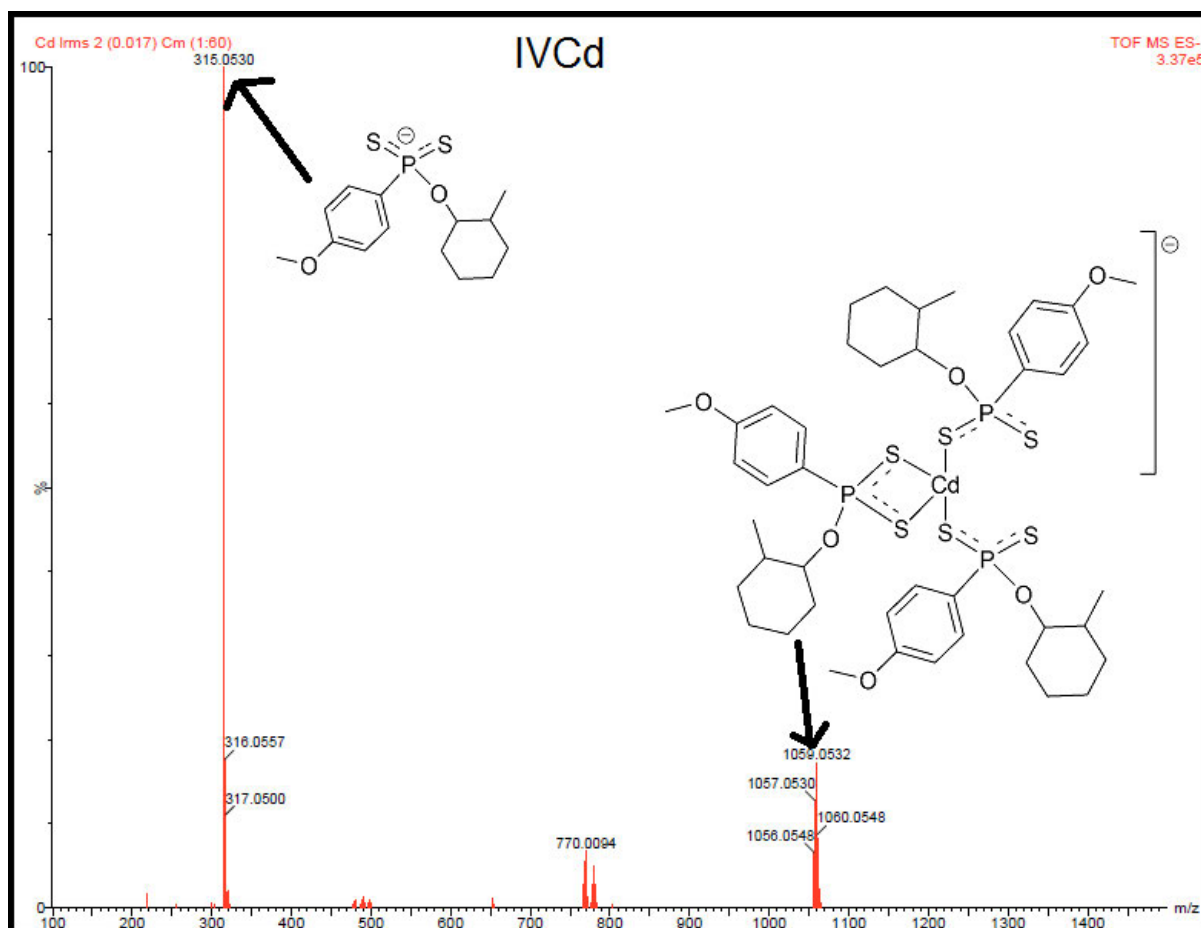


Figure 3-23: ESI (-) mass spectrum showing fragments of **4B**

3.1.1.6 2-methyl-3-hexanol derived compounds

A 2-methyl-3-hexanol derived dithiophosphate salt **5** was synthesised using LR and 2-methyl-3-hexanol. The synthesized ligand was thereafter complexed with silver, cadmium and zinc salts to form compounds **5A**, **5B** and **5C** respectively. This section details the characterisation data obtained.

3.1.1.6.1 2-Methyl-3-hexanol derived ligand (**5**)

Analysis with FT-IR indicated expected vibrations consistent with an ammonium dithiophosphate salt. Vibrations at 3192 cm^{-1} , 1017 cm^{-1} , 662 cm^{-1} , and 540 cm^{-1} were attributed to the $\nu(\text{N-H})$, $\nu(\text{P-O-C})$, $\nu_{as}(\text{P-S})$ and $\nu_s(\text{P-S})$ vibrations respectively. **Figure 3-24** shows the FT-IR spectrum with the vibrations annotated accordingly.

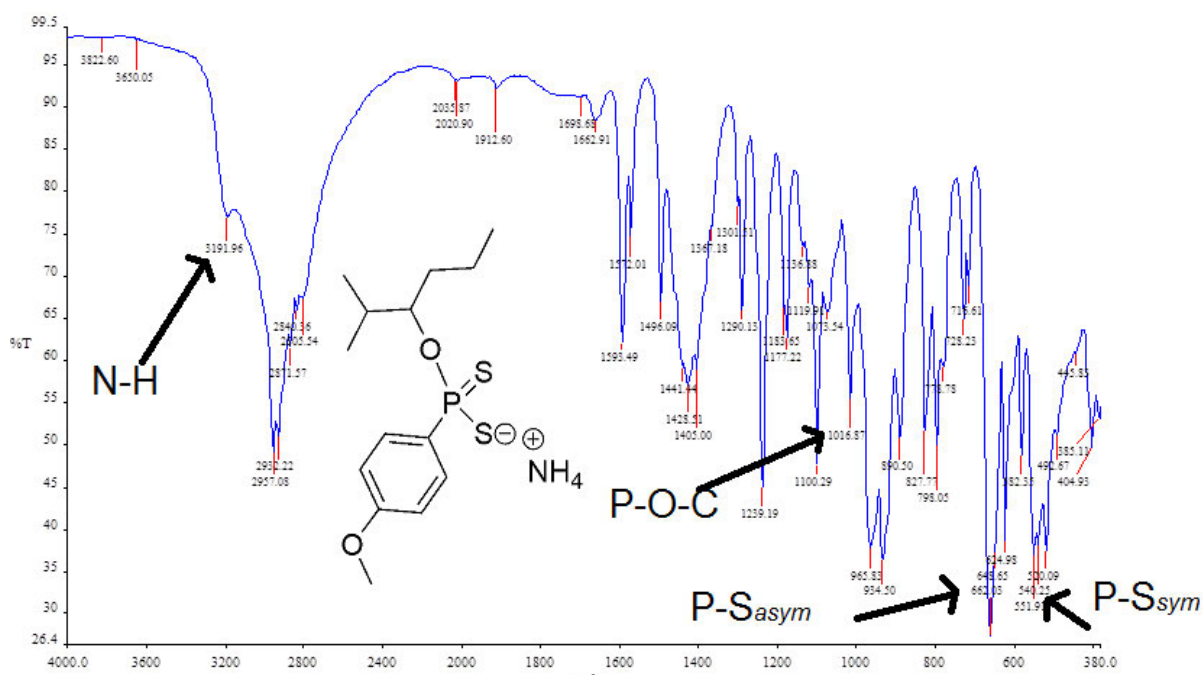


Figure 3-24: FT-IR spectrum for compound **5**

The ^{31}P -NMR analysis of compound **5** revealed a singlet at 103.83 ppm as shown by **Figure 3-25** which indicated the synthesis of a compound with a dithiophosphate moiety as it was within the expected dithiophosphate range.

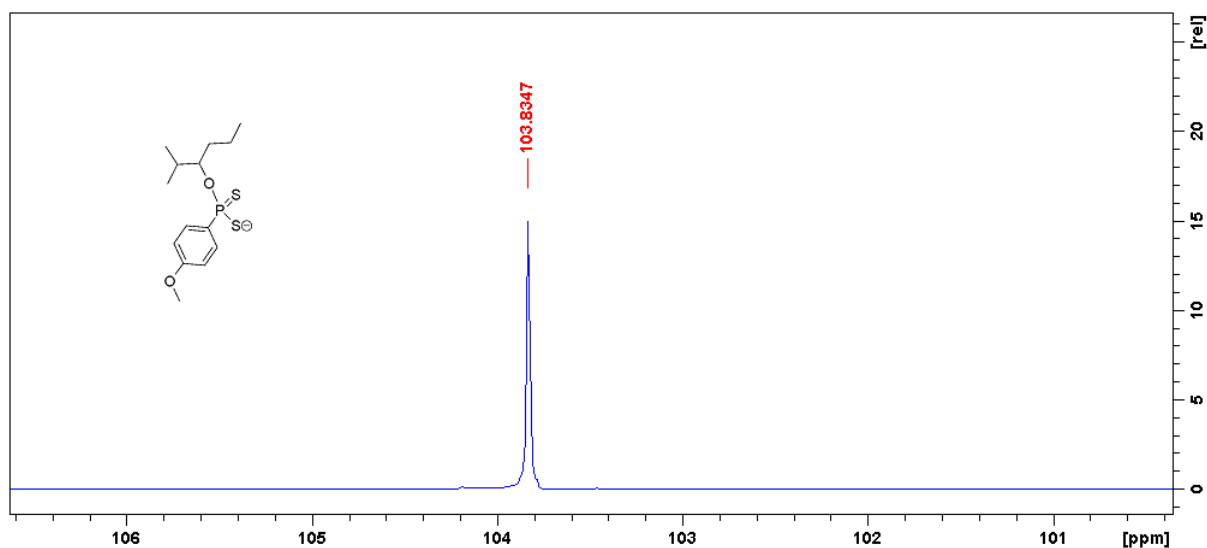


Figure 3-25: ^{31}P -NMR spectrum for compound **5**

Figure 3-26 shows the $^1\text{H-NMR}$ spectrum for compound **5** with three resonances *ca.* 8.10 ppm, 6.90 ppm and 3.81 ppm due to *meta*, *ortho* and the methoxy protons respectively on the anisyl side chain of the ligand. The methyl protons H-4, H-6 and H-10 were the least deshielded and were determined by their upfield chemical shifts, as well as the integration of their signal to nine protons corresponding to three methyl groups. H-7 was determined by its relatively downfield chemical shift compared to H-5 or H-8 due to a direct bond with an oxygen atom of the dithiophosphonate moiety. The signal at 2.04 ppm was assigned to the C-5 methine proton while the multiplets at 1.33-1.58 ppm were assigned to the methylene protons H-8 and H-9. The $^{13}\text{C-NMR}$ spectrum shown in **Figure 3-27** had twelve resonances at expected chemical shifts. The resonances for the anisyl carbon atoms due to the *para* carbon (C-1a), *ipso* carbon (3a), *ortho* carbons (C-3), *meta* carbons (C-2) and methoxy carbon (C-1) were at chemical shifts 162.3 ppm, 139.1 ppm, 132.9 ppm, 113.6 ppm and 55.9 ppm respectively. 81.90 ppm was assigned to C-7 directly bonded to the oxygen. Other carbon atoms were determined using their $^{13}\text{C-NMR}$ chemical shift values and HSQC as C-8, C-5, C-4,C-6 and C-10 at 34.43 ppm, 32.54 ppm, 19.77 ppm, 18.82 ppm, 18.24 ppm and 14.79 ppm. **Figure 3-28** shows the HSQC spectrum of compound **5** displaying the signals of the observed carbon atoms and their correlating protons.

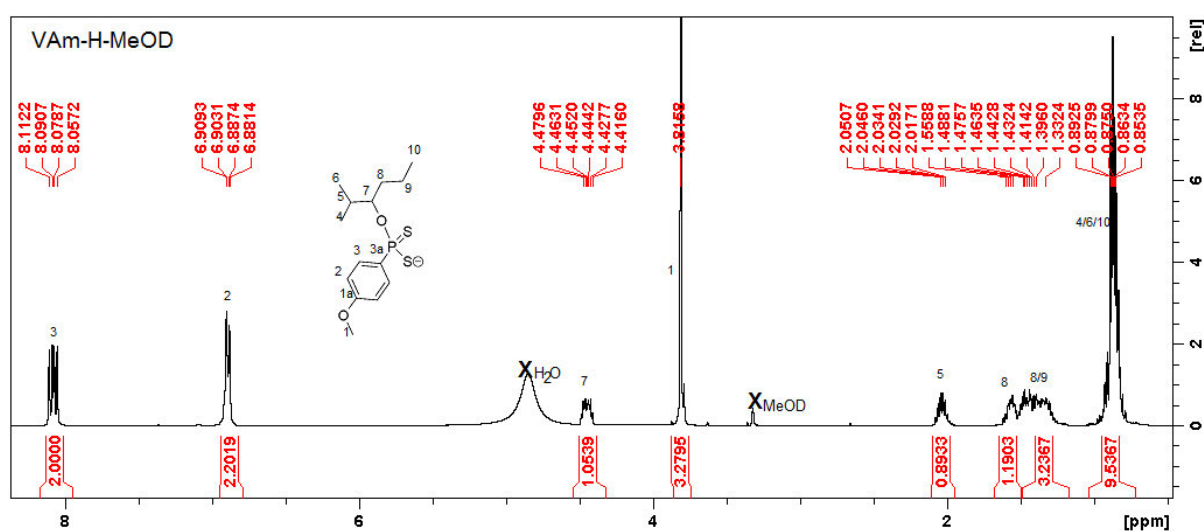


Figure 3-26: $^1\text{H-NMR}$ spectrum for compound **5**

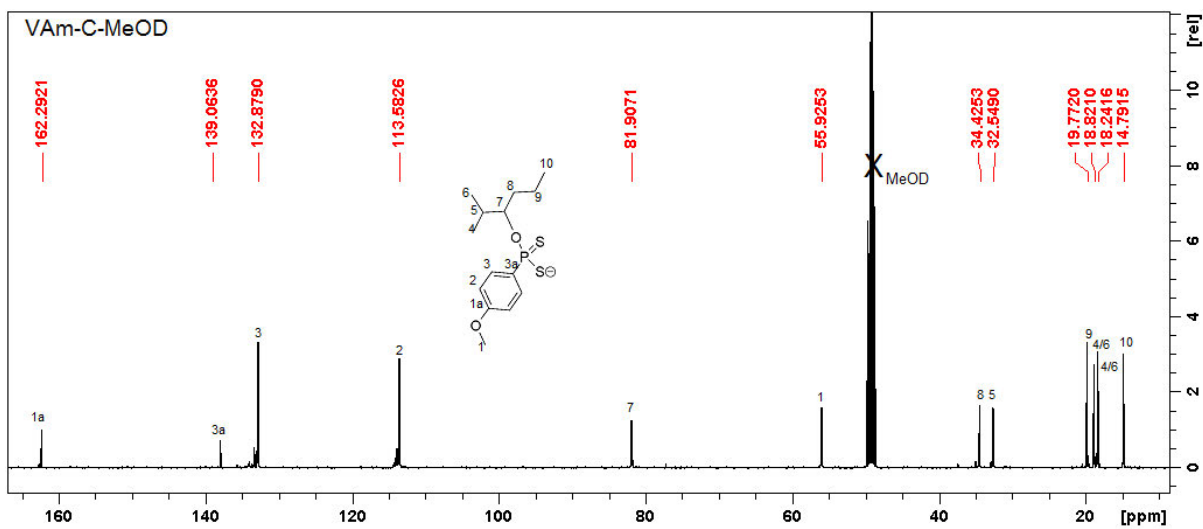


Figure 3-27: ^{13}C -NMR spectrum for compound 5

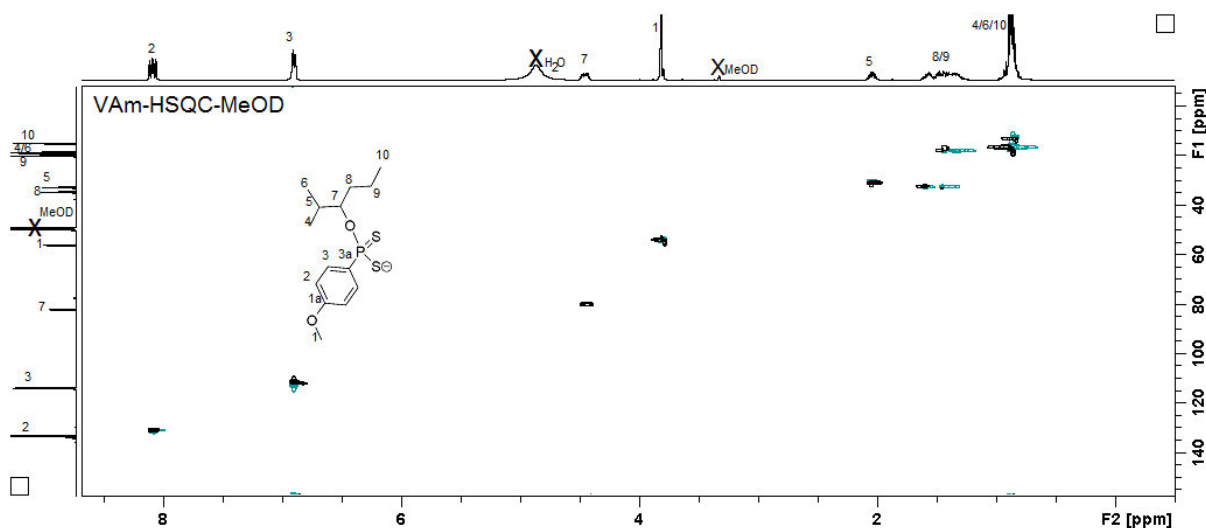


Figure 3-28: HSQC spectrum for compound 5

Mass spectrometry analysis confirmed the structure of **5** when a base peak was observed as $[\text{M}]^- = 317.09$ corresponding to the anticipated ligand with a molecular formula of $\text{C}_{14}\text{H}_{22}\text{O}_2\text{PS}_2^-$ as shown in the ESI (-) mass spectrum in the supporting information accompanying this work.

3.1.1.6.2 2 methyl 3 hexanol derived silver, cadmium and zinc complexes

The synthesised silver complex (**5A**) was yellow while the cadmium (**5B**) and zinc complexes (**5C**) were white in colour. The complexes were characterised by FT-IR analysis to ascertain the presence of the characteristic $\nu(\text{P-O-C})$, $\nu_{as}(\text{P-S})$ and $\nu_s(\text{P-S})$ vibrations as well as confirmation of the absence of the $\nu(\text{N-H})$ band after complexation.

The complexes were analysed with ^{31}P -NMR indicating the presence of the dithiophosphonate moiety. Singlets were obtained at 103.84 ppm, 100.17 ppm and 97.00 ppm for **5A**, **5B** and **5C** which proved that complexes contained the dithiophosphonate group derived from their ligand precursor **5**

^1H -NMR analysis of **5A**, **5B** and **5C** showed similar signal splitting compared to the precursor with minor differences in chemical shifts. The complexes showed the protons associated with anisyl as well as the alcohol residue *ca.* 7.99 ppm, 6.8 ppm, 4.7 ppm, 3.8 ppm, 2.1 ppm, 1.5 ppm and 0.9 ppm.

^{13}C -NMR spectra of **5A**, **5B** and **5C** also showed 12 resonances similar to **5**. The most notable difference as with the other ligands synthesized in this work was on the *ipso* carbon (C-3a) which was at 139.06 ppm on compound **5** but was upfield at 130.44 ppm, 130.11 ppm and 129.78 ppm in **5A**, **5B** and **5C** respectively as shown in **Table 3-5**.

Table 3-5: ^{13}C -NMR chemical shifts for 2-methyl-3-hexanol derived compounds

Carbon atom number and chemical shifts(ppm)												
	C-1	C-1a	C-2	C-3	C-3a	C-4	C-5	C-6	C-7	C-8	C-9	C-10
5	55.92	162.29	113.58	132.88	139.06	18.82/ 18.24	32.55	18.82/ 18.24	81.91	34.43	19.77	14.79
5A	55.45	162.41	113.66	131.72	130.44	18.74/ 18.00	31.49	18.74/ 18.00	84.03	33.10	19.87	14.26
5B	55.50	162.49	113.71	131.91	130.11	18.05/ 17.81	31.58	18.05/ 17.8	84.09	33.18	18.85	14.31
5C	55.43	162.42	113.48	131.84	129.78	17.98/ 17.74	17.98/ 17.74	14.24				

Fragment ion peaks were observed using mass spectrometry, indicating the formation of the desired compounds. The ESI (-) mass spectrum showed fragment ion peaks $[\text{M}-\text{Ag}]^- = 741.07$ for **5A** and $[\text{M}-\text{L} + \text{Na}^+]^- = 1168.07$ for **5C**. The ESI (+) spectrum displayed a fragment ion $[\text{M} + \text{Na}]^+ = 1517.56$ m/z for **5B** as shown in the supporting information. **Figure 3-29** shows the fragmentation of the **5B** which shows the loss of a cation and a ligand. Similar fragments were observed with **5A**.

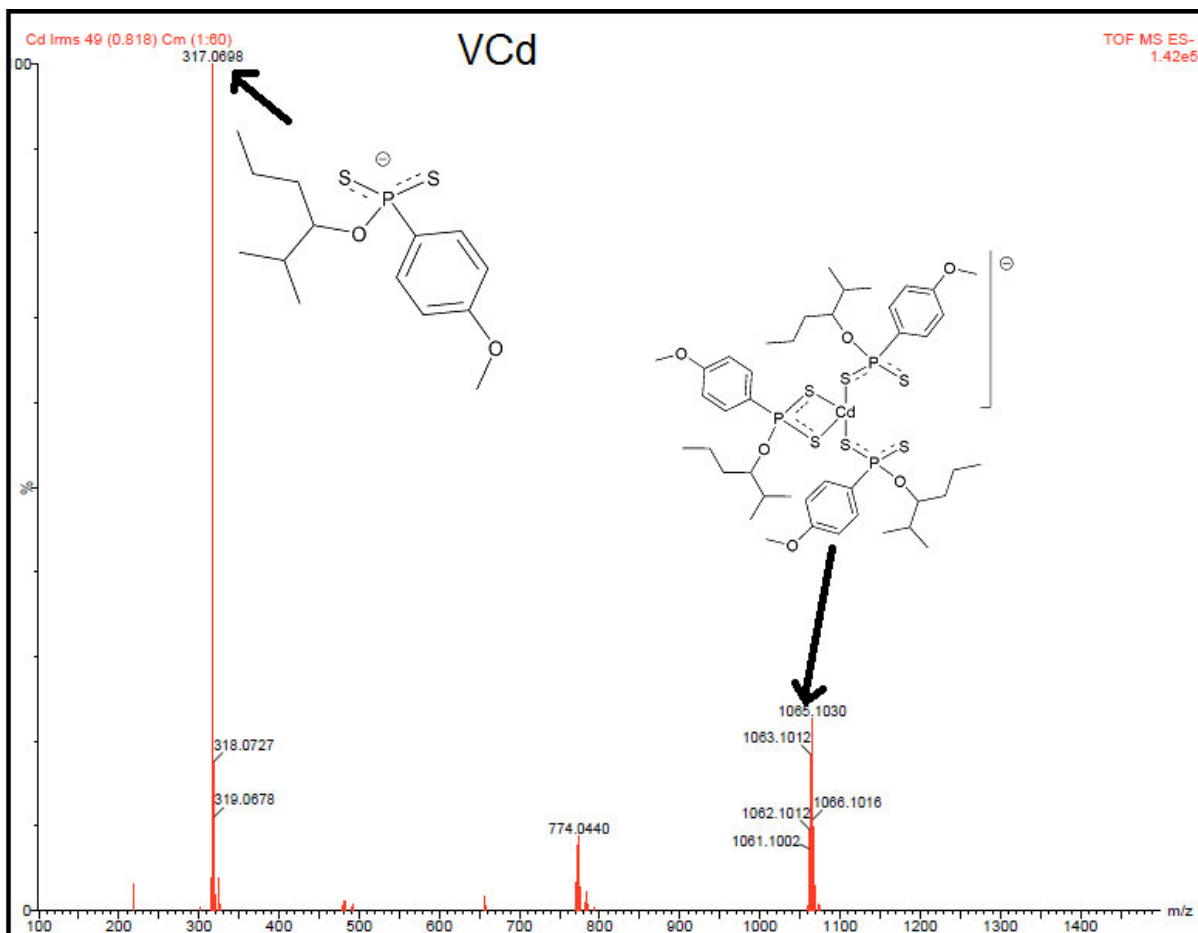


Figure 3-29: ESI(-) mass spectrum for compound **5B**

3.2 Conclusion

The FT-IR analyses conducted were used to characterise the synthesized compounds to prove the formation of an ammonium DTP salt based on the $\nu(\text{N-H})$, $\nu(\text{P-O-C})$, $\nu_s(\text{P-S})$ and $\nu_{as}(\text{P-S})$ vibrations observed. It was also used to determine the formation of a complex as observed by the disappearance of the broad $\nu(\text{N-H})$ band *ca.* 3200 cm^{-1} .

Single peaks were observed with $^{31}\text{P-NMR}$ within the expected range of 90-110 ppm, $^1\text{H-NMR}$ showed signals with expected splitting and chemical shifts, and was also useful to ascertain the bulk purity of the synthesized compounds. $^{13}\text{C-NMR}$ was used to predict the structures of the compounds, as the resonances were obtained at expected chemical shifts. It also showed the formation of the complex from the ligand as shown by the change in the chemical shift of the *ipso* carbon by *ca.* 10 ppm upon complexation. 2D-NMR was instrumental in resolving the structure of some compounds with overlapping peaks by the correlation of the carbons and protons involved.

ESI(-) MS showed the fragmentation of complexes in most cases shown by the largest fragment without the metal ion and ligand. Fragments corresponding to the ligands were also observed usually as base peaks. ESI(+) confirmed the suggested structures of the complexes either as M^+ or $[\text{M} + \text{Na}]^+$ peaks.

SC-XRD enabled the confirmation of the molecular structures of **3B** and **3C** which were observed to have similar structures. Both had a distorted tetrahedral geometry around their metal centres consisting of three ring structures including an eight membered $\text{M}_2\text{S}_4\text{P}_2$ ring comprising the metal, sulfur and phosphorus atoms which was formed *via* bridging coordination of the two ligands with two metal centres using their PS_2 moiety with the formation of an inversion centre within the complexes between the two metal atoms.

The characterisations discussed in this section confirmed the synthesis of the desired dithiophosphonate compounds, which were subsequently used for in-vitro antibacterial studies in Chapter 4.

CHAPTER 4

APPLICATION OF NEW DITHIOPHOSPHONATE COMPOUNDS IN ANTIBACTERIAL STUDIES

4.1 Introduction

Bacterial infectious diseases are a severe health challenge as evidenced by increased outbreaks. Bacterial antibiotic resistance and the emergence of new bacterial mutations are becoming increasingly more common.⁶⁵ Bacteria are prokaryotes known to infect humans and animals a few minutes after they are born.^{66,67} There are multitudes of bacteria that are fairly innocuous but have been known to develop virulent tendencies and become pathogenic.⁵⁷ An opportunity was created for the eradication of infections by these virulent bacteria with the discovery of antibiotics by Alexander Fleming in 1928. However, within a few years an increase in antimicrobial resistance (AMR) was observed resulting in reduced efficacy of formerly effective antibacterial agents.⁶⁸ Currently AMR has resulted in the treatment of patients becoming more costly and difficult,⁶⁹ or even impossible in some instances.⁷⁰ The virulence capability of such strains is determined by a combination of distinctive accessory traits, called virulence factors. The antibiotic resistance patterns are also to some extent determined by the local environment, selective acquisition and loss of plasmids carrying resistance genes and various other genetic mechanisms.⁷¹ In some cases, resistance extends to the entire range of the available therapeutic agents posing an arduous challenge to antimicrobial therapy. This is particularly worrisome in light of the current dearth of new compounds active against such bacteria.⁵⁹ Poor medical and agricultural practices of the past decades are suspected to have promoted resistance development and spread in both human and animal pathogens culminating in compromised chemotherapy.⁷²

Bacteria are classified as gram negative and positive differentiated by the Gram staining technique developed by Cristian Gram in 1884 using crystal violet as the staining technique. Gram positive

bacteria are more susceptible to antibiotics due to the absence of the outer membrane. Gram negative bacteria are less susceptible because they contain the outer membrane as shown by **Figure 4-1**

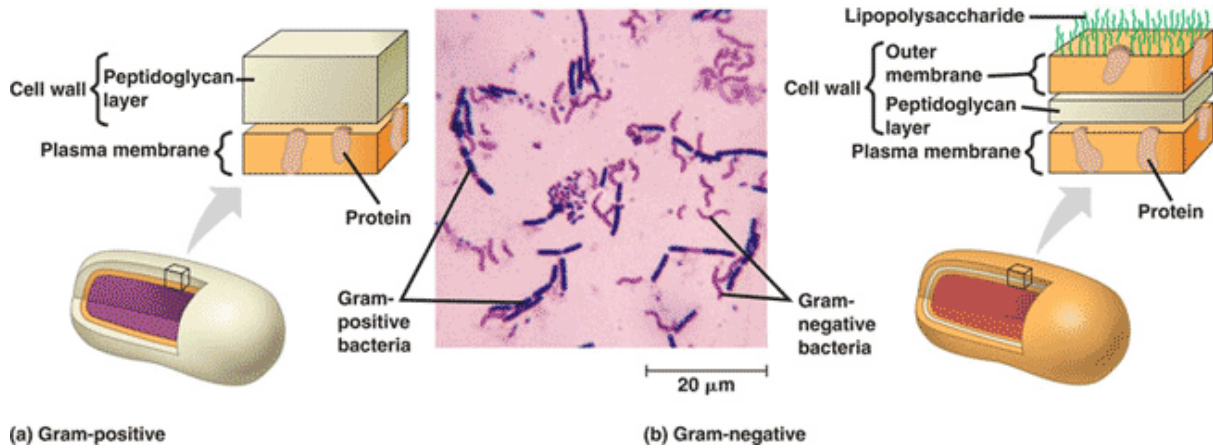


Figure 4-1: Structural comparison between gram positive and negative bacteria cell walls.⁸⁴

Gram positive bacteria contain a thick peptidoglycan cell wall along with teichoic acid, allowing the bacteria to stain in purple during gram staining whereas gram negative bacteria contain a thin peptidoglycan cell wall with no teichoic acid, which causes the cell wall to stain pink during counter staining. These two types of bacteria also appear differently under a microscope, as well as having different sizes, cell wall texture, lipid and lipoprotein content, presence/absence of pores on the outer membrane, resistance to physical disruption, cell wall disruption by lysozyme, pathogenicity and toxins produced.⁷³

Staphylococcus aureus is a Gram-positive aerobic organism frequently responsible for nosocomial bacteraemia, biofilm linked infections, catheter related infections and the infection of many implanted devices leading to longer term hospitalization and naturally higher care costs.^{68,74}

Escherichia coli is a Gram-negative, rod-shaped bacterium and versatile predominant facultative anaerobe of the human colonic flora. The organism typically colonizes the infant gastrointestinal tract within hours of life and co-existing in good health. However, several highly adapted *E. coli* variants have evolved the ability to cause a broad spectrum of human diseases⁶⁶ including bacteraemia,⁶⁷ urinary tract infections, neonatal meningitis and diarrheal diseases.⁴

Klebsiella pneumoniae is a Gram-negative, encapsulated, non-motile bacterium^{76,77} that resides in the environment, including soil and surface waters and on medical devices.⁷⁸ It causes a wide range of infections, including pneumonia, bacteraemia, urinary tract infections and liver abscesses. *K. pneumoniae* readily colonizes human mucosal surfaces, including the gastrointestinal (GI) tract and oropharynx.

Salmonella Typhimurium is a Gram-negative, flagellated, facultative anaerobic and primary enteric pathogen infecting both humans and animals. Infection is instigated by the ingestion of contaminated food or water allowing the salmonellae access to the intestinal epithelium and ultimately triggering gastrointestinal disease.⁷⁹

Pseudomonas aeruginosa is a ubiquitous bacterial species. It is a Gram-negative, rod-shaped bacterium. It is found in various environmental habitats including animal and human hosts, where they can act as opportunistic pathogens.⁸⁰ One of the most worrisome characteristics of *P. aeruginosa* is its low antibiotic susceptibility, which is attributable to the concerted action of multidrug efflux pumps with chromosomally encoded antibiotic resistance genes.⁷²

Dithiophosphonates have received attention due to their useful applications, which now include potential use in medicine. Dithiophosphonate compounds have appreciable antibacterial activity among other biological activities.²⁷ They are of particular interest because of the resistance of some bacteria to traditional antibiotics. Efforts are being made to improve and also develop better compounds for use in antibacterial applications to reduce unpleasant side-effects frequently associated with antibiotics as well as resistance.^{9,19}

4.2 Results and discussion

Of the synthesised compounds, only **1A** could not be used for screening as it was sparingly soluble in DMSO. As shown by **Table 4-1** each compound was effective against at least two bacterial strains. Cadmium complexes generally had poor antibacterial effectiveness against most of the strains tested in this study. Three of the four zinc complexes were effective against all of the tested bacteria although they were not the best against the bacterial strains in each case. The most effective metal complexes based on the largest zones of inhibition for each bacteria were silver complexes. The most resistant strain was *Salmonella Typhimurium*, most of the compounds were ineffective against this strain. Only a third were effective against the strain and even so with relatively small zones of diffusion showing that the synthesized compounds were mildly effective against it. Most of the compounds were effective against *Klebsiella Pneumoniae* but the most susceptible strain was MRSA. The largest zones of inhibition were recorded with MRSA, even the less effective cadmium complexes showed some activity against the strain. The most effective compounds against each strain, as shown by the largest zones of diffusion are highlighted in **Table 4-1** and were used for the next step of testing to determine their minimum inhibitory concentrations (MICs).

Table 4-1: Initial screening tests for synthesized dithiophosphonate compounds at 10 000ppm showing the diameter of zones of inhibition (mm)

Compound	Bacterial strains					
	Ec	Kp	MRSA	Sa	Pa	St
1	7	-	-	-	5	-
2	7	8	11	7	5	-
3	5	8	-	6	6	-
4	5	-	11	6	5	-
5	9	9	12	6	5	7
2A	-	19	18	-	11	-
3A	11	9	5	7	8	6
4A	9	14	-	7	6	-
5A	-	14	10	-	6	-
1B	-	12	-	7	-	-
2B	-	10	25	-	-	-
3B	-	10	23	9	-	8
4B	-	-	22	-	-	-
5B	-	12	19	7	-	-
1C	-	7	-	5	7	-
3C	7	5	6	7	9	10
4C	8	5	19	7	8	8
5C	8	7	18	7	6	8

Ec = *Escherichia Coli*; MRSA = Methicillin resistant *staphylococcus aureus*; Pa = *Pseudomonas aeruginosa*; St = *Salmonella Typhimurium*; Kb = *Klebsiella Pneumoniae*; Sa = *Staphylococcus aureus*.

3.3 Minimum inhibitory concentration (MIC)

These tests are crucial as resistance surveillance in epidemiological studies of susceptibility and in comparisons of new and existing agents. In MICs dilutions of antimicrobial agents are tested for their ability to stop visible growth on a series of agar plates. The lowest concentration of an antimicrobial agent (in mg/L) which under defined in-vitro conditions prevents the appearance of visible growth of the microorganism within a predefined period of time is referred to as the MIC. The MIC is used as a guide for clinicians to the susceptibility of the organism to an antimicrobial agent, thereby assisting in decision making based on the treatment options available.⁸¹ Compounds **2A**, **3A**, **2B**, **3B** and **3C** were used in the MIC tests. The minimum concentrations that inhibited bacterial growth are shown in **Table 4-2**.

Table 4-2: Minimum inhibitory concentrations (MICs) for dithiophosphonate complexes $\mu\text{g/mL}$ (ppm)

Microorganism	DTP compound	MIC $\mu\text{g/mL}$ (ppm)	MIC $\mu\text{g/mL}$ (ppm) Ciprofloxacin
Ec	3A	625	0.2
Kp	2A	10	1.6
MRSA	2B	20	25
Sa	3B	1250	25
Pa	2A	1250	0.8
St	3C	2500	0.4

Ec = *Escherichia Coli*; MRSA = Methicillin resistant *staphylococcus aureus*; Pa = *Pseudomonas aeruginosa*; St = *Salmonella Typhimurium*; Kb = *Klebsiella Pneumoniae*; Sa = *Staphylococcus aureus*.

Comparison with the standard drug ciprofloxacin showed that most of the compounds were not as effective as the standard drug. The MICs of the compounds were higher than those of ciprofloxacin when tested against the bacterial strains. However **2B** was more effective against MRSA than

ciprofloxacin as shown by the lower MIC of 20 ppm compared to 25 ppm of ciprofloxacin, **2A** also showed a relatively good MIC value of 10 ppm against *Klebsiella Pneumoniae* compared to the Ciprofloxacin value of 1.6ppm.

The results show that ligand **2** and **3** derivatives generally had larger zones of inhibition than other ligands. Overall, complexes had larger zones of inhibition compared to their free ligands as shown by **Table 4-1** which showed that they were more effective than their ligand precursors. These results corroborate reports using antimony DTP complexes which showed that the complexes had greater potency compared to their free ligands,⁸² another investigation by Saadat et al. using nickel DTP complexes had the same findings.⁶¹ Chauhan et al. have used other dithiolates like dithiophosphates in antimicrobial applications against similar bacteria and managed to get encouraging results.⁸² It is reported that chelation makes the ligand act as stronger and effective bactericidal agents, thus showing more antibacterial activity than the ligand. In a complex there is π -electron delocalization over the whole chelate due to the positive charge of the metal which is not fully shared with the ligand's donor atoms. This improves the lipophilic performance of these complexes which encourages infiltration through the lipid layer of the bacterial membranes and consequently improved efficacy⁸³

Other factors may also be responsible for the antimicrobial activity that was observed in this study, including solubility, conductivity, and bond length between the metal and the ligand. The results show the ligands being consistently active against *Escherichia coli* and *Pseudomonas aeruginosa* but all the cadmium complexes were ineffective despite having the same ligands as part of its complexes. It is also interesting to note that most of the ligands were ineffective against the most resistant strain *Salmonella Typhimurium* but the zinc complexes from the same ligands were consistently effective. The results of this study revealed that the bacteria were susceptible to the new dithiophosphonates tested on them and showed the effectiveness of this class of compounds against common bacterial strains.

4.3 Conclusion

This study reports on the antibacterial susceptibility tests for the 6 bacterial strains using new dithiophosphonate compounds and also the determination of the MIC values for selected compounds against the bacteria strains. The obtained result indicated that these compounds showed a range of antibacterial activities from zero to moderate and even significant, and it is evident that the microbial growth inhibition by metal complexes was in most cases higher than that of the free ligands as displayed by the larger zones of inhibition observed with complexes.

The most resistant bacterial strain was *Salmonella Typhimurium*, most of the compounds were ineffective against it. Even the most effective compound (**3C**) had a small zone of inhibition and a large MIC value which shows that the synthesized compounds were not very effective against this bacterial strain. The most susceptible bacterial strain was MRSA as shown by the large zones of inhibition that were observed against it.

As anticipated, the dithiophosphonate complexes were more effective than the free dithiophosphonate ligands, as shown by their larger zones of inhibition against the bacterial strains. Silver was the most effective metal, while cadmium was the least effective, zinc metals were generally effective against most of the bacterial strains even though they were not the most effective. Three of the four zinc complexes were effective against all the bacterial strains. In conclusion the findings of this investigation confirm that the ligand as well as the metal complex both play significant roles in effectiveness of the antibacterial properties of the compounds which can be useful in the design of antibiotics using this class of ligands.

CHAPTER 5

CONCLUSIONS AND FUTURE WORK

In this study, five new dithiophosphonate ligands were successfully synthesized from the reaction between alcohols (and diols) and Lawesson's Reagent. The study further prepared fourteen new dithiophosphonate complexes.

The compounds were characterised mainly by FT-IR, ^{31}P -NMR, ^1H -NMR, ^{13}C -NMR, mass spectrometry and SC-XRD. The FT-IR spectra showed similarities between the vibrations of the complexes and the ligands with regards to $\nu(\text{P-O-C})$, $\nu_s(\text{P-S})$ and $\nu_{as}(\text{P-S})$ vibrations which were used to confirm the POS_2^- moiety within the compounds. The absence of the $\nu(\text{N-H})$ band in the complexes was used to show the successful complexation of the ligand. ^{31}P -NMR was also used to confirm the synthesis of a dithiophosphonate compound as single peaks were observed within the expected 90-110ppm range associated with dithiophosphonate while ^1H -NMR and ^{13}C -NMR were used to determine the structure of the compounds. Mass spectrometry was used as the final confirmation of the successful synthesis of the compounds as shown by fragment ions and sometimes base peaks corresponding to the expected molecular mass. ESI (-) was useful for observing the fragmentation patterns of the complexes using prominent peaks in the spectra, generally the complex fragmented into a fragment ion with the loss of its metal cation as well as the whole ligand or its anisyl side chain. Two high quality crystals of **3B** and **3C** were obtained from complexes of cadmium and zinc respectively of a 2-butene 1, 4 diol derived ligand. SC-XRD was utilised to analyse them to obtain their structures. The complexes had similar structures. They were dinuclear complexes comprising two bidentate ligand molecules, bound to the metal centres in a chelating fashion, while also forming bridges between them. This formed an eight-membered ring $\text{M}_2\text{S}_2\text{P}_2$ comprising the metal, sulfur and phosphorus atoms as a result.

The in vitro antibacterial studies showed that *Salmonella Typhimurium* was the most resistant strain while MRSA was the most susceptible to the new DTP compounds used in this test. All of the

eighteen tested compounds had some degree of antibacterial effectiveness, as each compound was effective against at least two bacterial strains. The complexes, particularly silver complexes were generally more efficacious compared to their ligands, cadmium complexes were mostly ineffective while most zinc complexes were effective against all 6 bacterial strains used in this study.

Future work

In this study, only compounds derived from Lawesson's Reagent were utilised. But new compounds derived from phenetole and ferrocene analogues of Lawesson's Reagent can also be synthesised for application in antibacterial studies against common virulent bacterial strains.

This study was limited to the use of dithiophosphonate compounds in antibacterial applications, however, catalytic and optical (luminescence) applications can also be considered and attempted.

Further work can also involve the synthesis of the above mentioned compounds (including potential ferrocene and phenetole analogue compounds) using microwave radiation.

The synthesised compounds in this study and related compounds can also be investigated for use single-site metal precursors in the formation of metal chalcogenide, especially metal sulfide, (MS_x) nanoparticle synthesis. Such studies could give mechanistic insight into the formation of metal sulfide nanoparticles which can subsequently be used in catalysis studies.

The study using these dithiophosphonates can also be expanded to more bacterial strains that just the six that were used in this study. The study can also be extended using the same compounds to other types of microorganisms for example viruses and fungi to test for any efficacy.

More metals as well as alcohols can be used to synthesize new compounds which can then be tested for their antibacterial properties as the findings show that the combination of the ligand and metal cation is key to its inherent antibacterial properties.

CHAPTER 6

6.1 REFERENCES

1. Murugavel, R., Choudhury, A., Walawalkar, M. G., Pothiraja, R. & Rao, C. N. R. Metal complexes of organophosphate esters and open-framework metal phosphates: Synthesis, structure, transformations, and applications. *Chem. Rev.* **108**, 3549–3655 (2008).
2. Dauter, Z. & Adamiak, D. A. Anomalous signal of phosphorus used for phasing DNA oligomer: Importance of data redundancy. *Acta Crystallogr. Sect. D Biol. Crystallogr.* **57**, 990–995 (2001).
3. Tang, S. Y. H. & Chan, J. T. S. A review article on nerve agents Physicochemical characteristics. *Hong Kong J. Emerg. Med.* **9**, 83–89 (2002).
4. Alberti, E., Ardizzoia, G. A., Brenna, S., Castelli, F., Galli, S., A. Maspero, A. The synthesis of a new dithiophosphonic acid and its coordination properties toward Ni(II): A combined NMR and X-ray diffraction study. *Polyhedron* **26**, 958–966 (2007).
5. Van Zyl, W. E. & Woollins, J. D. The coordination chemistry of dithiophosphonates: An emerging and versatile ligand class. *Coord. Chem. Rev.* **257**, 718–731 (2013).
6. Van Zyl, W. E. Dithiophosphonates and related P/S-type ligands of group 11 metals. *Comments Inorg. Chem.* **31**, 13–45 (2010).
7. Maspero, A., Kani, I., Mohamed, A., Omary, A., Staples, R. and Fackler, J.P.Jr. Syntheses and structures of dinuclear gold(I) dithiophosphonate complexes and the reaction of the dithiophosphonate complexes with phosphines: diverse coordination types. *Inorg. Chem.* **42**, 5311–5319 (2003).
8. Gray, I. P., Milton, H. L., Slawin, A. M. Z. & Woollins, J. D. Synthesis and structure of $[\text{Fc}(\text{RO})\text{PS}_2]^-$ complexes. *Dalt. Trans.* 3450–3457 (2003).
9. Haiduc, I. Thiophosphorus and related ligands in coordination, organometallic and supramolecular chemistry. A personal account. *J. Organomet. Chem.* **623**, 29–42 (2001).
10. Banaei, A., McArdle, P., Saadat, A., Pourbasheer, E., Mina Goli, M.M., Parinaz Pargolghasemi, P. Synthesis, characterization, and molecular structures of Ni(II) and Cd(II) complexes derived from dithiophosphonates. *Heteroat. Chem.* 1–8 (2015).

11. Moodley, V. Synthesis and characterization of new gold and silver complexes based on P/N and P/S ligands ; P/S ligand-stabilized gold nanoparticles. (University of Kwazulu-Natal, 2013).
12. Gray, I. P., Bhattacharyya, P., Slawin, A. M. Z. & Woollins, J. D. A new synthesis of (PhPSe₂)₂ (Woollins Reagent) and its use in the synthesis of novel P–Se heterocycles. *Chem. - A Eur. J.* **11**, 6221–6227 (2005).
13. Sewpersad, S. New dithiophosphonate complexes of nickel , cadmium , mercury and lead. (University of Kwazulu-Natal, 2013).
14. Hua, G., Randall, R. A. M., Slawin, A. M. Z. & Woollins, J. D. Ammonium phenylphosphonamidodiselenoates and phenylphosphonamidodi-selenoic diamides from the selenation of primary and secondary amines. *Zeitschrift fur Anorg. und Allg. Chemie.* **637**, 1800–1806 (2011).
15. Kaleta, Z., Makowski, B. T., Soós, T. & Dembinski, R. Thionation using fluorous Lawesson's Reagent. *Org. Lett.* **8**, 1625–1628 (2006).
16. Van Zyl, W. E. & Fackler, J. P. A general and convenient route to dithiophosphonate salt derivatives. *Phosphorus. Sulfur. Silicon Relat. Elem.* **167**, 117–132 (2000).
17. Pieterse, H. Ferrocene-derivatized dithiophosphonate salts and their gold(I) and palladium(II) complexes. (University of Johannesburg, 2009).
18. Foreman, Mark, S. J. & Woollins, J. D. Organo-P–S and P–Se heterocycles. *J. Chem. Soc. Dalt. Trans.* 1533–1543 (2000).
19. Larik, F. A., Saeed, A., Muqadar, U. & Channar, P. A. Application of Lawesson's Reagent in the synthesis of sulfur-containing medicinally significant natural alkaloids. *J. Sulfur Chem.* **38**, 206–227 (2017).
20. Jesberger, M., Davis, T. P. & Barner, L. Applications of Lawesson ' s Reagent in organic and organometallic syntheses. *J. Synth. Org. Chem.* **13**, 1929–1958 (2003).
21. Sağlam, E. G. *et al.* Syntheses, characterization of and studies on the electrochemical behaviour of ferrocenyl dithiophosphonates and 4-methoxyphenyl dithiophosphonates. *Phosphorus. Sulfur. Silicon Relat. Elem.* **192**, 322–329 (2017).
22. Pillay, M. N., van der Walt, H., Staples, R. J. & van Zyl, W. E. C/O/P/S cycles derived from oxidative intramolecular disulfide (–S–S–) coupling of ferrocenyl dithiophosphonates. *J.*

- Organomet. Chem.* **794**, 33–39 (2015).
23. Manfred Fild , Oana Krüger , Ioan Silaghi-Dumitrescu, C. T. & A. W. Synthesis and properties of organogermanium and organotin dithiophosphonate complexes; crystal structures of $(C_6H_5)_2Sn(Cl)[(p\text{-MeOC}_6H_4)(EtO)PS_2-S, S']$, $Me_2Sn[(p\text{-MeOC}_6H_4)(MeO)PS_2-S]_2$, $Me_2Sn[(p\text{-MeOC}_6H_4)(i\text{-PrO})PS_2-S]_2$, and $Me_2Ge\{[(C_6H_5)_3SiO](p\text{-MeOC}_6H_4)PS_2\}$. *Phosphorus. Sulfur. Silicon Relat. Elem.* **182**, 2283–2310 (2007).
 24. Van Zyl, W. E., López-de-Luzuriaga, J. M., Mohamed, A. A., Staples, R. J. & Fackler, J. P. Dinuclear gold(I) dithiophosphonate complexes: synthesis, luminescent properties, and X-ray crystal structures of $[AuS_2PR(OR')]_2$ (R = Ph, R' = C₅H₉; R = 4-C₆H₄OMe, R' = (1S,5R,2S)-(-)-menthyl; R = Fc, R' = (CH₂)₂O(CH₂)₂OMe). *Inorg. Chem.* **41**, 4579–4589 (2002).
 25. Przychodzeń, W. New products of reaction of Lawesson's Reagent with diols. *Phosphorus. Sulfur. Silicon Relat. Elem.* **179**, 1621–1633 (2004).
 26. Karakus, M. & Yilmaz, H. Synthesis and characterization of Ni(II), Zn(II), and Cd(II) complexes with dithiophosphonate derivatives. *Russ. J. Coord. Chem.* **32**, 437–443 (2006).
 27. Nizamov, I. S., Terenzhev, D. A., Sabirzyanova, G. R., Salikhov, R. Z., Nizamov, I. D. & Cherkasov, R. A. New phosphorus dithioacids and their derivatives containing chiral centers and pharmacophoric groups. *Phosphorus. Sulfur. Silicon Relat. Elem.* **191**, 1578–1580 (2016).
 28. Pillay, M. N., Omondi, B., Staples, R. J. & van Zyl, W. E. A hexanuclear gold(I) metallatriangle derived from a chiral dithiophosphonate: synthesis, structure, luminescence and oxidative bromination reactivity. *CrystEngComm.* **15**, 4417–4421 (2013).
 29. Shabana, R., Oman, F. H. & Atrees, S. S. Organophosphorus compounds XIII. The reaction of 2,4-bis(4-methoxyphenyl)-1,3,2,4-dithiadiphosphetane-2, disulfide (LR) with dihydric alcohols. A new route to 1,3,2-dioxaphosphorinane. **49**, 1271–1282 (1993).
 30. Shabana, R., Osman, F. H. & Atrees, S. S. Organophosphorus compounds XV. The reaction of 2,4-bis(4-methoxyphenyl)-1,3,2,4-dithiadiphosphetane-2,4-disulfide (Lawesson's Reagent) with aromatic dihydroxy compounds. Simple new route to 1,3,2-dioxaphospholane-2-sulfide. *Tetrahedron.* **50**, 6975–6988 (1994).
 31. Ajayi, T. J., Pillay, M. N. & van Zyl, W. E. Solvent-free mechanochemical synthesis of dithiophosphonic acids and corresponding nickel(II) complexes. *Phosphorus. Sulfur. Silicon Relat. Elem.* **6507**, 1–7 (2017).

32. Haiduc, I. & Yoong Goh, L. Reactions of bis(thiophosphoryl)disulfanes and bis(thiophosphinyl)disulfanes with metal species: An alternative, convenient route to metal complex and organometallic dithiophosphates and dithiophosphinates. *Coord. Chem. Rev.* **224**, 151–170 (2002).
33. Haiduc, I., Sowerby, D. & Lu, S. Stereochemical aspects of phosphor-1, 1-dithiolato metal complexes (dithiophosphates, dithiophosphinates): Coordination patterns, molecular structures. *Polyhedron* **14**, 3389–3472 (1995).
34. Pillay, M. N. Complexes and Clusters of Group 9-11 Metal Dithiophosphonates : Synthesis , Reactivity , Luminescence Properties and Structural. (University of Kwazulu-Natal, 2016).
35. Haiduc, I. & Sowerby, D. B. Stereochemical aspects of phosphor-1,1-dithiolato metal complexes: Coordination patterns, molecular structures and supramolecular associations in dithiophosphinates and related compounds. *Polyhedron* **15**, 2469–2519 (1996).
36. Gray, I. P., Slawin, A. M. Z. & Woollins, J. D. Synthesis and Structure of $[\text{Fc}(\text{EtO})\text{PS}_2]^-$ Complexes. *Zeitschrift fur Anorg. und Allg. Chemie.* **630**, 1851–1857 (2004).
37. Karakus, M., Ikiz, Y., Kaya, H. I. & Simsek, O. Synthesis, characterization, electrospinning and antibacterial studies on triphenylphosphine-dithiophosphonates copper(I) and silver(I) complexes. *Chem. Cent. J.* **8**, 18 (2014).
38. Da Silva, A.C.R., Lopes, M.P., De Azevedo, M.M.B., Costa, M. C. M. Alviano, C. S. and Alviano, D. S. Biological activities of α -pinene and β -pinene enantiomers. *Molecules* **17**, 6305–6316 (2012).
39. Przychodźen, W. New products of reaction of Lawesson's Reagent with diols. *Phosphorus. Sulfur. Silicon Relat. Elem.* **1799**, 1621–1633 (2004).
40. Sağlam, E. G. Structural studies on some dithiophosphonato complexes of Ni(II), Cd(II), Hg(II) and theoretical studies on adithiophosphonato Ni(II) complex using density functional theory. *J. Mol. Struct.* **1099**, 490–501 (2015).
41. Karakus, M., Yilmaz, H. & Bulak, E. Synthesis and characterization of Zn(II) and Cd(II) complexes with bisdithiophosphonates. *Russ. J. Coord. Chem. Khimiya* **31**, 316–321 (2005).
42. Gimadiev, T. R. & Pinus, Æ. M. V. Complexes of podand-containing bis (dithiophosphonate) ligands with cobalt(II), nickel(II) and cadmium(II): recognition of CH_2Cl_2 . *Transit. Met. Chem.* **48**, 921–924 (2008).

43. Solak, S. Novel gold(I) and silver(I) complexes of novel gold(I) and silver(I) complexes of phosphorus-1,1 , -dithiolates and molecular. *Chem. Cent. J.* **7**, 89 (2013).
44. Çekirdek, P., Solak, Osman, A., Aydın, A. & Yılmaz, H. Reduction of some dithiophosphonates in aprotic, media on freshly copper plated glassy carbon electrode. *Fen Bilim. Derg.* **12**, 1–16 (2011).
45. Karakus, M. Synthesis and characterization of novel organothiophosphorus compounds : X-ray crystal structure of $H_3COC_6H_4P(OC_2H_4S)(S)$ synthesized by a new method. *Zeitschrift für Anorg. und Allg. Chemie* **632**, 1549–1553 (2006).
46. Ozcan, Y. Ö., Karakus, M., Yılmaz, H. & Semra, I. Crystal and molecular structures of trans - nickel(II)-bis[(O-propyl n)-(p-methoxyphenyl) dithiophosphonate]. *Anal. Sci.* **18**, 1285–1286 (2002).
47. Kabra, V., Mitharwal, S. & Singh, S. Synthesis and insecticidal activity of novel dithiophosphonates synthesis and insecticidal activity of novel dithiophosphonates. *Phosphorus. Sulfur. Silicon Relat. Elem.* **184**, 2431–2442 (2009).
48. Kır, E., Yalımlı, Ş., Kurtulmuş, S., Aydın, A. & Yılmaz, H. Facilitated transport of Ni(II) through supported liquid membranes containing dithiophosphonates as ion carrier. *Phosphorus. Sulfur. Silicon Relat. Elem.* **190**, 178–190 (2015).
49. Karakus, M. *et al.* A kinetic study of mercury(II) transport through a membrane assisted by new transport reagent. *Chem. Cent. J.* **5**, 2–7 (2011).
50. Fackler, J. P. Forty-Five Years of Chemical Discovery Including a Golden Quarter-Century. *Inorg. Chem.* **41**, 6959–6972 (2002).
51. Van Zyl, W. E. Luminescence studies of dinuclear gold (I) phosphorus-1 , 1-dithiolate complexes. *J. Mol. Struct.* **516**, 99–106 (2000).
52. Kvitek, L. & Panacek, A. Silver nanoparticles : synthesis , properties , toxicology , applications and perspectives. *Adv. Nat. Sci. Nanosci. Nanotechnol.* **4**, (2013).
53. Jones, N., Ray, B., Ranjit, K. T. & Manna, A. C. Antibacterial activity of ZnO nanoparticle suspensions on a broad spectrum of microorganisms. *FEMS Microbiol. Lett.* **279**, 71–76 (2008).
54. Salem, W. *et al.* Antibacterial activity of silver and zinc nanoparticles against *Vibrio cholerae* and enterotoxigenic *Escherichia coli*. *Int. J. Med. Microbiol.* **305**, 85–95 (2015).

55. Guzmán, M. G., Dille, J. & Godet, S. Synthesis of silver nanoparticles by chemical reduction method and their antibacterial activity. *Int. J. Chem. Biomol. Eng.* **2**, 104–111 (2009).
56. Munita, J. M., Arias, C. A., Unit, A. R. & Santiago, A. De. HHS Public Access. *Microbiol. Spectr.* **4**, 1–37 (2016).
57. Vila, J., S´aez-L´opez, E., Johnson, J.R., Romling, U., Dobrindt, U., Cant´on, R., Giske, G., Naas, T., Carattoli, A., Mart´inez-Medina, M., Bosch, J., Retamar, P., Rodr´iguez-Ba˜no, J., Baquero, F. and Soto, S.M. Escherichia coli: An old friend with new tidings. *FEMS Microbiol. Rev.* **40**, 437–463 (2016).
58. Palena, A. A. P. & Mata, E. G. Thionation of bicyclic β -lactam compounds by Lawesson’s Reagent. *ARKIVOC* **2005**, 282–294 (2005).
59. Aydemir, C., Solak, S., Doganlı, G.A., Sensoy, T., Arar, D., Bozbeyoglu, N., Dogan, N.M., Lönnecke, P., Hey-Hawkins, E., Sekerci, M. and Karakus, M. Synthesis, characterization, and antibacterial activity of dithiophosphonates and amidodithiophosphonates. *Phosphorus. Sulfur. Silicon Relat. Elem.* **190**, 300–309 (2015).
60. McKenna, C.E., Li, Z., Ju, J., Pham, P. T., Robert Kilkuskie, R., Loo, T.L. and James Straw. Simple and conjugate bifunctional thiophosphonates: synthesis and potential as anti-viral agents. *Phosphorus. Sulfur. Silicon Relat. Elem.* **74**, 469–470 (1993).
61. Saadat, A., Banaee, A., Mcardle, P. & Zare, K. Ni(II) complexes of dithiophosphonic acids. *J. Chem. Sci.* **126**, 1125–1133 (2014).
62. Van Zyl, W. E., L´opez-de-Luzuriaga, J. M., Mohamed, A. a, Staples, R. J. & Fackler, J. P. Dinuclear gold(I) dithiophosphonate complexes: synthesis, luminescent properties, and X-ray crystal structures of $[\text{AuS}_2\text{PR}(\text{OR}')_2]_2$ (R = Ph, R' = C₅H₉; R = 4-C₆H₄OMe, R' = (1S,5R,2S)-(-)-menthyl; R = Fc, R' = (CH₂)₂O(CH₂)₂OMe). *Inorg. Chem.* **41**, 4579–89 (2002).
63. Solak, S., Lönnecke, P. & Karakus, M. Novel gold(I) and silver(I) omplexes of novel gold(I) and silver(I) complexes of phosphorus-1, 1, -dithiolates and molecular. *Chem. Cent. J.* **7**, 89 (2013).
64. Wang, X., Li, Y., Ma, Q., and Zhang, Q. Ruthenium complexes with dithiophosphonates $[\text{Ar}(\text{RO})\text{PS}_2]^-$ and. *Organometallics* **29**, 2752–2760 (2010).
65. Sirelkhatim, A., Mahmud, S., Seeni, A., Kaus, N.H.M., Ann, L.C., Bakhori, S.K.M., Hasan, H., Dasmawati, M. Review on zinc oxide nanoparticles: Antibacterial activity and toxicity

- mechanism. *Nano-Micro Lett.* **7**, 219–242 (2015).
66. Nataro, J. P., and J. B. K. Diarrheagenic *Escherichia coli*. *Clin Microbiol Rev* **11**, 142–201 (1998).
 67. Kaper, J. B., Nataro, J. P. & Mobley, H. L. T. Pathogenic *Escherichia coli*. *Nat Rev Microbiol* **2**, 123–140 (2004).
 68. Chambers, H. F. & Deleo, F. R. Waves of resistance: *Staphylococcus aureus* in the antibiotic era. *Nat. Rev. Microbiol.* **7**, 629–41 (2009).
 69. Lally, R. T., Ederer, M. N. & Woolfrey, B. F. Evaluation of mannitol salt agar with oxacillin as a screening medium for methicillin-resistant *Staphylococcus aureus*. *J. Clin. Microbiol.* **22**, 501–504 (1985).
 70. Walsh, F. M. & Amyes, S. G. B. Microbiology and drug resistance mechanisms of fully resistant pathogens. *Curr. Opin. Microbiol.* **7**, 439–444 (2004).
 71. Mehndiratta, P., Bhalla, P. & Org Pmid, W. I. Typing of Methicillin resistant *Staphylococcus aureus*: A technical review. *Indian J. Med. Microbiol.* **30**, 16 (2012).
 72. Poole, K. Efflux-mediated multiresistance in Gram-negative bacteria. *Clin. Microbiol. Infect.* **10**, 12–26 (2004).
 73. Panawala, L. Difference Between Gram Positive and Gram negative Bacteria (2017).
 74. Tong, S. Y. C., Davis, J. S., Eichenberger, E., Holland, T. L. & Fowler, V. G. *Staphylococcus aureus* infections: Epidemiology, pathophysiology, clinical manifestations, and management. *Clin. Microbiol. Rev.* **28**, 603–661 (2015).
 75. Croxen, M. A. & Finlay, B. B. Molecular mechanisms of *Escherichia coli* pathogenicity. *Nat. Rev. Microbiol.* **8**, 26–38 (2010).
 76. Paczosa, M. K. & Mecsas, J. *Klebsiella pneumoniae*: Going on the Offense with a Strong Defense. *Microbiol. Mol. Biol. Rev.* **80**, 629–61 (2016).
 77. Dorman, M. J. & Short, F. L. Genome watch: *Klebsiella pneumoniae*: when a colonizer turns bad. *Nat. Rev. Microbiol.* **13**, 2017 (2017).
 78. Ullmann, U. 6 *Klebsiella spp.* as Nosocomial Pathogens Epidemiology, Taxonomy, Typing Methods, and Pathogenicity Factors. **11**, 589–603 (1998).

79. Fàbrega, A. & Vila, J. *Salmonella enterica*, serovar Typhimurium skills to succeed in the host: Virulence and regulation. *Clin. Microbiol. Rev.* **26**, 308–341 (2013).
80. Klockgether, J., Cramer, N., Wiehlmann, L., Davenport, C. F. & Tümmler, B. *Pseudomonas aeruginosa* genomic structure and diversity. *Front. Microbiol.* **2**, 1–18 (2011).
81. Hasselmann, C. & Diseases, I. Determination of minimum inhibitory concentrations (MICs) of antibacterial agents by broth dilution. *Clin. Microbiol. Infect.* **9**, ix–xv (2003).
82. Chauhan, H. P. S., Singh, U. P., Shaik, N. M., Mathur, S. & Huch, V. Synthetic, spectroscopic, X-ray structural and antimicrobial studies of 1,3-dithia-2-stibacyclopentane derivatives of phosphorus based dithiolato ligands. *Polyhedron* **25**, 2841–2847 (2006).
83. Al-Amiery, A. A., Kadhum, A. A. H. & Mohamad, A. B. Antifungal and antioxidant activities of pyrrolidone thiosemicarbazone complexes. *Bioinorg. Chem. Appl.* **2012**, (2012).
84. McGee, M. Chapter 27 - Bacteria and Archaea (detailed), available from <https://www.quia.com/jg/2536816list.html>, [retrieved 30 April 2018].

SUPPORTING INFORMATION

The accompanying CD serves as a soft copy Appendix to this dissertation and contains ^{31}P -NMR, ^1H NMR, ^{13}C -NMR, HSQC-NMR, FT-IR and mass spectra. As well as X-ray crystallographic data (including *cif* files).